FORMULATION AND CHARACTERIZATION OF PROTOTYPE PARTICLEBOARDS USING SELECTED CROP RESIDUE AND STARCH FROM CASSAVA PEELS AS A BINDER

STEPHEN WARUI KARIUKI

A THESIS SUBMITTED IN PARTIAL FULFILLMENT OF THE REQUIREMENTS FOR THE AWARD OF THE DEGREE OF DOCTOR OF PHILOSOPHY IN CHEMISTRY IN THE UNIVERSITY OF EMBU

NOVEMBER, 2020

DECLARATION

This thesis is my original work and has not been presented elsewhere for a degree award

Signature : 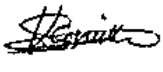 …… Date ……

Stephen Warui Kariuki

Department of Physical Sciences

B801/168/2016

This thesis has been submitted for examination with our approval as University Supervisors

Signature …… Date ……

Prof. Jackson Wachira Muthengia

Department of Physical Sciences

University Of Embu

Signature …… Date ……

Dr. Erastus Millien Kawira

Department Of Physical Sciences

University Of Embu

Signature …… Date ……

Dr. Genson Murithi

Department Of Physical Sciences

University Of Embu

DEDICATION

This study is dedicated to my ever-supportive mother Agnes Muthoni, my dear wife Christine Gacheri, my daughter Julienne Muthoni and my sons Richmond Kariuki and Liam Mutugi

ACKNOWLEDGEMENT

I am obliged to my able supervisors Prof. Wachira Jackson Muthengia, Dr. Erastus Millien Kawira and Dr. Genson Murithi for their continued excellent supervision, tireless guidance, support and advice throughout the research.

I am also thankful to the lecturers for their advice and the cooperative technical team of the staff University of Embu for their support. Special gratitude is due to my fellow course mate Peterson Mutembei. I also wish to thank my uncles and especially engineer Raphael Kabugu for his tireless financial support and encouragement.

I owe most sincere gratitude to my lovely mum Agnes Muthoni, my siblings the late Hannah Njeri, Isaiah Gichanga, Phyllis Nyawira, Simon Kinyua and Peter Kamau for their moral and financial support.

I am also grateful to my wife Christine Gacheri, my daughter Julienne Muthoni and my son Richmond Kariuki for their encouragement, patience and understanding during my absence.

Above all most sincerely the Omnipotent God for life and perfect health to pursue this doctoral course.

TABLE OF CONTENTS

LIST OF TABLES

LIST OF FIGURES

LIST OF PLATES

LIST OF APPENDICES

LIST OF SCHEMES

LIST OF ABBREVIATIONS / ACRONYMS

AAS	Atomic Absorption Spectroscopy
ANOVA	Analysis of Variance
ANSI	American National Standards Institute
ASTM	American Society for Testing and Materials
ATR	Attenuated Total Reflection
BC	Bacteria Cellulose
CP	Cassava Peel
E	Energy
EN	European Standards
Ɛ	Molar Absorptivity
FAO	Food and Agriculture Organization
FTIR	Fourier Transform Infra-Red
GHG	Greenhouse gas
HCl	Hydrochloric acid
HD	High Density
KS	Kenyan Standards
LBL	Layer by Layer
LD	Low Density
MC	Moisture Content
MD	Medium Density
MDF	Medium Density Fiberboard
MOE	Modulus of Elasticity
MOE	Modulus of Elasticity
MOR	Modulus of Rupture
MRG	Mount Royal Gabbro
nm	Nano Metre
NMR	Nuclear Magnetic Resonance
PF	Phenol-Formaldehyde
PVA	Polyvinyl Acetate
PVOH	Polyvinyl Alcohol
SEM	Scanning Electron Microscopy
SY	Syenite
T	Transmittance
TS	Thickness Swelling
UV	Ultra Violet
VOC	Volatile Organic Compounds
WA	Water Absorption
XRD	X-ray Diffraction
XRFS	X-Ray Fluorescence Spectroscopy
$\bar{x}$	Arithmetic mean
δ	Chemical Shift
υ	Frequency

ABSTRACT

Particleboards are formulated from lignocellulose material bound with adhesives. Conventional lignocellulose material used is wood particles and adhesive is formaldehyde-based resin. Due to reduction of tree cover, wood has become scarce leading to search for alternative lignocellulose material. Crop residues, as a lignocellulose material, pose disposal problems due to their low biodegradability, hence disposed off mainly by burning. Crop residues are lignocellulose materials of low nutritional value for use as livestock feed. Conventional formaldehyde-based resins hydrolyse in water to form formaldehyde. Epidemiological studies have shown that formaldehyde are carcinogenic and thus harmful. Efforts to reduce the health hazard effects of the formaldehyde-based resins in the particleboard formulation have included, among others, the use of chemical scavengers for formaldehyde and use of an alternative binder. In this study, single layer particleboards were made from cassava peels starch and selected lignocellulose materials. This was done by *in-situ* chemical oxidation of cassava peels starch and hydrolysis of lignocellulose sources from crop residue followed by condensation polymerization to form composite material. The resultant composite material was moulded to form particleboards. Crop residues used in this study included bagasse, maize straw and rice husks. The residues were sampled from farm and disposal sites in Kirinyaga, Kisumu and Narok Counties. Sawdust was used as a control for the source of lignin. Lignin content was determined following the Klason method. Cassava peel starch adhesive used in this study was analyzed for pH. Na^{+}, Zn^{2+}, Ca^{2+} and Mg^{2+} in starch and crop residues were determined using atomic absorption spectroscopy (AAS) and X-ray fluorescence (XRF). The mineralogical content of particleboards was determined using X-ray Diffractometer (XRD). Structure elucidation of compounds in raw materials and particleboards was determined by the use of fourier transform infra-red (FTIR) and nuclear magnetic resonance (NMR). Data obtained from this study were subjected to statistical analysis using Tukey one way analysis of variance (ANOVA). Particleboards were formulated and tested per American Standard for Testing and Materials (ASTM D1037). Average densities for particleboards was between 0.608 gcm^{-3} to 0.627 gcm^{-3}, moisture content of 9.51 % to 9.85 %, deionized water absorption (WA) ranged from 61.33 % to 83.87 % and thickness swelling (TS) 18.23 % and 23.43 %. Modulus of Elasticity (MOE) for particleboards was between 2364.2 Nmm^{-2} to 33329.92 Nmm^{-2}, Modulus of rupture (MOR) ranged from 13.55 Nmm^{-2} to 14.83 Nmm^{-2}, internal bonding (IB) ranged from 1.613 Nmm^{-2} to 2.370 Nmm^{-2}. Elemental analysis for both starch sources and polyphenolic materials for Na^{+}, Zn^{2+}, Ca^{2+} and Mg^{2+}. Na^{+} and Zn^{2+} was less than 1 %. Ca ranged from 4.55 to 13.46 % and Mg ranged from 5.95 to 6.55 %. FTIR and NMR analysis for starch and polyphenolic materials showed that peaks of –OH and -COOH decreased as those of -C-O-C- increased. Particleboards formulated in this study have similar characteristics to medium density fiberboards. They can thus be used for making furniture and doors.

CHAPTER ONE
INTRODUCTION

1.1 Background Information

Particleboard is a panel produced when particles are compressed while simultaneously bonding them with an adhesive. Particleboard is also defined as wood particles bonded using synthetic resin and with pressure and heat, moulded into a panel product (Kasim *et al.*, 2014). Particleboard is formulated with small particles of lignocellulose material bonded together by adhesives (Tay *et al*., 2016; Matuana and Carlborn, 2012; Nasser, 2012b). Particleboards are formulated either as a medium, low or high-density boards. The criterion of the three categories depends on particleboard standards and certification bodies. According to American Standards for material testing (ASTM), low-density particleboards have densities of < 600 g/cm^3, medium density have densities that range from 640 g/cm^3 to 0.85 g/cm^3 and high-density particleboards have densities > 0.85 g/cm^3.

Particleboard is formulated through the encapsulation of lignocellulose particles with adhesive resins. Commonly used resins involve phenol-formaldehyde and urea-formaldehyde (Akhtar *et al*., 2011). These resins undergo condensation polymerization to form a network of interlinked polymer that holds lignocellulose particles together at high pressure in a process known as curing (Grenier-Loustalot *et al*., 1996). The pressure used in the process reduces the spaces between the lignocellulose particles before the adhesive cures. Lignocellulose particles involved are wood chips, flakes, or wafers among others.

Adhesives determine the strength of the resultant composite material formulated. However, the particle size and particle shapes affect the strength of the bonds (Ullah *et al.*, 2014). Particleboard applications depend on the properties of adhesive used. Adhesives used have a partial or complete water-resistant. Adhesives that have partial water-resistance are mainly used for interior applications whereas complete water-resistant are mainly used for exterior applications due to the exposure to high moisture. Particleboards are mainly used in the construction industry for making doors, partitioning of rooms, packaging, paneling and frames.

Conventional adhesive used is mainly formaldehyde-based resins. Formaldehyde based resins undergo hydrolysis in the presence of water to form free formaldehyde. According to epidemiologic studies, formaldehyde is carcinogenic, hence harmful to health. Efforts to reduce formaldehyde-based resins in the particleboard formulation have included among others use of chemical scavengers for formaldehyde and the use of alternative binder (Magalhaes *et al*., 2013; Takagaki *et al*., 2000). There are no findings that the use of chemical scavengers eliminates the emission of formaldehyde from particleboard (Magalhaes *et al*., 2013).

According to the European Panel Federation (EPF) 2016 – 2017 reports, more than 30,250,000 m^3 of particleboards were produced. Germany is leading with 5,500,000 m^3, France, 3,630,000 m^3, Poland, 2,793,000 m^3, Italy, 2,569,000 m^3, Austria, 2,300,000 m^3, United Kingdom, 1,949,000 m^3, Spain, 1,806,000 m^3, Belgium, 1,050,000 m^3 among other countries (Mantanis *et al.*, 2017). Other major particleboards producing countries included Bulgaria, Croatia, Czech Republic, Denmark, Estoria, Finland, Greece, Hungary, Lavia, Lithuania, and Norway. Kenya remains a main importer of particleboards (Mantanis *et al.*, 2017).

In Kenya, there has been a steady rise in demand for particleboard (KNBS, 2018). Primarily, wood and wood products including sawdust, have acted as the main source of lignocellulose material for particleboard formulation. This has been a major factor contributing to deforestation. Due to decreasing wood sources, there is a need for research on the use of alternative sources for lignocellulose material for the formulation of particleboards. According to 2017 Kenya National Bureau of Statistics (KNBS) reports, wood and wood products decreased by 13.2 percent, an indication of a reduction in the production of wood as a raw material for making these materials (KNBS, 2018).

The focus of this study was to investigate the possibility of using alternative lignocelluloses and adhesive material to make prototype particleboards. The study investigated the use of crop residues as an alternative source of lignocellulose material and use of cassava starch as an adhesive for formulating the particleboard. The resultant formulated particleboards are suitable for interior design and construction.

1.2 Statement of the Problem

Particleboards made currently for furniture and interior designs are expensive due to high cost raw materials thus making them unaffordable. This is due to the high cost of the conventional raw materials used in their formulation. The use of wood as a source of lignocellulose material has led to deforestation. This has led to the utilization of alternative, but low-quality construction materials. Since use of crop residues in particleboard formulation will enhance the use of alternative lignocellulose material which is otherwise disposed of mainly through burning in open fields. The use of cassava peel starch to formulate an adhesive will result in the elimination of formaldehyde-based resins. The use of formaldehyde in particleboard formulation poses a health risk associated with oncological health hazards. Cassava peel starch is, therefore, an alternative binder for particleboard formulation. Making particleboards from these agricultural by-products would introduce an alternative waste disposal method for the agricultural by-product.

1.3 Significance of the Study

Particleboards formulated with sugarcane bagasse, rice husks and maize stalk solve a problem in waste disposal. Alternative methods of waste disposal are provided in the production of particleboards. In this case, agricultural wastes are not burnt as a way of their disposal. Since burning of agricultural waste leads to environmental pollution. Greenhouse gases causes climatic conditions such as to global warming. In turn, it will result in a reduction in climate change.

Agricultural by-products are estimated to increase globally to more than 496.4 million tones every year (FAO, 2015). This will lead to the production of more agricultural-based crop residues. Disposal of these agriculture materials is mainly by burning (Kartini, 2014a) which gives rise to fine silica particles in the air causing air pollution (Anderson *et al.*, 2016) and evolution of greenhouse gases such as carbon dioxide, methane gas and dinitrogen oxide (Boonyanopakun and Pavasant, 2012; Okoba *et al*., 2012). Greenhouse gases cause global warming (Haysa *et al.*, 2015) and are emitted due to human activities. The use of these wastes, in developing countries like Kenya, and the world at large, is the most suitable way of their disposal.

Agricultural based materials such as rice husk contain 75 to 90 percent of organic matter which is mainly lignin (Ummah *et al.*, 2015; Sangwan *et al*., 2013). Lignin, a natural polymer, has been used in formulating adhesives (Pfungen, 2015; Ghaffar and Fan, 2014) and particleboard yet it is still underutilized (Boon *et al.*, 2019; Abdelmouleh *et al.*, 2007; Mwaikambo and Ansell, 2002). Lignin can be blended with established biopolymers such as starch-based adhesives (Vengal and Srikumar, 2015) to make composite material used to formulate particleboards. Particleboards made from biomaterials do not pollute the environment as they are biodegradable. Starch is used in the manufacture of processed material such as garri and starch flour (Tonukari, 2014; Grace, 2012). Starch is a natural biopolymer of adhesive which can be obtained from agricultural materials like cassava, sorghum, wheat, corn, rice, among others (Tonukari, 2014). It's fine, smooth texture, non-staining and non-poisonous nature make it useful in the formulation of bio-based adhesives for domestic use (Hardy *et al.*, 2017).

Kenya produces waste especially husks, corn stalk, cassava peels and bagasse from sugarcane and rice as crop residues in largescale (KNBS, 2018; Okeyo *et al.*, 2016). Reports show that cassava has the highest output of residues generated in Kenya with residues of about 29,000,000 metric tonnes in one year. Middle-income countries, like Kenya, find cassava peels of no use, thus disposed of by burning, which produces greenhouse gases. Crop residues produced in large quantities include rice husks, sugar bagasse, and wheat straw among others. Agricultural crop residue disposal is a challenge leading to low tillage of farms (Okeyo *et al.,* 2016). Poor crop residue disposal management has led to burning as an alternative way of waste disposal.

1.4 Research Questions

i. What is the starch, Na, Mg, Zn and Ca content in cassava tubers, maize, wheat, sorghum and millet grains?
ii. What is the lignin content in bagasse, maize stalks, rice straw, rice husks, grass straw, wheat straw and sawdust?
iii. What is the mineralogical composition of particleboards formulated from selected agricultural materials?

iv. What is the structure of compounds found in particleboards formulated from selected agricultural-based materials?
v. What are the mechanical, physical and chemical properties of the formulated particleboards?

1.5 Study Objectives

1.5.1 The General Objective

Investigation of particleboards formulated using selected crop residues as sources of lignocellulose materials and starch from cassava peels as a binder

1.5.2 Specific Objectives

1. To determine the starch, Na, Mg, Zn and Ca content in cassava tubers, maize, wheat, sorghum and millet grains
2. To determine the lignin content in bagasse, maize stalks, rice straw, rice husks, grass straw, wheat straw and sawdust
3. To investigate the mineralogical composition of formulated particleboard made through copolymerization of crop residues and starch as a binder using X-Ray Diffraction
4. To elucidate the structural composition of the particleboards using FTIR and NMR spectroscopy.
5. To investigate the physical and mechanical properties of the formulated particleboards

1.6 Scope and Limitation

This study was limited to formulating particleboards from selected agricultural residues such as sugarcane bagasse, maize stalk and rice husks and starch from selected sources. The study has not included synthetic polymeric materials used in commercial particleboards formulation.

CHAPTER TWO

2 LITERATURE REVIEW

2.1 Particleboards

A Particleboard is a panel made of lignocellulose materials bonded together by resin under high pressure and temperature (Nasser, 2012a; Wang and Sun, 2002). Particleboard can also be defined as an engineered wood product formulated from wood particles, such as wood chips, sawmill shavings, sawdust and a synthetic resin as a binder (Nemli *et al*., 2009; Nemli *et al*., 2007). It can also be made by compressing the small prtion of wood while simultaneously bonding them with adhesive (Youngquist, 2012). Primary lignocellulose materials used in particleboard formulation are usually wood particles. Agro-based crop residues such as palm stalks, rice straw, rice husks and other crop residues are being investigated for producing particleboards. Utilization of crop residues reduces the demand of wood and mitigates environmental pollution (Zarifa *et al*., 2018).

Particleboards are categorized on the basis of the size of the particle. There are various types of particles such as fiberboard, orient starnd board (OSB), medium density board (MDF) and others (Akgul and Camlibel, 2008). Particle sizes specification is different for each particleboard plant requires slender particles for attaining high strength. Fine particles are used for face layers and coarse particles are used for the core layer. Once particles are prepared, they are dried by means of rotary, disk or suspension drying. Particle drying is a critical step in production of particleboard and the moisture content of the particles leaving the dryer is usually in the range of 4% to 8%. After drying, the particles are blended with an adhesive and additives. The adhesive-blended particles typically have a final moisture content of near 10% (Diop *et al.*, 2017). Then the adhesive-blended particles are formed into a mat and pre-pressed to reduce mat thickness prior to hot pressing. Hot-press temperature usually ranges from 140 °C to 165 °C, and pressure in the range of 1.37 to 3.43 MPa for medium density particleboard.

2.2 Particleboard Binders

Particleboard binders are used to hold the lignocellulose materials together. They are categorized into two: synthetic and natural. Synthetic adhesives commonly used in particleboard formulation include phenol-formaldehyde (PF) and urea-formaldehyde

(UF) (Yan *et al*., 2017a; Mamza *et al*., 2014; Paul *et al*., 2014). Natural adhesives include starch (Yang *et al*., 2013; Qiang *et al*., 2013; Sridach *et al*., 2013) and soybean (Bai *et al*., 2020; Ciannamea *et al*., 2010; Cheng *et al*., 2004; Sun *et al*., 2004b). Synthetic adhesives undergo hydrolysis to form carcinogenic formaldehyde. The main challenge with natural adhesive is their water solubility which limits their outdoor applications. Due to this limitation, natural adhesives require chemical modifications to increase their stability in particleboard formulation (Masina *et al*., 2017; Lewicka *et al*., 2015; Liu and Li, 2002; Bayazeed *et al*., 1998). Other adhesives used in particleboard formulation include sodium silicate (Zuo *et al*., 2015), melamine-formaldehyde (Ullah *et al*., 2014; Merline *et al*., 2012; De Barros Filho *et al*., 2011) and methylene diphenyl diisocyanate (Sattayarak *et al*., 2012; Pan *et al*., 2006).

2.2.1 Starch-Based Adhesive

Starch is a biodegradable polymer with a demand in adhesive industries (Chang *et al.*, 2010). Due to its abundance, non-food applications have been developed (Lawton, 2016). Non-food use of starch includes paper-making and adhesives (Gu *et al.*, 2016; Xu *et al.*, 2016). Currently, less than 30 percent of starch in developed countries is used as food (Lawton, 2016). In Kenya, starch is mainly used as a source of carbohydrates for both human and domestic animals. Starch is a renewable and bio-degradable material convertible to bioplastic and binders in the manufacture of concrete (Kulshreshtha *et al.*, 2017)

Starch is a primary carbohydrate that is composed of amylose and amylopectin (Tester *et al.*, 2014). Structurally, starch has amylose that is joint with α-1,4-glycoside linkages and branched amylopectin with α-1,6-glycoside linkages. Amylose and amylopectin are important fractions in grafting polymer formation such as lignin, cellulose and hemicellulose (Tester *et al.*, 2014; Buleon *et al.*, 2012; Parker and Ring, 2001). Amylopectin is shown in Figure 2-1 and Amylose structure is shown in Figure 2-2.

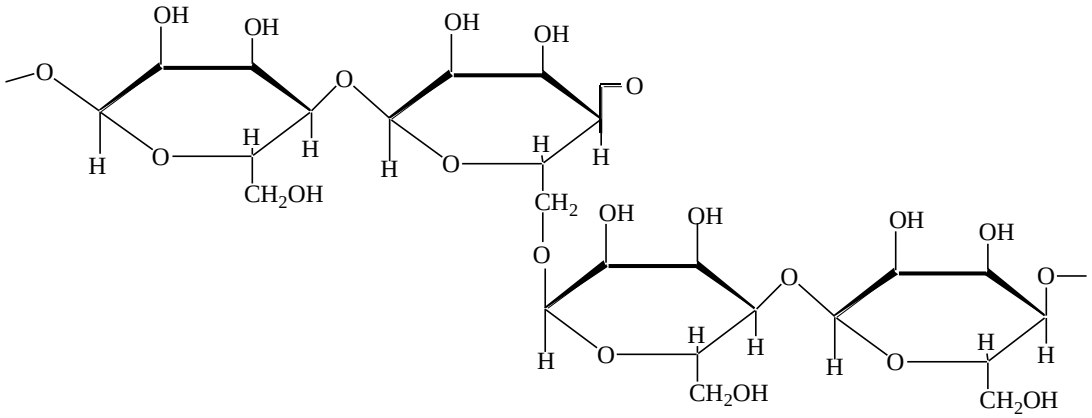

Figure 2-1. Molecular structure of amylopectin

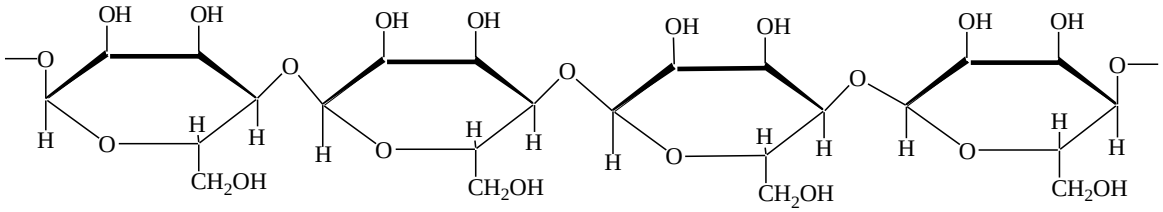

Figure 2-2. Molecular structure of amylose

Raw starch is mainly stored in root tubers, cereal grains and fruits (Chang *et al.*, 2010). Plants that contain high starch content include potatoes, corn, wheat, cassava and rice grains. Raw starch also contains wax, amino acids, and minerals with phosphorus (P), magnesium (Mg), and calcium(Ca) as main elemental composition (Tester *et al.*, 2014). Elements present in starch are mainly supplied from fertilizers used during crop production.

Raw starch has a high number of free hydroxyl groups. The hydroxyl groups form hydrogen bonding with water. When used in the formulation of composite materials, free hydroxyl groups result in high water absorption (WA), thus treatment of starch to reduce the free hydroxyl groups is done using various structural modifications using chemical, physical, enzymatic (Chen *et al.*, 2009; Murphy, 2000) and genetic methods (Neelam *et al.*, 2012).

Chemical modification of starch is done through oxidation, cationization and esterification where new functional group is introduced to starch structure (Haroon *et al.*, 2016) and new functional groups introduced are mainly carboxyl, acetyl,

hydroxypropyl, amine and amide which give specific properties. Oxidation to carboxylic group thus increases carboxyl content (Patel *et al*., 1974). Cationization of starch is involved during the introduction of an amino group to the starch chain (Xie *et al*., 2016; Siau *et al*., 2004). Esterification leads to the replacement of –OH in –C-OH with an alkanoyl group (Qiao *et al*., 2016).

Chemical treatment affects the crystallinity nature of starch molecules. Crystallinity is attributed to the presence of inter-molecule and intra-molecule hydrogen bonding as shown in Figure 2-3 (Huang *et al.*, 2017).

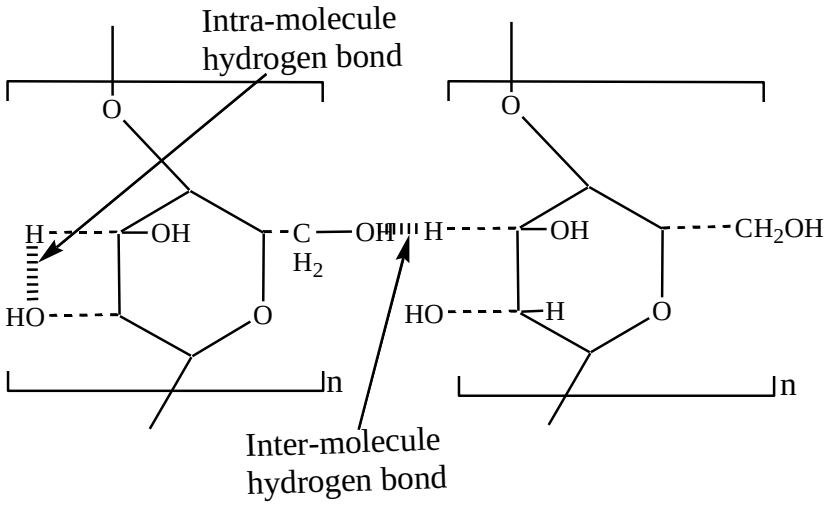

Figure 2-3. Crystalline nature of starch

Crystalline starch contains a fewer number of free hydroxyl groups used to combine with the lignocellulose materials. Crystallinity is broken by weakening hydrogen bonding in the starch, a process known as gelatinization. Gelatinization increases the number of free hydroxyl groups that act as reactive sites in the starch (Meimoun *et al.*, 2017; Le Corre and Dufresne, 2013; Lu *et al.*, 2004).

Hydrogen bonding between starch molecules is achieved by substitution of hydrogen in the hydroxyl group with a cation, a process known as cationization. Scheme 2-1 shows the cationization of starch molecules using an alkali such as sodium hydroxide. Cationization reduces starch granule size and starch fragmentation (Liu *et al.*, 2016; Siau *et al.*, 2013).

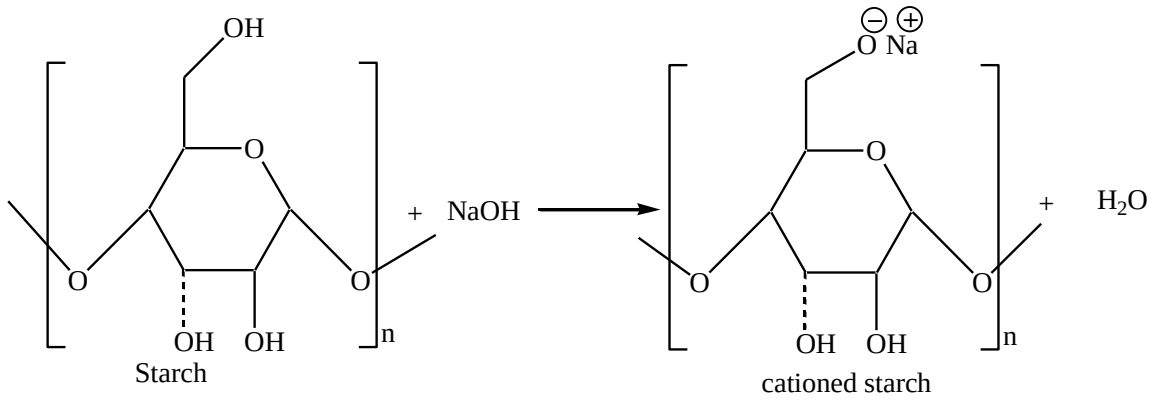

Scheme 2-1. Alkalization of starch using sodium hydroxide

Chemical modifications of starch also involve grafting (Gayathri *et al.*, 2013; Polnaya *et al.*, 2013). Grafting of starch with long polyurethane is possible through grafting polymerization (Barikani and Mohammadi, 2007). Hydroxyl groups from starch react with isocyanates (NCO) from polyurethane to form an ester bond as shown in Scheme 2-2. The resultant polymer contains fewer hydroxyl groups. Reduced numbers of the hydroxyl group in starch increases water resistance making it more hydrophobic (Zia *et al.*, 2015).

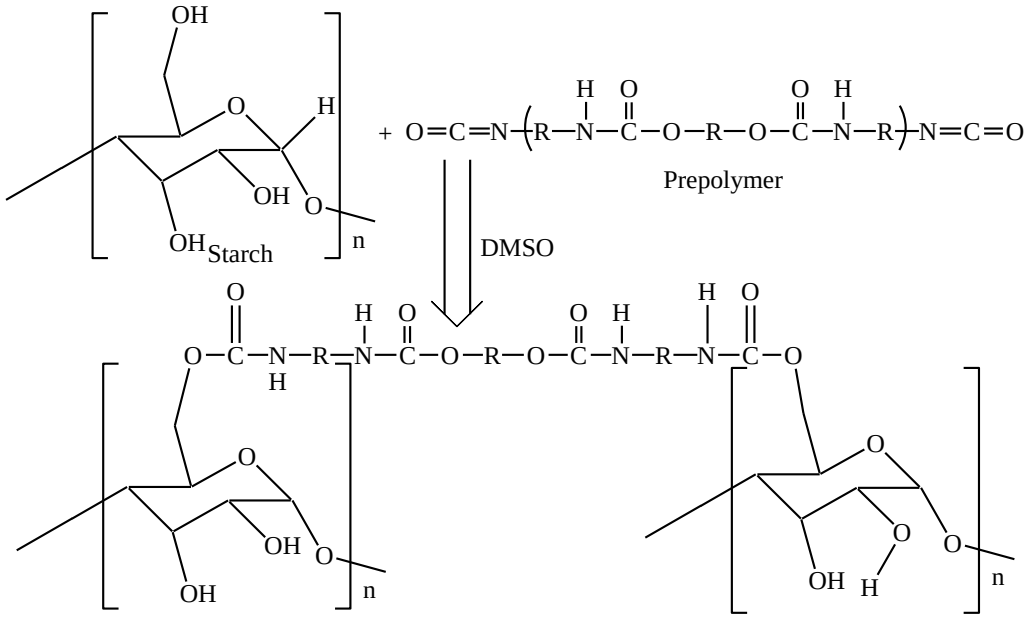

Scheme 2-2. Grafting of starch and polyurethane

Cross-linking involves a combination of starch molecules with other molecules that consist of two or more hydroxyl groups, known as polyols, such as hydrolyzed

borax. Hydrolyzed borax reacts with starch (Narkchamnan and Sakdaronnarong, 2013) as shown in Scheme 2-3.

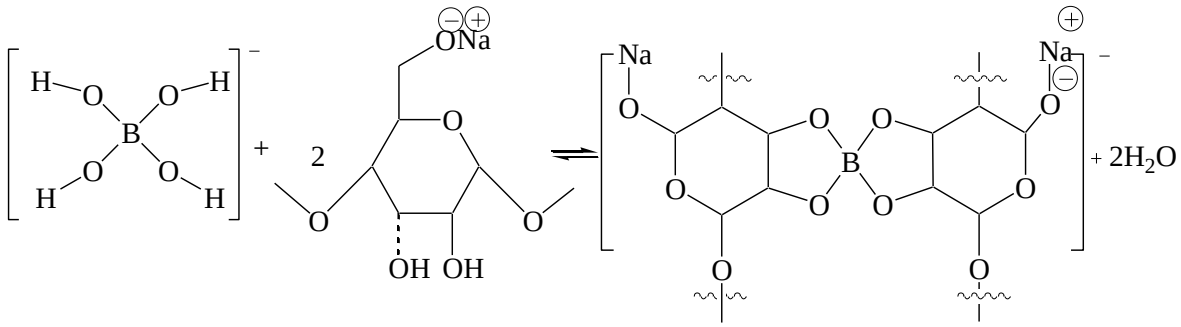

Scheme 2-3. Starch molecules crosslinked with borax

Starch is oxidized by the use of oxidizing agents such as hydrogen peroxide, sodium hypochlorous among others. Hydrogen peroxide in alkaline media oxidizes starch through a mechanism shown in equations 2.1 to 2.7.

$$H_2O_{2(l)} + OH_{(aq)} \rightarrow HOO^-_{(aq)} + H_2O_{(l)} \quad 2.1$$

$$H_2O_{2(l)} + HOO^-_{(aq)} \rightarrow {}^{\cdot}OH_{(aq)} + H_2O_{(l)} + {}^{\cdot}O_{2(aq)} \quad 2.2$$

$${}^{\cdot}OH_{(aq)} + {}^{\cdot}O_{2(aq)} \rightarrow OH_{(aq)} + O_{2(aq)} \quad 2.3$$

$$H_2O_{2(l)} + {}^{\cdot}O_{2(aq)} \rightarrow {}^{\cdot}OH_{(aq)} + OH_{(aq)} + O_{2(g)} \quad 2.4$$

$$3H_2O_{2(l)} \rightarrow 2{}^{\cdot}OH_{(aq)} + 2H_2O_{(l)} + O_{2(aq)} \quad 2.5$$

$$RCH_2OH_{(l)} + {}^{\cdot}OH_{(aq)} \rightarrow R{}^{\cdot}CHOH_{(l)} + H_2O_{(l)} \quad 2.6$$

$$R{}^{\cdot}CHOH_{(l)} + H_2O_{2(l)} \rightarrow RCHO_{(aq)} + {}^{\cdot}OH_{(aq)} + H_2O_{(l)} \quad 2.7$$

Oxidation reduces swelling capacity and viscosity of starch (Gambus *et al.*, 2014; Patel *et al.*, 2013). The process introduces carboxyl and carbonyl groups into the starch molecules (Haroon *et al.*, 2016). Carboxyl groups undergo a condensation reactions with hydroxyl groups to form covalent bonds through esterification (Gu *et al.*, 2016). This reduces the hydroxyl groups that hold the molecules together in starch crystals thus depolymerizing the starch molecules. Oxidation of starch converts the primary C-OH into aldehydes and carboxylic groups (Carey, 2003) while secondary C -OH groups are converted to ketones. Oxidation results in the cleavage of the glycocidic starch molecules (Lewicka *et al.*, 2015) and reduces the

number of hydroxyl groups hence improved water solubility, lower viscosity and retrogradation of starch.

Starch hydroxyl groups are used during substitution reactions modifications especially acetylation (Lewicka *et al.*, 2015). The process of acetylation involves the replacement of the hydroxyl groups from starch with acetyl groups from chemicals such as ethanoic acid, acetic anhydride. The resultant acetyl groups in starch reduce the number of free hydroxyl groups that form hydrogen bonding between starch molecules thus increasing the starch stability (Colussi *et al.*, 2015). Acetylation leads to a reduction in the gelatinization heat due to the weakening of hydrogen bonding. Acetylation using ethanoic acid (Kapelko-Zeberska *et al*., 2015) is represented in the scheme 2-4.

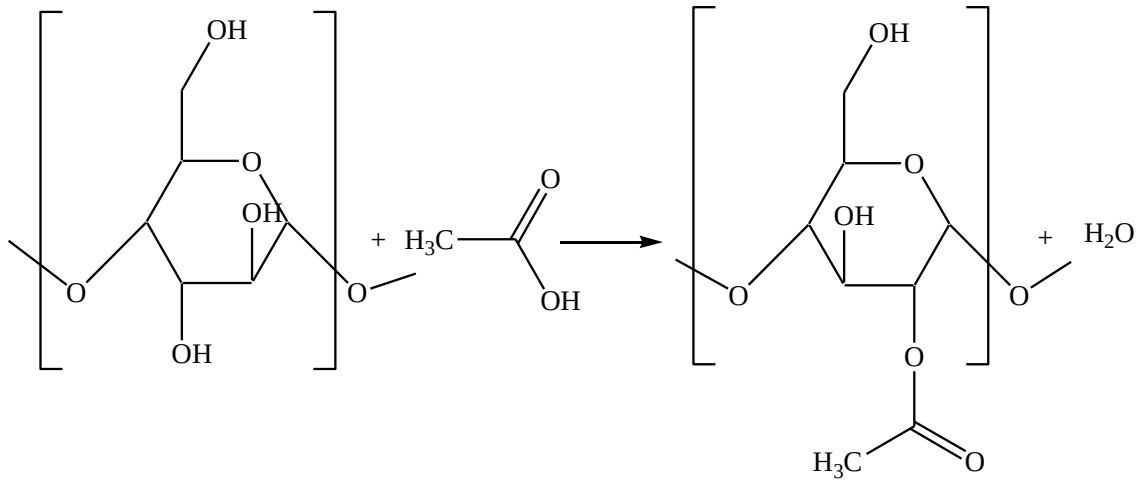

Scheme 2-4. Acetylation of starch using ethanoic acid

Carboxylmethylation is another chemical modification process used for starch. The primary hydroxyl group in starch is replaced with a carboxymethyl group from monochloroacetic acid. The reaction between starch and monochloroacetic acid takes place in the presence of an alkali base such as sodium hydroxide to form carboxymethyl starch (Barrios *et al*., 2012). Carboxymethylation takes place in two major steps. Step one involves the reaction between starch with sodium hydroxide to form sodium alkoxide (Milotskyi *et al*., 2018) as shown in equation 2.8.

$$St - OH + NaOH \leftrightarrow St - O^{-}Na^{+} + H_2O \qquad 2.8$$

Sodium alkoxide reacts with the monochloroacetic acid to form carboxymethyl starch as shown in equation 2.9.

$$St - O^{-}Na^{+} + ClCH_2COO^{-}Na^{+} \rightarrow St - O - CH_2COO^{-}Na^{+} + NaCl \quad 2.9$$

Carboxylmethylation improves the physicochemical properties of starch, such as reducing its crystallinity. Reduced crystallinity makes resultant starch less prone to damage by heat and bacteria thus making it suitable for making adhesives (Alizadeh *et al.*, 2017).

Starch reacts with polymers such as polyvinyl acetate through grafting (Tout, 2000). Grafting involves the formation of radicals from starch and monomers such as vinyl acetate initiated by reducing agents (Xiao *et al*., 2011; Samaha *et al*., 2005). Radicals coalesce after water loss through the heating or hot press to form polyvinyl acetate (PVA). Radicals formed covalently bond to form a grafted supramolecule. PVA is thermoplastic thus softens on heating making it lose bonding strength especially at a temperature beyond 70 °C (Tout, 2000; Motohashi *et al.*, 1984). PVA improves moisture and temperature resistance of adhesives (Cho *et al.*, 1999). PVA adhesives are commonly applied in veneering, edge banding and jointing in furniture production (Tout, 2000). Grafted chains are terminated by disproportionation, coupling or chain transfer to give graft copolymer (Samaha *et al.*, 2005) as shown in equations 2.10 to 2.15.

$$St - OH + R^{\cdot} \rightarrow St - O^{\cdot} + RH \quad 2.10$$

$$R^{\cdot} + CH_2CHOCOCH_3 \rightarrow RCH_2\dot{C}HOCOCH_3 \quad 2.11$$

Propagation involves a combination of molecules with the radicals as shown in reaction equation 2.12 to 2.14.

$$St\dot{O} + CH_2CHOCOCH_3 \rightarrow RCH_2\dot{C}HOCOCH_3 \quad 2.12$$

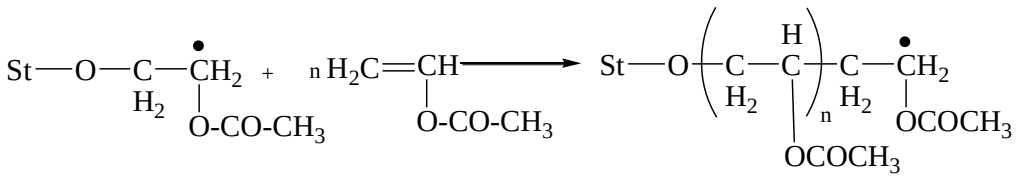

2.13

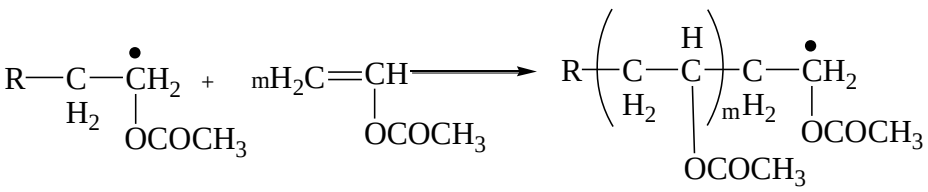

2.14

Termination involves a combination of radicals to produce a molecule during grafting as shown in equation 2.15 to 2.17.

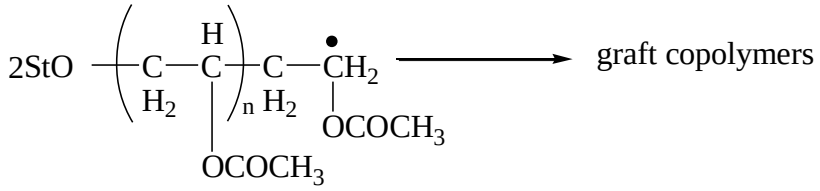

2.15

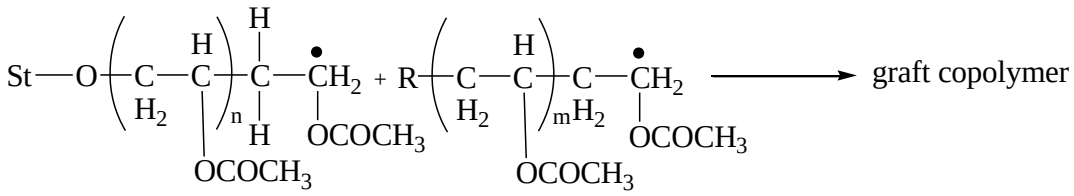

2.16

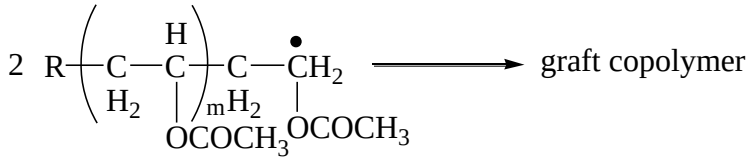

2.17

2.2.2 Formaldehyde-based adhesives

Formaldehyde-based adhesives are synthesized from petrochemical products. Petrochemical products such as phenol, urea and formaldehyde form the monomers used to synthesize the adhesive resins. The resins undergo condensation polymerization to form a network of interlinked supramolecules that encapsulate the lignocellulose materials during particleboard formulation (Biswas *et al*., 2011). The two main formaldehyde-based adhesives include phenol-formaldehyde and urea-formaldehyde. The structures of the two monomers used in making phenol-formaldehyde resins are shown in Figure 2-4.

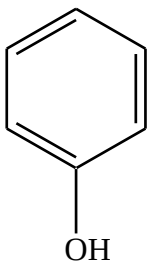

Phenol

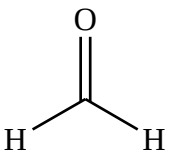

Formaldehyde

Figure 2-4. The structural formula of phenol and formaldehyde

Phenol-formaldehyde based adhesives are synthesized from phenol and formaldehyde through condensation polymerization to form a resin (Mitsunaga *et al.*,

2000) as shown in equation 2.18.

$$HOC_6H_{5(l)} + HCHOH_{(l)} \rightarrow HOC_6H_4CH_2OH_{(l)} \quad 2.18$$

Phenol formaldehyde molecules undergo further condensation reactions to form polyphenol formaldehyde (Grenier-Loustalot *et al.*, 1996) as shown in equation 2.19.

$$2HOC_6H_{5(l)} + HCHOH_{(l)} \rightarrow (HOC_6H_4CH_2)_2O_{(l)} + H_2O_{(l)} \quad 2.19$$

Other side reactions involve hydroxyl groups in phenol-formaldehyde and phenols (Bhattacharjee *et al.*, 2014) as illustrated in equation 2.20.

$$HOC_6H_4CH_2OH_{(l)} + HOC_6H_{5(l)} \rightarrow (HOC_6H_4)_2CH_{2(l)} + H_2O_{(l)} \quad 2.20$$

Urea-formaldehyde is another main adhesive synthesized from petrochemical products. The adhesive, which is conventionally used for non-wood materials, is synthesized by condensation polymerization of formalin with urea as shown in equation 2.21.

$$CO(NH_2)_{2(l)} + HCHO(l) \xrightarrow{pH=7\text{-}8} H_2NCONHCH_2OH_{(l)} \quad 2.21$$

Urea-formaldehyde undergoes condensation polymerization to form poly-(urea-formaldehyde) (Dunky, 1998) as illustrated in equation 2.22.

$$2H_2NCONHCH_2OH_{(l)} \rightarrow \text{-[-NHCONHCH}_2\text{O-]-}_{(l)} + H_2O_{(l)} \quad 2.22$$

2.2.3 Other binders

Other binders used in particleboard formulation include methylene diphenyl diisocyanate (MDI) and soy flour adhesive. MDI is synthesized from formaldehyde, a carcinogenic material whereas biobased adhesive results in low water resistance and thus require chemical modification with a chemical such as epichlorohydrin.

Biobased adhesives from starch and soybean are readily available. Their uses are hindered by low water absorption resistance and thus require chemical modification. The focus of the study, is to chemically modify the starch, obtained from cassava peels, through oxidation using hydrogen peroxide in an alkaline media.

2.3 Particleboard Component

Lignin is one of the main components of lignocellulose biomass. The wood matrix consist of 20 to 30 percent of lignin as an aromatic polymer (Watkins *et al.*, 2015). It is also an amorphous and highly branched phenolic polymer. Lignin is strong and

therefore provides support (Lu *et al.*, 2017) and protection of plants mainly from chemical attacks (Welker *et al.*, 2015; Miedes *et al.*, 2014). Lignin is used to replace phenol in the synthesis of phenol-formaldehyde resin. Phenol-formaldehyde is used as an adhesive in particleboard formulation (Cetin and Ozmen, 2002). Lignin use in adhesives is cheaper compared to phenols mainly due to its low thermomechanical pulping (Ago *et al.*, 2013). Lignin also has low polydispersity (Jablonskis *et al.*, 2016), high water resistance and low melting point and therefore suitable in the adhesive formulation (Wang *et al*., 2013b). Lignin is used during particleboard formulation to reduce water absorption and thickness swelling (Warui *et al*., 2019). Lignin, therefore, plays an important role in particleboard formulation.

Lignin mainly consists of three alcohols that have few free hydroxyl groups. These alcohols include coniferyl (G), synapyl (S), and *p*-coumaryl (H) as shown in figure 2-5 below (Cai *et al.*, 2015).

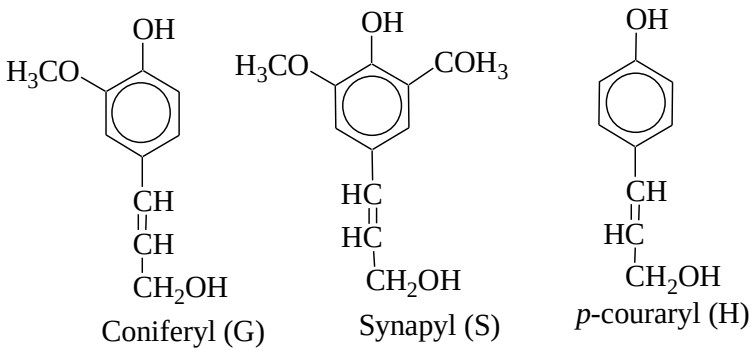

Figure 2-5. Three structural units of lignin

Alcohol reaction with aldehydes depends on several factors such as the source of lignin, the molecular mass and the predominant alcohol in the lignin. Lignin from softwood, for example, is more reactive than lignin from hardwood (Welker *et al.*, 2015). Lignin with a higher molecular weight decomposes faster on heating compared to those with low molecular mass (Ago *et al.*, 2013). Lignin from sugarcane bagasse has shown uniform thermal stability when used in adhesives (Yan *et al*., 2017b). Purification of lignin using suitable reagents may also enhance the reactivity of lignin. Sugarcane lignin purified with the cyclohexane-ethanol mixture, for example, was found to increase the reactivity of the lignin (Tana *et al.*, 2016). Lignin in formaldehyde-based resin improved the mechanical characteristics of particleboard due to its fiber nature (Tana *et al.*, 2016). Lignin treated with

multicopper oxidases has been found to enhance the binding with the starch matrix due to formation of carboxylic groups (Narkchamnan and Sakdaronnarong, 2013).

Lignin used as a crosslink between starch and urea reduces the biodegradability of starch-urea adhesive (Majeed *et al.*, 2018). Untreated lignin results in low compatibility with natural polymers like starch (Cavalcante *et al.*, 2017). Lignin treatment improves mechanical characteristics and increases water absoption (WA) resistance of starch (Kaewtatip and Thongmee, 2013). Composites made from thermoplastic starch and esterified lignin showed a reduction in water absortpion and increase in tensile strength (Kaewtatip and Thongmee, 2013). Treatment of lignin and lignin model compound generate more hydrophilic materials which are further modified to create a wide range of applications (Collinson and Thielemans, 2010).

Alkalization of lignin increases the reactivity of lignin with starch leading to oligomerization/condensation reactions (Liu *et al.*, 2017). Condensation reaction leads to increased lignin-starch interaction in the formation of a composite material (Ramachandra and Shekar, 2018) which is the basis for making particleboards. Lignin plasticizes starch thus reducing its solubility in water (Baumberger *et al.*, 1998), making it useful in the formulation of particleboards. Composite material formulated is moulded into particleboard by compression (Rahman and Netravali, 2018a) which is a process used in particleboard formulation.

Treatment of lignin using alkali weakens hydrogen bonding hence increase free –OH groups (Akhtar et al., 2016b). Free hydroxyl groups provide reactive sites of lignocellulose material thus increasing the mechanical interlocking. Sodium hydroxide removes wax and oils besides delignification. Breaking of lignin structure exposes cellulose and hemicellulose thus reducing the crystallinity of the lignocellulose material (Akhtar *et al.*, 2016b). Alkalization results in the replacement of hydrogen in the hydroxyl group with sodium to form alkoxides, as illustrated in equation 2.23 (Chand and Fahim, 2008).

$$\text{Fiber} - \text{O-H} + \text{NaOH} \rightarrow \text{Fiber-ONa} + H_2O \qquad 2.23$$

Sodium hydroxide exposes more free hydroxyl groups used in condensation reactions (Xu *et al.*, 2017). Besides, sodium hydroxide forms soluble lignin derivatives (Lim *et al.*, 2015) therefore increasing interlocking sites (Gomes *et al.*,

2016). More molecular bonding leads to higher modulus of elasticity (MOE), internal bond (IB) and modulus of rupture (MOR) (Jacob *et al.*, 2004).

Sodium hydroxide cleaves the β-O-*4* ether bond in lignin (Roberts *et al.*, 2011), as illustrated in Scheme 2-5.

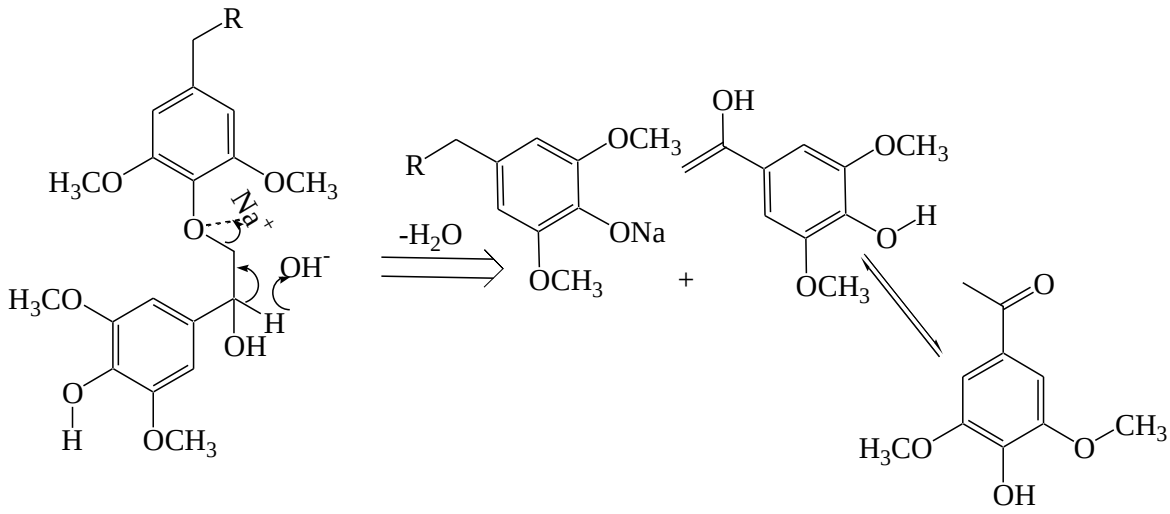

Scheme 2-5. Cleavage of lignin to form syringyl derivatives

Chemically modified lignin reacts with other functional groups other than formaldehyde resins. Hydrogen peroxide (H_2O_2) dissociate in sodium hydroxide (NaOH) to produce hydroperoxy group (HOO^-) (He *et al*., 2017; Hocking and Crow, 1994) as shown in equation 2.24

$$H_2O_{2(aq)} \leftrightarrow HOO^-_{(aq)} + H^+_{(aq)} \qquad 2.24$$

Hydroperoxy anion reacts with undissociated H_2O_2 to form hydroxyl radical ($^{\cdot}OH$) and superoxides (O_2^-) as shown in equation 2.25.

$$H_2O_{2(aq)} + HOO^-_{(aq)} \rightarrow {}^{\cdot}OH_{(aq)} + O^-_{2(aq)} + H_2O_{(l)} \qquad 2.25$$

Conyferyl alcohol is oxidized by H_2O_2/NaOH to carboxylic acids as shown in Figure 2-6.

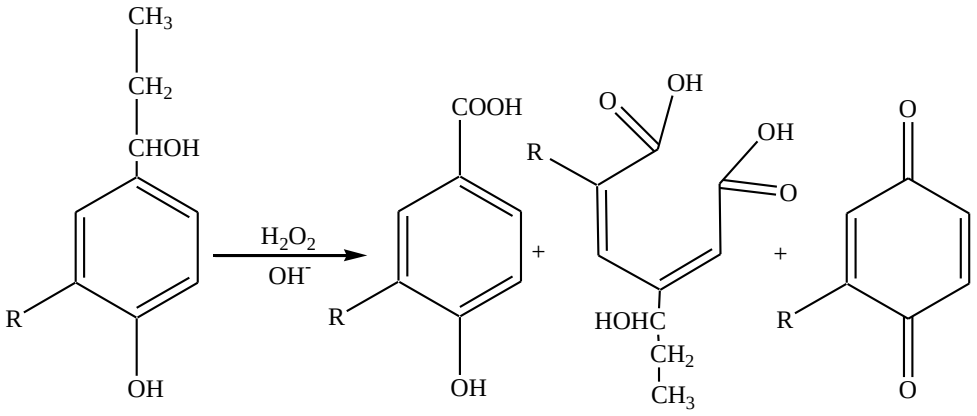

Figure 2-6. Perhydroxyl anion cleavage and oxidation of coniferyl alcohol in Lignocellulose Material

Hydrogen peroxide oxidizes synapyl alcohol in the presence of the alkaline solution (Gu *et al.*, 2012; Xiang and Lee, 2000) as shown in figure 2-7.

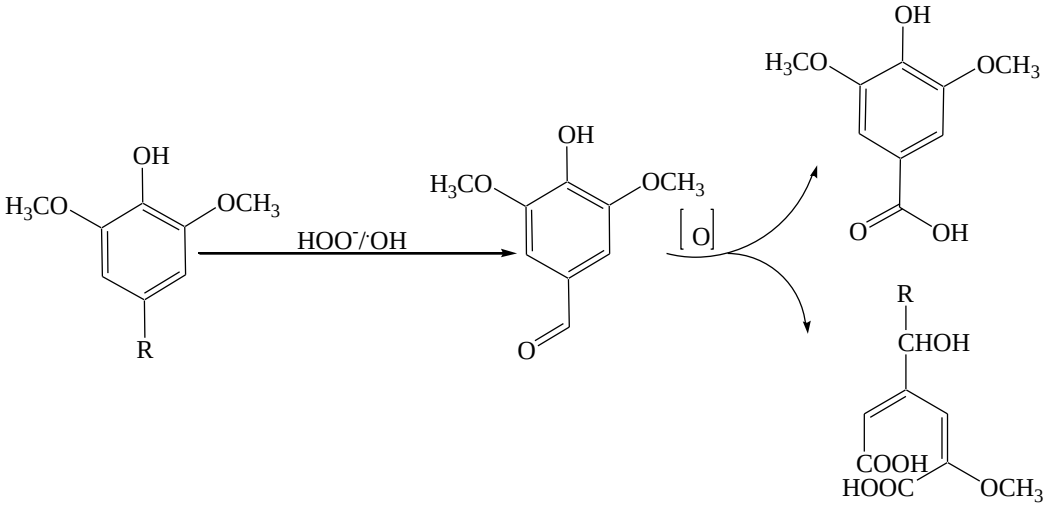

Figure 2-7. Reaction sequence of sinapyl alcohol under alkaline conditions

Perhydroxyl anion (HOO^-) is a strong nucleophile from hydrogen oxidation in an alkaline medium. HOO^- groups cleave ether bonds within the lignin structure. Lignin derivatives such as vanillin and syringaldehyde are rapidly degraded by hydrogen peroxide (Gu *et al.*, 2012; Xiang and Lee, 2000). Chemical modifications include lignin depolymerization that produces new reactive sites such as hydroxyl groups. These hydroxyl groups are chemically transformed so that lignin graft with other hydroxyl group-containing material to form copolymers (Figueiredo *et al.*, 2018).

Kraft lignin in thermoset polymers with polyurethane (Hatakeyama, 2012), phenol-formaldehyde (PF), and epoxy thermosetting resins are brittle (Kelley *et al.*, 2010).

Phenolic groups in lignin exhibit better characteristics than petrochemical phenol in PF resin. Up to 50 % of phenols in petrochemical products could be replaced with lignin without losing panel properties.

Raw lignin requires chemical modification to activate the functional groups. Chemical modification of lignin using sodium hydroxide enhances the reaction between the lignin and the starch. This leads to the formation of covalent bonds that hold the composite material together (Achyuthan *et al.*, 2010). The focus of this study was to improve the interaction between the lignin from lignocellulose material and modified cassava peel starch. Lignin forms more intermolecular associations in solution.

2.4 Cellulose

Cellulose is the major component of lignocellulose material. Cellulose constitutes between 30 to 50 percent of lignocellulose material and is mainly used in food, medical, paper and paper products, textile and pharmaceutical industries (Agarwal, 2019). Cellulose has a general formula $(C_6H_{10}O_5)_n$, where n, which is over 10,000, is the degree of polymerization. Although cellulose mainly occurs in wood, other cellulose-containing materials include crop residues, water plants, grasses among others.

Cellulose is a homopolymer of glucose linked by a β-1,4-glycoside link (Ruel *et al.*, 2012) as shown in figure 2-8.

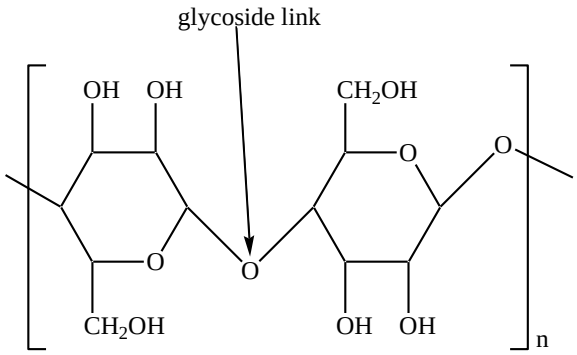

Figure 2-8. The structural formula for cellulose

Cellulose linear structure enhances the interaction between -OH through hydrogen bonding (Kanga *et al.*, 2016). The crystallinity of cellulose, therefore, is due to the

strong hydrogen bond between the glucose molecules. Cellulose in crystalline form exhibits little interaction with water. This is attributed to the smaller number of hydroxyl groups exposed that interact with water through hydrogen bonding. Depending on the number of free hydroxyl groups, cellulose ends up affecting the WA and mechanical properties of composite material.

Chemical treatment of cellulose with H_2O_2/NaOH converts hydroxyl groups in -C-OH into -COOH as shown in Scheme 2-6.

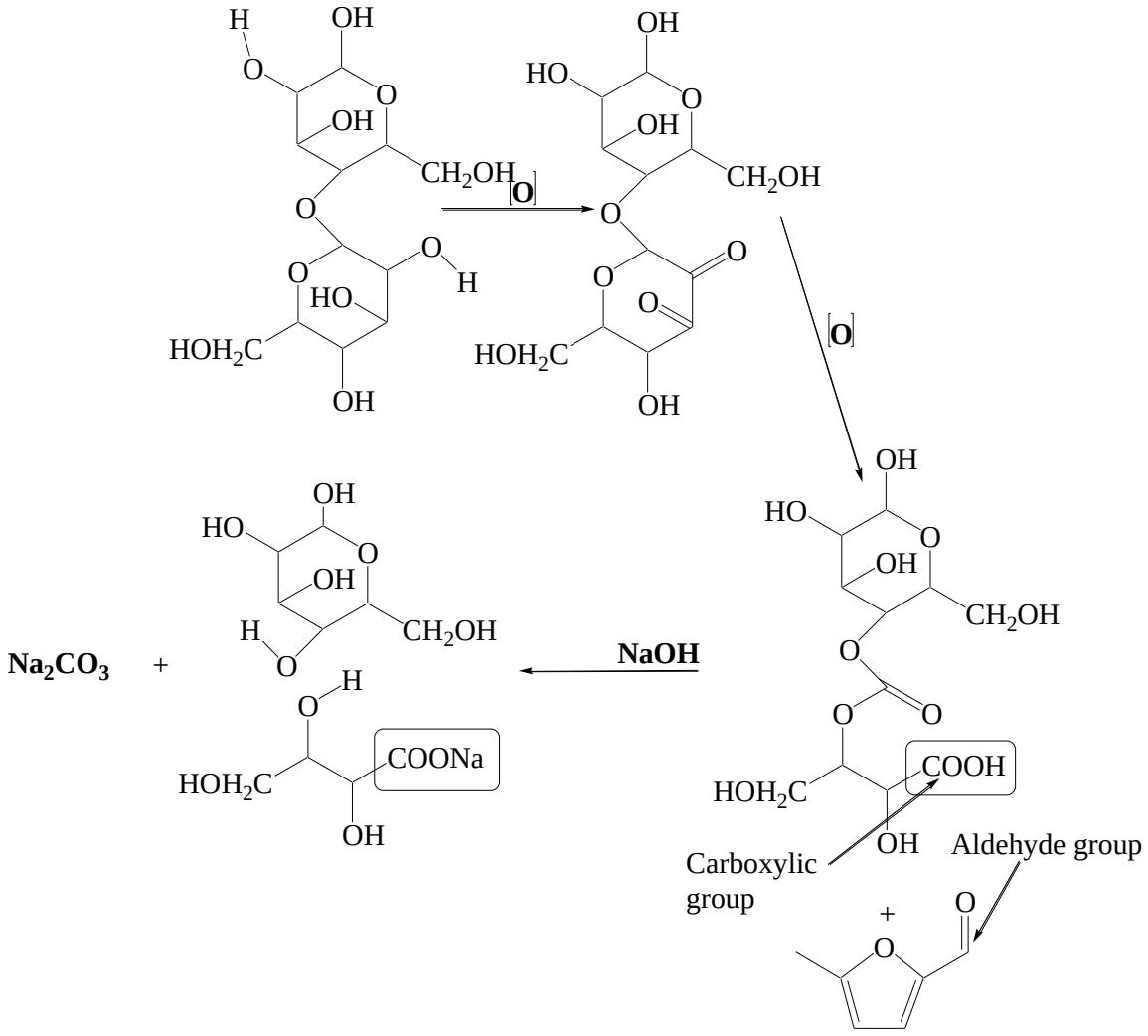

Scheme 2-6. Cellulose oxidation with alkaline hydrogen peroxide

Cellulose combine with hydrolyzed silica to form hybrid (Han *et al*., 2019). Another way through which organic-inorganic hybrids are prepared is the use of electrostatic interactions. An organic compound such as cellulose reacts with silica to form a composite material through silication (Root *et al.*, 2017; Kaushik *et al.*, 2015).

Cellulose undergos chemical modification to reduce the number of free –OH by substituting them with an inorganic material. Inorganic material such as silica improves the properties of polymer-silica hybrid formed such as hardness and thermal stability (Zhou *et al.*, 2019).

Cellulose-silica linkage can be achieved using the interaction between ions to form layer by layer (LBL) (Borges and Mano, 2014). This concept deals with the attraction between unlike charges on the surface of composite material. LBL results in overlaying of many layers in a composite material. Interaction between each layer depends on the interaction between the unlike charges. Inorganic compounds, such as silica, are adsorbed onto the surface using the interaction of unlike charges. Silica having negatively charged ion require a positively charged ion to be adsorbed. SiO_2-NaOH treatments thus lead to the formation of oppositely charged ions enhancing the interaction. This principle was used in this study.

Cellulose-silica blends can also be achieved through a sol-gel technique especially on a large scale (Chen *et al.*, 2019). Cellulose from fibers and silica combine through sol-gel during the synthesis of organic-inorganic hybrids. Hydrophobic silica-based material such as polysiloxane can be used in coating organic material through sol-gel. Covering of organic material using inorganic material require chemical treatments. Sulfite pulp is hydrolyzed with water when using compounds with silicon (Unger *et al.*, 2012). Sol-gel is used to reduce water absorption in organic composite materials. Hydrolysis of metal alkoxides undergoes a condensation reaction with inorganic compounds containing hydroxyl groups such as silicic acid. Treated silica undergoes condensation reaction after hydrolysis (Gao *et al.*, 2016). The two-phase process of hydrolysis and condensation is used to form a cellulose-silica composite (Guangbao, 2014) as shown in Scheme 2-7.

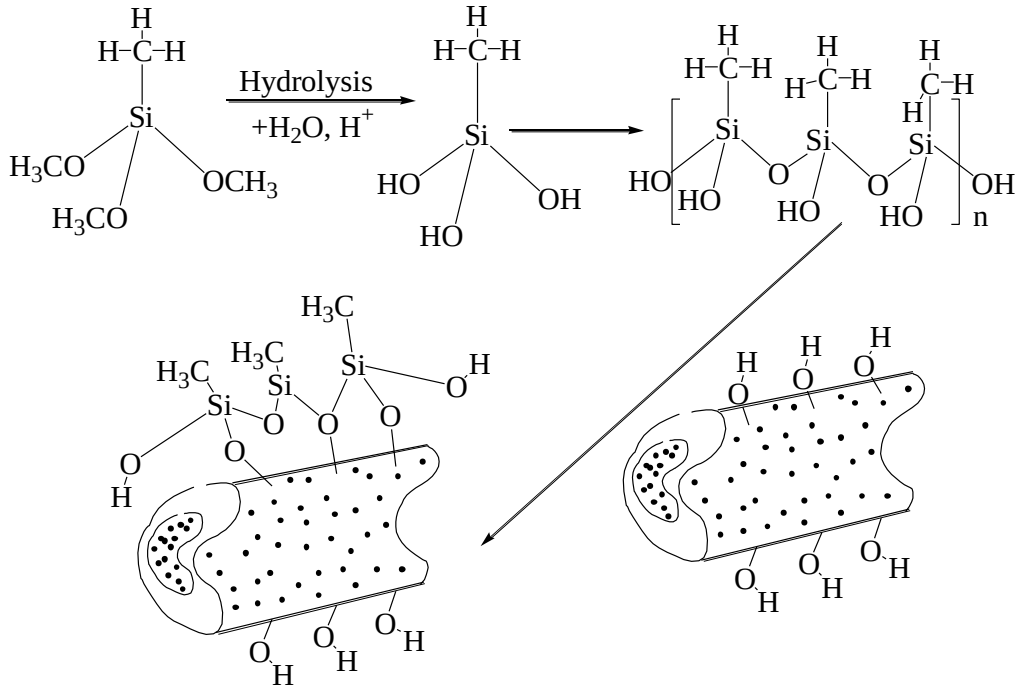

Scheme 2-7. Reaction process of production of cellulose-silica hybrid

Biomineralization is another process used in the synthesis of inorganic-organic hybrids and can happen naturally or artificially. Naturally, bacteria release metabolic products that react with metal ions to form a precipitate (Han *et al*., 2019). Natural biomineralization is greatly enhanced by the use of bacteria especially bacterial cellulose (BC) (Maeda *et al.*, 2006). The precipitate formed through biomineralization includes bones, egg shells and teeth in animals and rice husks that contain silica. Rice plant growth involves the biomineralization of cellulose with silica through a condensation reaction. Condensation reactions between organic and inorganic materials are the main process through which they are combined. Polymethylmethacrylate reacts with ferric oxides to form a hybrid (Sharif *et al.*, 2017). The introduction of a covalent bond between organic and inorganic materials increases MOE, MOR and IB of composite materials (Papageorgiou *et al.*, 2017).

Silica derivatives such as tetraethoxysilane (TEOS) and sodium silicate undergo hydrolysis. TEOS is hydrolyzed to form silanol solution in the presence of bacteria cellulose to form a hydro-gel whereas sodium silicate undergoes hydrolysis to form silicic acid (Annenkov *et al*., 2017). Silanol and silicic acid contain hydroxyl groups that react with hydroxyl groups from organic material through a condensation reaction. Silica is also hydrolyzed in the presence of bacterial cellulose to silanol

(Ashori *et al*., 2012). Rice husks contain silica that undergoes hydrolysis in sodium hydroxide to form silicic acid (Visser, 2018; Angelova *et al.*, 2015). Silicic acid contains hydroxyl groups that combine with hydroxyl groups from biomass. Covalent bonds formed result in improved mechanical properties such as MOR and MOE as the structure is strengthened.

Biomineralization leads to the production of two hybrids as shown in Scheme 2-8.

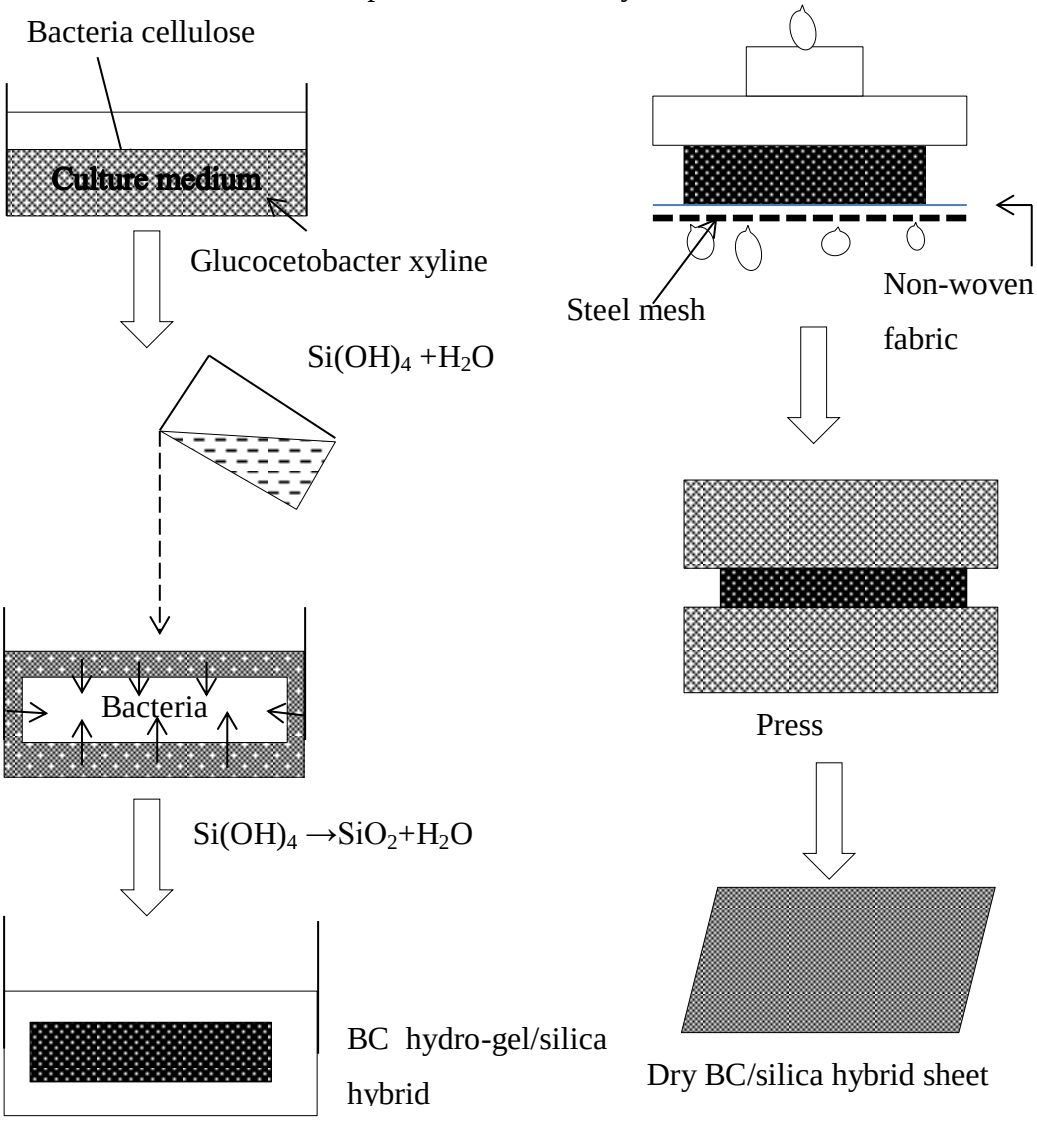

Scheme 2-8. BC hydro-gel/silica mixture and dry BC/silica mixture

Composite materials made from cellulose treated with silica are used as an alternative of fibers due to their improvements in their mechanical properties (Papageorgiou *et al.*, 2017). Cellulose-silica is a rigid composite material that is resistant to any structural deformation. Silica becomes part of the organic network through linkages between silica and cellulose in lignocellulose material. Silica can be

combined with cellulose through hydrolysis followed by condensation (Tadanaga *et al.*, 2013).

Cellulose in its natural form interacts less with other organic and inorganic materials. Treatment with an alkali such as sodium hydroxide reduces hydrogen bonding. Rice husks treatment with sodium hydroxide serves two main purposes. First, it increases the number of free hydroxyl groups and secondly, conversion of silica to sodium silicate. Silica-based derivatives are converted to silanol to increase their reactivity with organic materials.

2.5 Hemicellulose

Hemicellulose polysaccharides that represent 20 to 35 % of lignocellulose material. Hemicellulose is a mixture of low-branched sugar with C_6 and C_5 units (Mounguengui-Diallo *et al.*, 2019). These sugars include xylan ($C_5H_{10}O_6$), xylose ($C_5H_{10}O_5$), glucose ($C_6H_{12}O_6$), mannose ($C_6H_{12}O_6$), glucuronic acid ($C_6H_{12}O_7$) and 4-methyl glucuronic acid ($C_7H_{12}O_7$) (Gao *et al.*, 2020). Hemicelluloses act as a link between cellulose and starch that make the cell walls of plants (Waldron *et al.*, 2003). Hemicellulose glycoside linkages vary in terms of side chains, localization and distribution throughout its main macromolecular structure (Ebringerova *et al.*, 2005). Hemicellulose is mainly in form of xylans grouped into homoxylans that are mainly polysaccharides bonded via β-(1→3) and β-(1→4), glucuronoxylans that have single side chains, arabinoxylans, and heteroxylans.

Hemicellulose is chemically modified through crosslinking, acetylation, dehydration, oxidation, reduction, esterification and etherification of hydroxyl groups. Hemicellulose contains only one or two hydroxyl groups for esterification which makes it more challenging to modify compared to cellulose and starch that have three free hydroxyl groups (Fischer and Heinze, 2005; Ebringerova *et al*., 2005). Crosslinking involves the combination of hemicellulose with biopolymers such as starch and cellulose (Fang *et al*., 2000). Hemicellulose is treated through acetylation to replace free hydroxyl groups with acetyl groups (Fang *et al*., 2000). This reduces the number of free hydroxyl groups thus increasing its hydrophobic character (Ebringerova *et al.*, 2005). Heteroxylan structures are mainly found in bran, cereals and gum discharge (Ebringerova *et al.*, 2005).

Hemicellulose C_5 oligomers undergo hydrolysis to form xylose (Zhou and Zhang, 2016) as shown in Scheme 2-9.

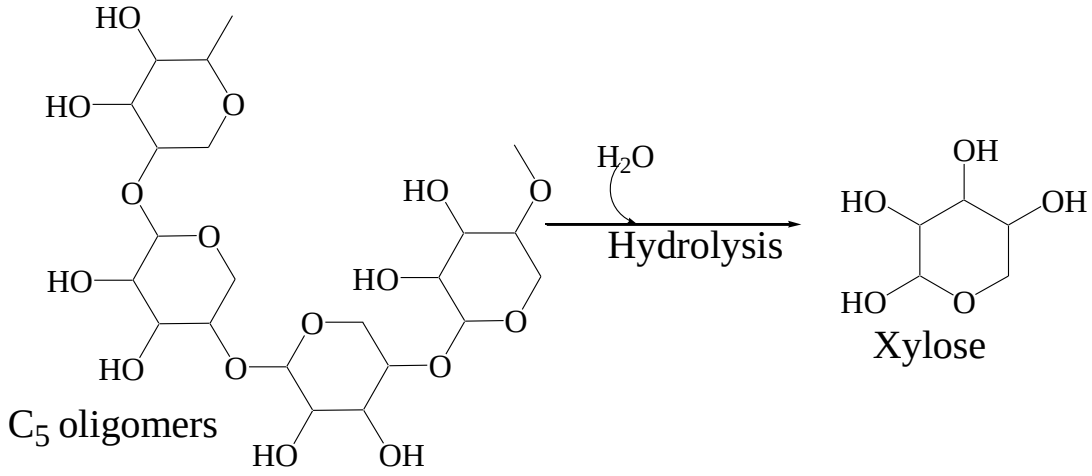

Scheme 2-9. Hydrolysis of hemicellulose to form xylose

Xylose undergoes dehydration to form furfural (Dulie *et al.*, 2020; Zhou and Zhang, 2016) as shown in Scheme 2-10. Furfural is a substitute for formaldehyde that is used as a cross-link during the formulation of particleboard.

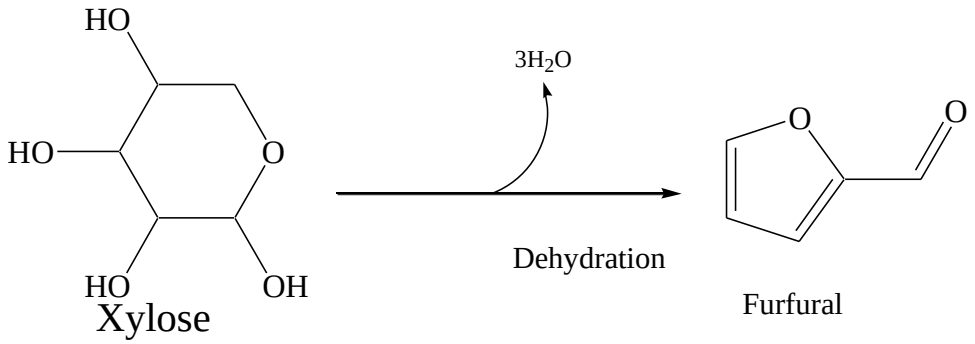

Scheme 2-10. Conversion of xylose molecules to furfural molecules

2.6 Starch Additive Using Borax

Borax is a compound whose molecular formula $Na_2B_4O_7.10H_2O$ contains Na^+ and $B_4O_5(OH)_4^{2-}$ (Zhang *et al.*, 2016). Borate additives are inter-chain linkages between polymers through hydroxyl groups of borate anion structure (Moussa *et al.*, 2013) as shown in Figure 2-9. Hydroxyl group in borax increase bonding that result to increase in resistance to the biodegradability of bio-based materials. Borax cross-linking is another way of polymer modification, especially for starch. Borax increases the molecular weight of molecules of interest and results in a more rigid material.

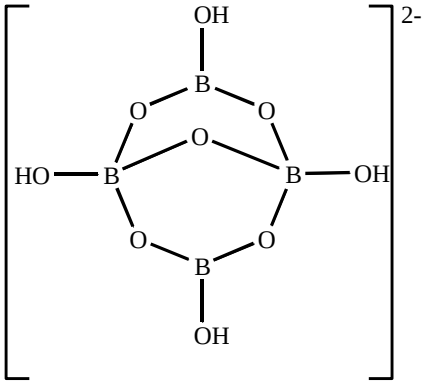

Figure 2-9. Arrangement of elements in a borate ion

Cross-links are formed when the hydroxyl groups in borate ions react with molecules containing more than one free hydroxyl groups called polyols such as starch (Zhang *et al.*, 2016). The condensation reaction between polyols and borate ion leads to the elimination of water molecules producing strong covalent bonds. Borate ions are formed through hydrolysis of borax in water (Wang *et al.*, 2013a) as shown in equations 2.26 to 2.28.

$$B_4O_{7\,(aq)}^{2-} + H_2O_{(l)} \rightarrow HB_4O_{7(aq)}^{-} + OH_{(aq)}^{-} \qquad 2.26$$

$$B_4O_{7\,(aq)}^{2-} + H_2O_{(l)} + 2H_{(aq)}^{+} \rightarrow 4B(OH)_{3(aq)} \qquad 2.27$$

$$B(OH)_{3\,(aq)} + H_2O_{(l)} \rightarrow H_{(aq)}^{+} + 4B(OH)_{4(aq)}^{-} \qquad 2.28$$

Boron in sodium borate exhibit two major structural geometry that is tetrahedral and trigonal planar that enables linkage with other polyols (Zhang *et al.*, 2016) as illustrated in Scheme 2-11.

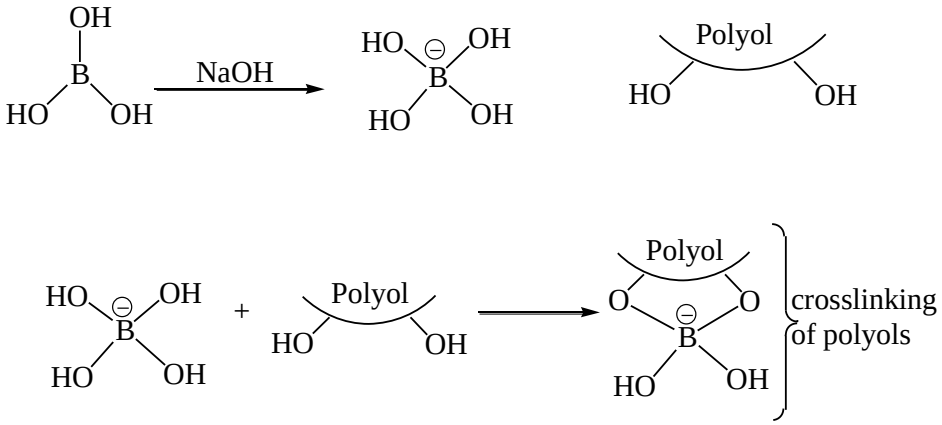

Scheme 2-11. Crosslinking borax to polyols

2.7 Particleboards Formulation

Particleboards are panels product manufactured from discrete lignocellulose particles bound with a synthetic binder under heat and pressure. Pressure forces the particles to come together before the resin cures. This could leave space between resin and lignocellulose material particles that may expose the inherent hydroxyl group. Hydroxyl functional groups interact with polar solvents such as water thus increasing the WA and TS (Adhikary *et al.*, 2008). Commonly used lignocellulose material is wood from trees and synthetic binders are mainly formaldehyde-based resins.

Conventional method in making particleboard involves encapsulation of lignocellulose material using formaldehyde-based resins. Phenol-formaldehyde resins is formulated by reacting phenols and formaldehyde as shown in equation 2.29.

$$HOC_6H_{5(l)} + HCHOH_{(l)} \rightarrow HOC_6H_4CH_2OH_{(l)} \qquad 2.29$$

The synthesized phenol-formaldehyde undergoes condensation polymerization with phenols to form polyphenol-formaldehyde as shown in equation 2.30

$$HOC_6H_5CH_2OH + HOC_6H_5 \rightarrow (HOC_6H_4)_2CH_2 + H_2O \qquad 2.30$$

Under high pressure applied on the lignocellulose particles and heat, polyphenol-formaldehyde undergoes curing process thus holding the particles together (Mamza *et al.*, 2014) as illustrated in Scheme 2-12. Polyphenol-formaldehyde encapsulates lignocellulose particles.

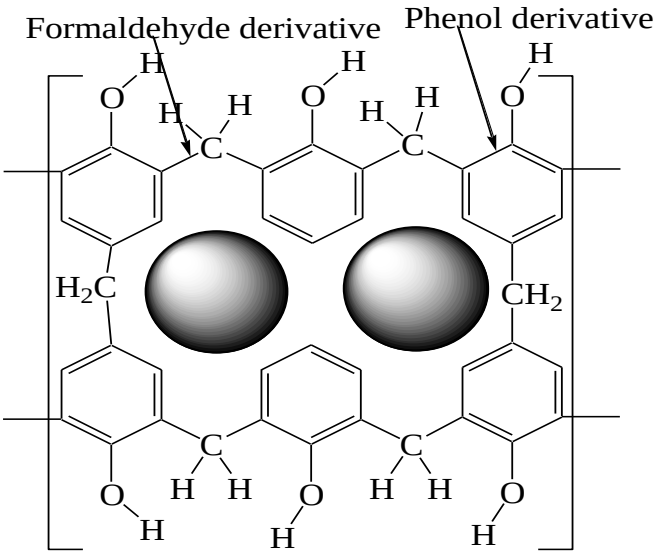

Scheme 2-12. Encapsulation of wood particles using cured phenol-formaldehyde resin

Urea-formaldehyde undergoes a similar process to that of phenol-formaldehyde. Urea-formaldehyde resin is sprayed on lignocellulose particles and, with pressure and heat, it encapsulates the lignocellulose material (Gürü *et al.*, 2006) as shown in the Scheme 2-13.

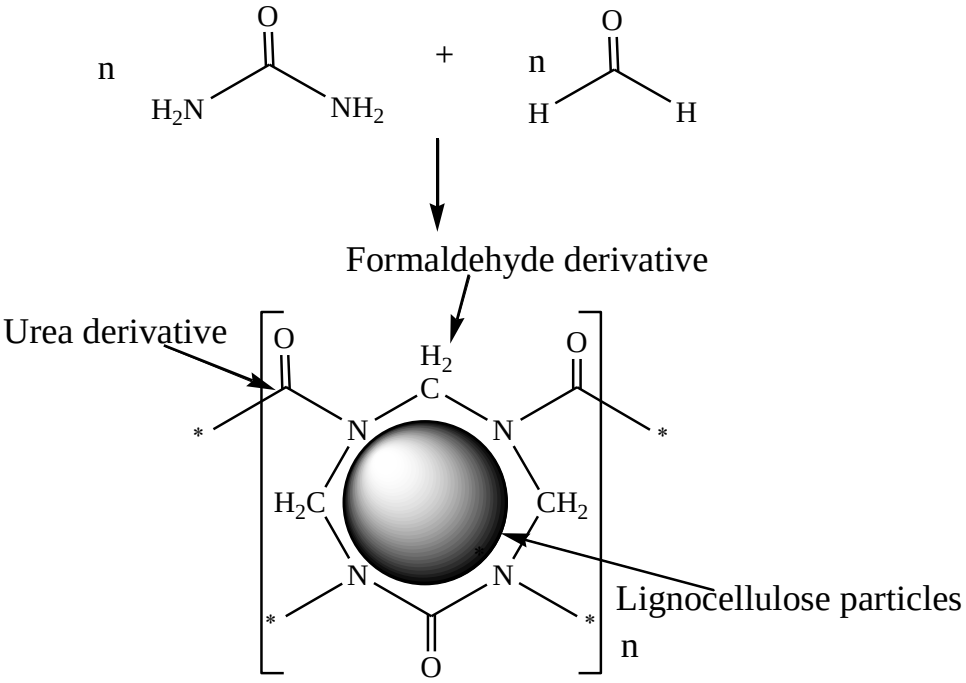

Scheme 2-13. Encapsulation of lignocellulose particles with poly(Urea Formaldehyde)

Post-industrial wood particle waste is feedstock for making composite materials for particleboards (Diyamandoglu and Fortuna, 2015; Vefago and Avellaneda, 2013). Sawdust is a conventional lignocellulose material for making particleboards with formaldehyde-based resin binders. Rahman, *et al.*, (2013) used sawdust as a lignocellulose material and polyethylene terephthalate as a binder. Polyethylene terephthalate is non-biodegradable. Binders such as polyethylene terephthalate are mixed with coupling agents such as formaldehyde and polymethylene polyphenol isocyanate. These coupling agents increase their interaction with wood waste by introducing a mixture of reactive functional groups (Rahman and Netravali, 2018a; Lu *et al*., 2005). Coupling agents introduce alternative functional groups that enhance interaction between binders and chemically treated lignocellulose materials which increase their compatibility with the adhesive (Ndazi *et al.*, 2006).

Bioplastics are formed between starch and lignin molecules. Starch –lignin matrix showed low enthalpy of combustion (Majeed *et al.*, 2016). Fibers containing cellulose and lignin undergo chemical treatment to enhance their interaction with biobased binders such as starch (Narkchamnan and Sakdaronnarong, 2013). Hydroxyl groups in lignin are activated by the use of a base such as NaOH (Erdocia *et al.*, 2014). Hydroxyl groups in activated lignin avail linkage point thus increase sites for condensation reactions to form copolymers (Lepifre *et al.*, 2004). Copolymers are joined through covalent bonds, a strong bond used in the formulation of fiber-reinforced composite material (Shekar and Ramachandra, 2018). Lignin in lignocellulose material improved the physicochemical properties of starch in particleboard formulation (Baumberger *et al.*, 2010).

Starch has been blended with lignin in forming a starch-lignin copolymer (Vengal and Manu, 2016). Lignin has several hydroxyl groups that can be used for polymerization reactions. They include phenolic hydroxyl groups, aliphatic hydroxyl groups and unsubstituted 3- or 5- positions on phenolic C_9 units (Cai *et al.*, 2015). Phenolic hydroxyl groups react through an oxidative coupling initiated by the removal of a hydrogen ion from the phenolic hydroxyl group. Oxidative degradation of phenolic structures of lignin converts them to carboxylic acid groups that react with the hydroxyl group from starch to form esters (EraghiKazzaz *et al*., 2019). Lignin with high aliphatic hydroxyl groups can easily undergo an esterification reaction with carboxylic acid groups (Gao and Fatehi, 2019). Lignocellulose materials interact with chemically modified starch to form composite material moulded to particleboards. Composite material formulation through condensation reactions from various sites of lignin from lignocellulose materials is as shown in scheme 2-14.

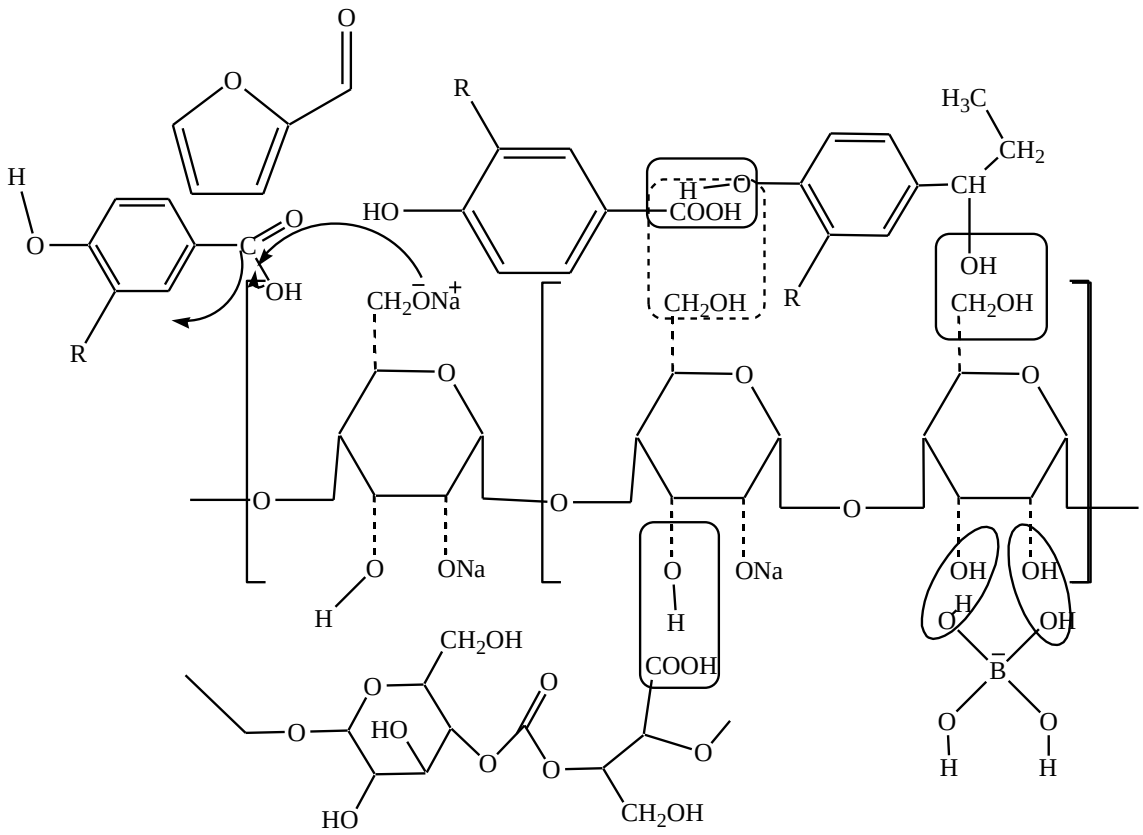

Scheme 2-14. Interaction sites between lignocellulose material and starch

Crop residues can be used as an alternative to wood as a source of lignocellulose material (Ferreira *et al.*, 2015). Polymerizing natural polymers from crop residues with starch produces composite material for particleboards (Alessandra *et al.*, 2015). The polymerization of crop residues and starch depends on free hydroxyl groups in their molecules which depend on the chemicals used during the treatment step. Hydrolysis with sodium hydroxide produces few free hydroxyl groups which are crucial in a condensation reaction (Yamada *et al*., 2001). Particleboards made from untreated cassava root and cassava starch consist of few hydroxyl groups that lack sufficient linkage sites during the formulation of composite materials (Nurul *et al.*, 2016).

Lignin structure interacts with hemicellulose structure through covalent bondage. Lignin interacts with cellulose through hydrogen bonding (Choong *et al.*, 2016) as shown in Figure 2-10.

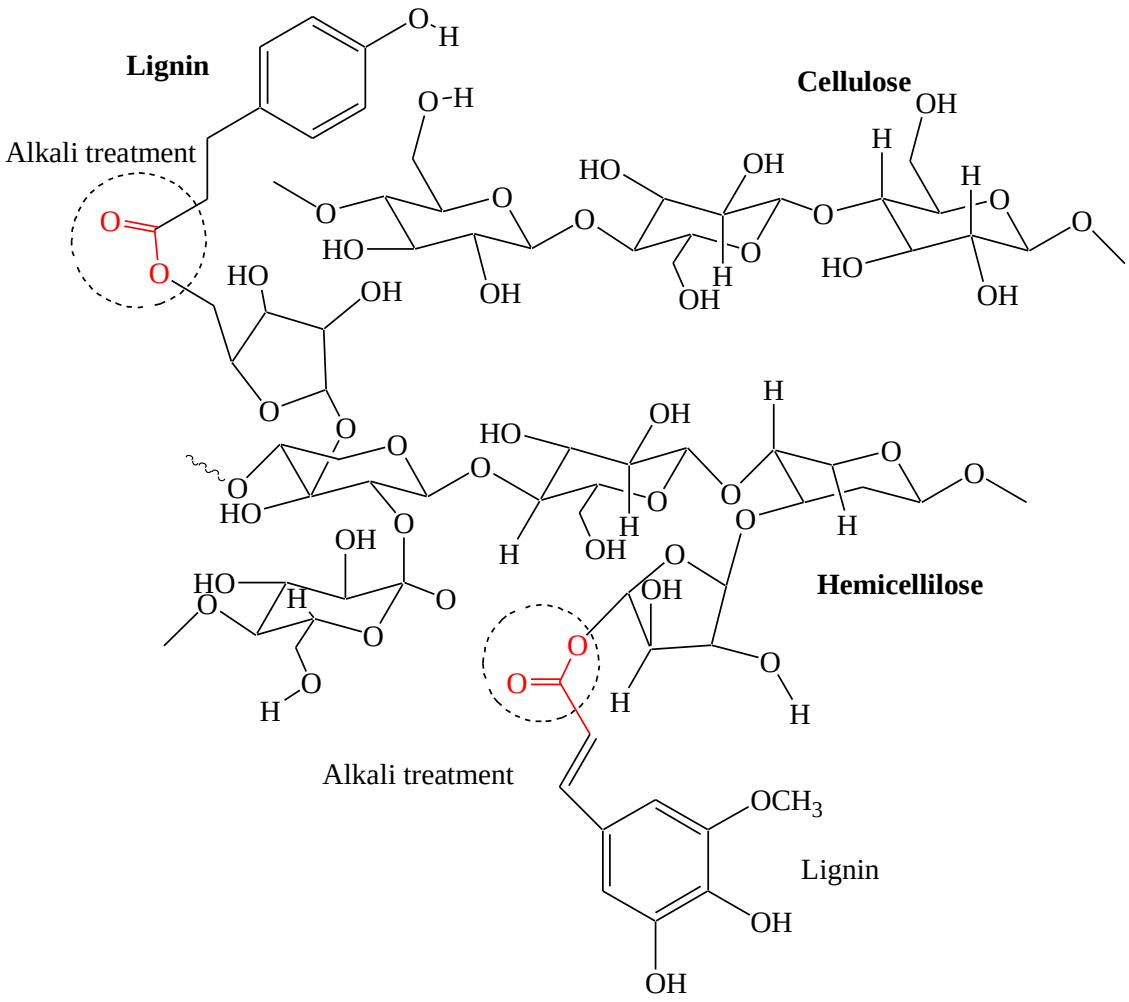

Figure 2-10. Lignin-hemicellulose covalent linkages

The above interactions result in four major linkage points between lignocellulose material and carbohydrates (Giummarella *et al*., 2016). The linkages include benzyl and ether bondage, benzyl and ester, phenyl and glycoside as well as acetal bonds. Phenolic and carboxyl groups react with quinone methide in hydrophobic conditions to form benzyl alcohols, ester and ethers (Sivasankarapillai and McDonald, 2011; Ghosh *et al*., 2000). Hydroxyl group reacts with a carboxylic group from glucuronic in xylan to form a benzyl ester. Phenolic hydroxyl groups in lignin undergo a condensation reaction with hydroxyl groups in polysaccharides to form phenyl glycoside. Acetal bond, on the other hand, is synthesized when two hydroxyl groups from polysaccharides react. Acetal groups undergo acid hydrolysis to form hydroxyl groups and carbonyl groups (Kapelko-Zeberska *et al*., 2015; Chotipratoom *et al*., 2014; Fang *et al*., 2000).

Crop residues such as corn cob and sawdust have been used in particleboard formulation bound with urea-formaldehyde (Akinyemi *et al*., 2016a), rice husk bound with silica (Battegazzore *et al.*, 2017), almond shell bound with urea-formaldehyde (Gürü *et al.*, 2006), sugarcane bagasse bound with urea-formaldehyde (Jonoobi *et al*., 2016b).

Biomass is a renewable material of growing interest in achieving global sustainability (Collinson and Thielemans, 2010). Biomass such as lignocellulose materials and starch are used to prepare biobased composite films (Wu *et al*., 2009b). Lignin in the lignocellulose matrix reacts with starch to form a biopolymer film of low enthalpy of combustion (Mansor *et al.*, 2016). This has increased resistance of composite material to microbial attack thus increasing the stability of composite materials (Mansor *et al.*, 2016). Biomass such as starch and cellulose improves mechanical, thermal conductivity, and hindrance of flexible thermoplastic (Ferreira *et al.*, 2015).

The discussion above show how components of lignocellulose combine with other polymers such as starch. Starch interacts with components of lignocellulose material through covalent bonds. This indicates that natural polymers can be combined without the use of synthetic resins such as formaldehyde-based resins that are carcinogenic. The study focuses on the use of inherent functional groups in biomass to form a composite material free from formaldehyde-based resins. Activated functional groups in biomass can undergo crosslinking, esterification and etherification among other reactions.

2.8 Characterization of Particleboard Adhesion

Adhesive tests are used for comparison of properties, quality checks for a "batch" of adhesives to determine the recommended standard. In addition, it checks on the effectiveness of surface, and determination of parameters useful in predicting performance of the particleboards (Landrock and Sina, 2015). Bond strength determines the quality of adhesives used in particleboards. Bond strength of a particleboard describes the overall adhesion and depends on the type of stress experienced by the bond and temperature.

2.9 Thermal Properties

Thermal conductivity in composites depends strongly on phase geometries, orientations and volume fractions of materials used in particleboard (Altendorf *et al.*, 2014). Simple two-phase composite structures are considered and are shown in Figure 2-11, (a) phase randomly dispersed and Figure 2-11 (b) lamella structure and the two phases having different conductivities.

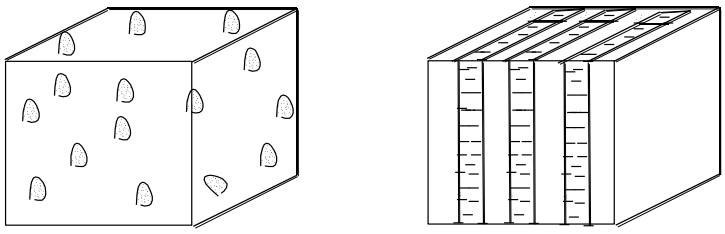

Figure 2-11. Phase arrangements in composite material

When one phase consists of dispersed particles, the composite has conductivity approximately equal to the volume-fraction-weight average. When the phases are in the form of parallel slabs, the magnitude of the conductivity in directions parallel and perpendicular to the slabs varies analogously to the flow of current in a resistive electrical circuit (Altendorf *et al.*, 2014). Parallel to the particleboard slabs, both phases contribute independently to the heat flow, similar to current flow through resistors in parallel, and the resultant thermal properties are always higher than that contributed by the phase with the larger conductivity (Altendorf *et al.*, 2014).

Perpendicular to the particleboards, heat must flow sequentially through each of the particleboard links. Heat flow is reduced by the lower-conductivity phase. This phenomenon is related to the current flowing through particleboard in series. In the latter case, the conductivity is lower than that contributed by the cooler phase alone (Altendorf *et al.*, 2014).

2.10 Methods Used for Adhesives Analysis and Thermal Properties

2.10.1 Atomic Absorption Spectroscopy (AAS)

AAS is used for the analysis of group two and higher group elements mainly from solubilized solution (Nerdy, 2018). The sample solution is nebulized into atoms that are directed into a flame where they absorb radiation of specific wavelengths. The amount of radiations absorbed is quantified and used for identification as different

atoms absorb at different wavelengths. The AAS depends on the efficiency of atomizer and monochromator. This technique requires standardization with analytical content which establishes an absorbance-concentration relationship that depends on Beer-Lambert's law (Mendham *et al.*, 2000) shown in equation 2.31.

$$A = \log_{10}(\frac{I_o}{I}) = \varepsilon.cL \qquad 2.31$$

Where A represents the absorbance, I_o represents radiation at a given wavelength, I represent radiations that are attenuated, L represents path length of the sample in cm, c represents the concentration of species in mol/dm^3) and ε represents the molar absorptivity in L/mol/cm.

AAS is used to determine the amount of metal in materials (Ghanemi *et al.*, 2011) and has been used to determine Pd and Rh in the characterization of nanoparticles of composite materials (Scaccia and Goszczynska, 2012).

2.10.2 X-Ray Diffraction (XRD) Spectroscopy

XRD is used for the elucidation of crystallinity. The X-rays waves are diffracted by particles in the crystal planes and a diffraction pattern is formed on the screen. Diffraction peaks are observed at different angles and intensities are as a result of the crystal lattice. Crystal lattices give rise to diffracted X-rays in the form of a wave with unique peaks at specific angles with different intensities as shown by Bragg equation 2.32.

$$n\lambda = 2d\sin\theta \qquad 2.32$$

Where λ represents the wavelength of x-rays, θ represents the angle in between the x-ray beam and atomic planes, n represents the order of the intensity. The inter-plane particle distance, d in Bragg's equation 2.32 can be calculated using the maximum intensity of constructive interference.

Bragg's equation is represented in figure 2-12.

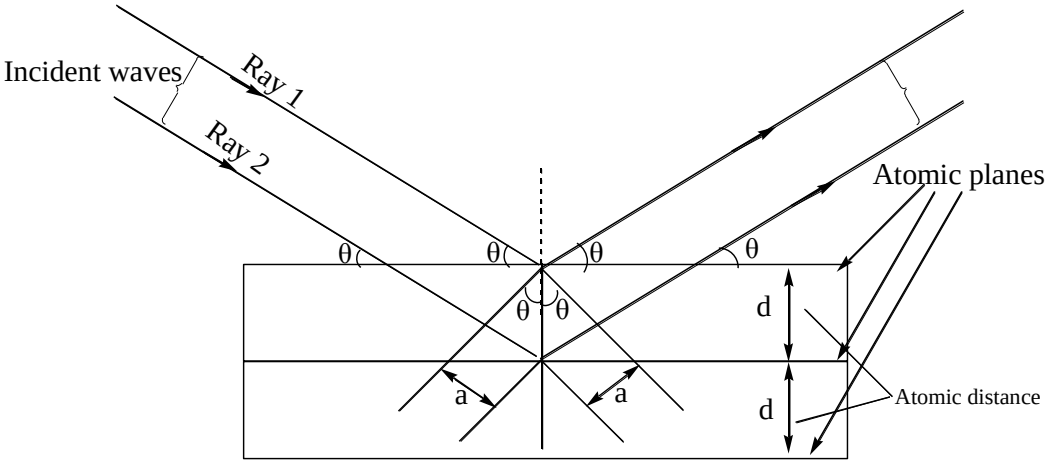

Figure 2-12. Bragg's law reflection

Diffraction pattern analysis provides information on atom arrangement in the material being in a plane. Arrangement of these atoms gives information on a unit cell in terms of shape and size whereas the position of atoms is determined by the use of relative peaks of the diffractograms (Myers, 2002). These techniques are used in the elucidation of the structure of materials as wavelengths in order of one angstrom (Å) which is equivalent to the magnitude of distance between atoms in test materials.

Electrons are propelled toward a certain metal by the use of a high voltage passed between electrodes. The high-density metal bombarded with these electrons emits rays with a certain wavelength characteristic of the specific target metal (Jones and Childers, 2003). Copper is used for standardizing that emits X-rays of 1.54 Å. Particles in the sample diffract the X-rays in all directions that form a pattern in the fingerprint of the sample. Various X-ray intensities are recorded at two angle theta (2θ). Distance between crystal planes in the matter is then calculated using Equation 2.32. A small diffraction angle shows a larger distance between atoms. Samples are identified using the handbook of mineral diffraction patterns (Poppe *et al.*, 2015).

XRD determines the mineralogical content of cellulose in sugarcane bagasse with different treatments (Umemura *et al.*, 2016). Cellular matrix exists in crystalline form in lignocellulose materials (Agarwal, 2019). XRD was used to show the effect of additives and water on lignocellulose materials (Zhao *et al.*, 2013). The introduction of additives into lignocellulose materials reduces the crystallinity nature of cellulose. This was observed in sugarcane bagasse treatment with citric acid where citric acid esterified with –OH in cellulose (Umemura *et al.*, 2016).

2.10.3 X-Ray Fluorescence (XRF)

XRF technique does not change the matrix of the tested materials during elemental identification and their concentrations in either solid or liquid state samples (Brouwer, 2010). Samples are bombarded with high energy photons from an X-ray tube more than the binding energy of the electron in the energy levels. Excited electrons move to a higher energy level from lower energy levels creating vacant spaces in energy levels which make atoms unstable. Stability is achieved when electrons from outer energy levels provide electrons that fill the energy levels in inner orbitals. The transition of electrons from outer energy levels to inner energy levels is accompanied by the emission of photons, a phenomenon called fluorescence. Emitted photons are energy waves that are lost by higher orbital electrons (Kalnicky and Singhvi, 2012).

Energy (E) emitted through fluorescence is determined by the difference between initial energy denoted as E_i and the final energy denoted as E_f for individual transition as shown in equation 2.33.

$$E = E_i - E_f = h\nu \qquad 2.33$$

This energy difference is related to the frequency (ν) of the photon by equation 2.34.

$$c = \lambda\nu \qquad 2.34$$

On substitution of equation 2.29 to that of equation 2.30, we obtain equation 2.35

$$E = \frac{hc}{\lambda} \qquad 2.35$$

Where h represents the Planck's constant, c for light velocity, and λ represents the photon wavelength.

Equation 2.35 shows that as wavelength increases energy produced decreases and this is unique for each element to be tested. The intensity of emitted photons varies directly to the element concentration in the sample, a basis of the XRF technique in the elemental analysis (Kalnicky and Singhvi, 2012).

2.10.4 Fourier Transform Infrared (FT-IR) Spectrophotometric Method

FT-IR provides information used in the elucidation of molecules in organic samples at the molecular level and characterization of proteins, lipids, nucleic acids, and carbohydrates. Calibration is done by collecting infra-red spectra of clay mixtures of known amounts of phosphatidylcholine (Polnaya *et al*., 2013).

Optical spectroscopy utilizes the interaction of electromagnetic radiation with matter. The medium infrared (MIR) spectral range covers the electromagnetic frequency regime from approx. 4000 - 400 cm^{-1}, which enables the excitation of vibrational or vibrational-rotational transitions of molecules involving transitions from/to rotational and/or vibrational levels in the same ground electronic state. MIR spectra are frequently characteristic of various functional groups within a molecule, particularly in the so-called "fingerprint" region (approx. 1200- 400 cm^{-1}), the vibrations of the related specific bonds show specific absorption patterns (Bec *et al.*, 2017). Consequently, MIR spectra determine the chemical nature and molecular structure of a constituent. MIR spectroscopy is used in qualitative and quantitative analysis of materials such as organic, inorganic, and biological substances.

Wavelength dependents on light reduction are calculated and defined as transmittance (Tinti *et al*., 2015) (T) as shown in equation 2.36:

$$T = \frac{I}{I_o} \qquad 2.36$$

Where I_o represents the incident radiation intensity, I represent radiation intensity after it passes through the sample.

Quantitative applications of IR spectroscopy is usually rearranged and expressed as absorbance (A) (Palencia, 2018), equation 2.37:

$$A = -\log(T) = -\log\left(\frac{I}{I_0}\right) \qquad 2.37$$

For quantitative measurements, absorbance may also be defined by the Lambert-Beer law (Parnis and Oldham, 2013), as illustrated in equation 2.38:

$$A = \varepsilon Cl \qquad 2.38$$

Where: ε represents absorptivity, C represents concentration; *l* represents sample thickness (the optical distance of light through the sample). Therefore, equation 2.38 shows a linear dependence of absorbance on the thickness of the sample, or more generally, the absorption path length.

Attenuated total reflection (ATR) is brought about by internal reflections of radiations by the matter. Radiations from optically denser medium with refractive index n_1 propagate to a lesser optically active media with refractive index n_1. The total reflectance in the media occurs at the interface where the angle of incident rays (θ) exceeds critical angle (θ_c) as shown in Figure 2-13.

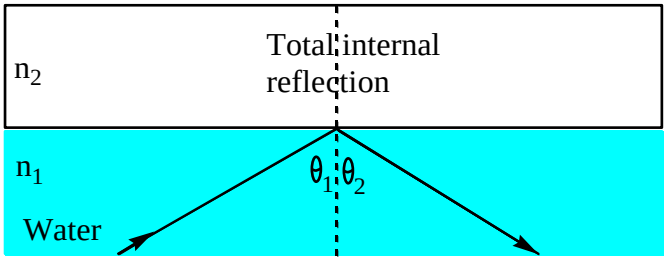

Figure 2-13. Total internal reflection in the interface of the two media

The θ_c representation of two media as a function of refractive indices is as shown in equation 2.39:

$$\theta_c = \sin^{-1}\left(\frac{n_2}{n_1}\right) \qquad 2.39$$

Evanescent fields extend into adjacent media that is rarer for each reflection. This resembles a standing electric wave that makes an angle of 90^o with the two media. Standing electric (E) amplitude decreases at an exponential rate to the distance as shown in equation 2.40.

$$E = E_0 e^{-\left(\frac{z}{d_p}\right)} \qquad 2.40$$

Where E_0 represents electric field amplitude, E represents the amplitude of standing electric field, z represents interface distance, and d_p represents the depth it penetrates (d_p).

The d_p which is an equivalent to $^1/_e$ of E_o is determined as shown in equation 2.41:

$$d_p = \frac{\lambda}{2\Pi\sqrt{n_1^2 \sin^2\theta - n_2^2}} \qquad 2.41$$

2.10.5 Nuclear Magnetic Resonance (NMR) Spectroscopy

Radiofrequency energy radiates a precessing nucleus. The system resonates and transition occurs from parallel to anti-parallel orientation. Absorption of energy occurs that is detected by a radiofrequency receiver (Baker and Kim, 2012). Resonance causes the transition which can be expressed by Equation 2.42.

$$\text{Energy} = h\nu = 2\mu H \qquad 2.42$$

Where h represents Planck's constant, υ represents radiofrequency, H represents static magnetic field strength whereas μ represents the magnetic moment of the nucleus.

Samples in solution were put in small tubes made of glass are placed between the poles of a magnet. The glass tube spins. The sample is irradiated with radiofrequency through the antenna coils from a radiofrequency source. The sample absorbs the radiofrequency (RF) energy; the absorbed RF energy is emitted through the receiver coil which surrounds the sample tube (Neudecker *et al*., 2009). Emitted RF energy is detected and recorded by electronic devices and computers. The resonance between the nucleus and the rotating magnetic field is achieved by varying the strength of the magnetic fields at constant radiofrequency and or sweeping (varying) radiofrequency while the extended magnetic field is constant. Different resonance signals give rise to a spectrum (Tan *et al*., 2007). Different resonance signals are observed for each of the different types of the proton. Different signals arise because different protons exist in different chemical environments. Electrons in the bonds between hydrogen and other atoms in the molecules such, as H-C, H-O, and H-N screen the neighboring hydrogen nucleus, altering the effective magnetic field at the nucleus (Capanema and Balakshin, 2015). Therefore protons are shielded to a different extent according to their chemical environment. Hence different protons resonate at different frequencies (Baker and Kim, 2012).

Chemical shift of protons is expressed in (delta). Generally, the chemical shift of resonance is expressed as shown in equation 2.43.

$$\delta = \frac{V_S - V_{TMS}}{\text{Operating frequency of spectrometer}} \times 10^6 \text{ppm} \qquad 2.43$$

Where υ_S represent the frequency of the signal and υ_{TMS} represents the frequency of the reference material assigned 0 ppm.

Chemical shifts of carbon – 13 are shown in Table 2-1

Table 2-1. Chemical shifts for various functional groups in carbon-13

Types of Carbon	Chemical Shift
RCH_3	10-15
R_2CH_2	16-25
CH_3CO-	20-50
R_3CH	25-35
RCH_2NH_2	30-65
RCH_2Cl	30-60
RCH_2O-	50-90
C=C (Alkenes)	115-140
C (in aromatic rings)	125-150
C=O (in acids and esters)	160-185
C=O (in aldehydes)	190-200
C=O (in ketones)	205-220
C-C	0-50
C-O	50-100
C=C	100-150
C=O	150-200

Among the isotopes of carbon, carbon-13 has magnetic properties, because it has an odd mass number and is capable of giving rise to a NMR signal (Wen *et al*., 2013). It has a spin quantum number I = ½ and is detectable by NMR. Carbon-13 makes up 1.1% of naturally occurring carbon (Balakshin and Capanema, 2015; Capanema and Balakshin, 2015; Neudecker *et al*., 2009). This natural abundance is high enough to make ^{13}C useful in the structure determination of molecules. Low natural abundance of ^{13}C, is about 6000 times more difficult to observe than proton resonance. Similar to ^{1}H NMR, ^{13}C shifts are measured in ppm downfield of TMS. Chemical shifts for ^{13}C range from 0-200 ppm relative to TMS, which is about 20 times the range for ^{1}H chemical shifts (Capanema *et al*., 2005). The structural environment of a carbon influences its chemical shift. The chemical shift of carbon is a function of its

hybridization, the polar and steric effects of the substituents as well as ring current (Zia *et al*., 2019).

^{1}H NMR provides information on peak areas, chemical shifts, and splitting of peaks due to the coupling of nuclei. ^{13}C NMR, does not provide information on peak area (integration) (Tan *et al*., 2007). However, chemical shifts and peak splittings are the two features of ^{13}C NMR spectra. ^{13}Carbon easily exhibits coupling with nearby protons, .i.e. protons directly attached to carbon resulting in split signal (Capanema and Balakshin, 2015; Stark *et al*., 2015). The resulting splitted signals are so complicated, signal to noise ratio is so low that ^{13}C NMR spectra are usually obtained under proton splitting condition, in which each non-equivalent carbon is seen a single peak (Zia *et al*., 2019). The line intensities do not reflect the relative number of carbon atoms. However, what is usually observed is that in carbons without hydrogen such as C=O carbons, the intensity of the line will be less than those having hydrogen (Choong *et al.*, 2016). For those carbons having hydrogen, the relative height of the peak estimates the relative number of carbon. Because an aromatic carbon atom which is attached to a substituent is not attached to hydrogen, such carbons appear with lower intensity than the other carbon atoms in that molecule, but they also appear with higher intensity than carbonyl carbons (Capanema and Balakshin, 2015; Stark *et al*., 2015; Sun *et al*., 2013).

NMR spectroscopy is used to elucidate structures for the grafted copolymer (Stark *et al.*, 2015). Copolymers were between cellulose and poly(β-hydroxybutyrate) /3-hydroxybutyrate-co-3-hydroxy valerate) composites were successfully determined by the use of NMR for quantification of phenolic hydroxyl groups in lignin (Capanema and Balakshin, 2015). Research findings have shown that three phenolic groups in lignin were identified by the use of NMR (Sun *et al*., 2013). This made it possible to determine the main functional groups formed when new phenolic groups were formed.

2.11 Adhesive Bonding Strength Analysis

Adhesion allows the transfer of mechanical stress from one material to the other through the bond formation. Polymers interact through physical as well as chemical ways by forming forces that put the materials together (Marhmood, 2005).

Interactions emanate from atomic attractions that form the functional groups. Adhesion creates a rigid solid after curing due to the formation of new compounds through a cohesive linkage such as cross-linking. Cohesive linkage establishes joints that bring materials together (Marhmood, 2005). Adhesion is measured through mechanical tests of the composite material formed (Mittal, 1995) which is dependent on the material under investigation.

Adhesion in particleboards is based upon thermosetting or thermoplastic polymeric matrices. Intrinsic adhesion involves the establishment of molecular contact between the substrate and adhesive. Inherent interactions mainly occur from interatomic as well as intermolecular attractions between an adhesive and material surfaces (Baldan, 2012). These intermolecular forces include hydrogen bonding whereas intra-molecules attractions are covalent and ionic bonding. Surface pretreatment of materials enhances the attraction between the materials.

2.12 Thermal Conductivity of Particleboards

Thermal conductivity reffers transfer of heat from one side of a particleboard to the another measured in watts per square surface. It measures the potential of a particleboard to be used as an insulator (Mati *et al*., 2015). It is affected by density, MC and ambient temperature where their increase corresponds to an increase in thermal conductivity and vice versa. It measures the basic properties of particleboards such as insulation. particleboards with large voids consist of more air trapped in the matrix results into low conductivity, a characteristic required in materials for internal applications.

Thermal conductivity is measured through two basic properties; steady and non-steady (Kerschbaumer *et al.,* 2019). The steady technique measures the thermal conductivity when there is complete equilibrium. The non-steady technique measures thermal conductivity during the heating process using a guarded hot plate instrument. This instrument measures the thermal conductivity of particleboards in a solid-state where the test material is placed between two plates. One side plate is heated and the other one is not heated at a specific lower temperature (Kerschbaumer *et al*., 2019). Transfer of temperatures across the material being tested is monitored until there is no more change is observed.

Cross-section of a guarded hot plate indicating the position of the test particleboard is shown in Figure 2-14.

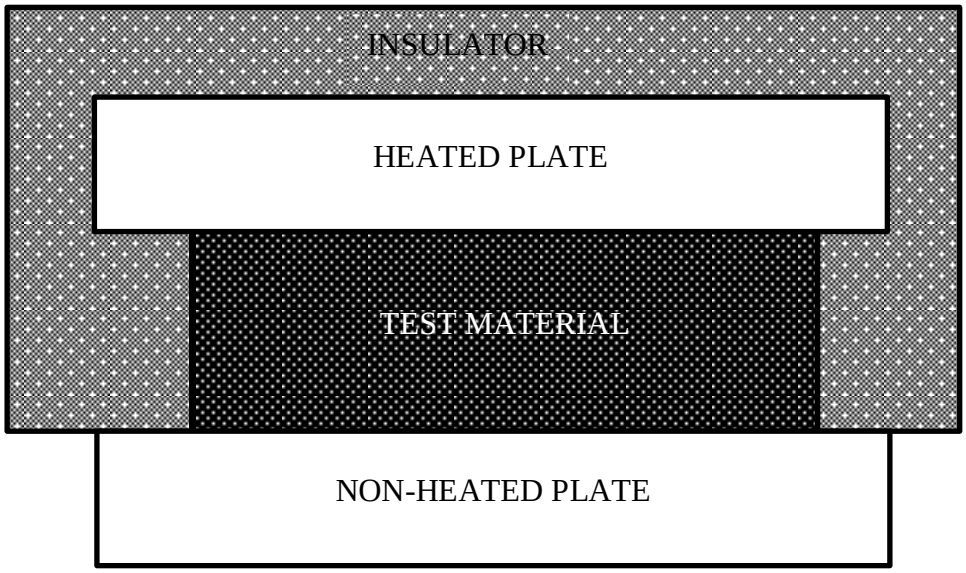

Figure 2-14. Scheme of guarded hot plate

Thermal conductivity, λ, for a steady-state is calculated (Kerschbaumer *et al*., 2019) using equation 2.44

$$\lambda = \frac{q \times d}{T_1 - T_2} \qquad 2.44$$

Where q represents the quantity of heat in W/m^2, d sample thickness in m, T_1 represents a higher temperature in kelvin, K, T_2 for a lower temperature in K.

Heat transferred across the particleboard is determined by equation 2.45.

$$q = \frac{Q}{A}\left[W/m^2\right] \qquad 2.45$$

Where Q represents heat passing through the particleboard sample in watts, A represents the surface area of test material in m^2.

2.13 Material Emissions

Material emissions are the results of several mass transport processes. Emissions are produced through processes such as diffussion (Zhang and Niu, 2003). Diffusion through a material as a result of a concentration, pressure, temperature, or density gradient and the surface emissions occurring between the material and the overlying air as a consequence of several mechanisms, such as evaporation, convection and

diffusion. Compounds in wet materials evaporate and the vapor pressures of the compound overly in the air depending on their concentrations. The mass transfer coefficient depends on the environment where they take place. Environmental factors include air temperature, relative humidity, surface air velocity, turbulence fluctuations, and surface characteristics (Zhang and Niu, 2003; Yang *et al.*, 2001).

2.13.1 Volatile Organic Compounds and Formaldehyde

Volatile Organic Compounds (VOC) include several hundred organic chemical gases from particleboard. In the particleboard, these are released by drying the wood particles and during hot-pressing at high temperatures. In the wood particles, VOCs can be attributed to wood extractives, including terpenes, and aldehydes; and in the resins, they can be mainly found in thinners and adhesives. The most commonly found VOCs in particleboard are formaldehyde, methanol, phenol and toluene (Santos *et al.*, 2007). VOC emissions have been linked to ozone destruction and photochemical smog.

2.13.2 Formaldehyde

Formaldehyde (HCHO) is the simplest and most common aldehyde and is found in low concentrations in our environment as a consequence of natural processes. At normal ambient temperatures, it is a transparent gas with a strong odor. It boils at 21^0C and melts at 92^0C (Ge *et al.*, 2020).

Wood-based composite materials are bonded through thermosetting (heat curing) adhesive resins, such as UF, with curing temperatures that vary from 130 °C to 195 °C. UF is among the less expensive thermosetting resin used as a binder in wood; they are non-flammable, strong, have a very rapid cure rate, and are light in color. UF adhesives are the predominant adhesives for interior grade plywood and particleboards (Bekhta *et al*., 2016; Tan *et al*., 2011; Hoong *et al*., 2010). UF adhesive can only be used in particleboards for interior applications such as furniture and partitioning as they are destroyed by excess moisture and heat (Yan *et al*., 2017b; Pfungen, 2015; Mamza *et al*., 2014). Moisture and heat breakdown of the bond-forming carcinogenic formaldehyde fumes continues to emerge from the adhesive. The formaldehyde emissions are high initially because of unreacted formaldehyde. Formaldehyde emissions decrease with time but do not disappear

(Paiman *et al*., 2019; Khanjanzadeh *et al*., 2013). The carcinogenic nature of formaldehyde is attributed to the crosslinking of proteins with DNA (Lu *et al*., 2010). The first step involves the reaction between proteins and formaldehyde (Kerns *et al*., 1983; Swenberg *et al*., 1980) as shown in equation 2.46

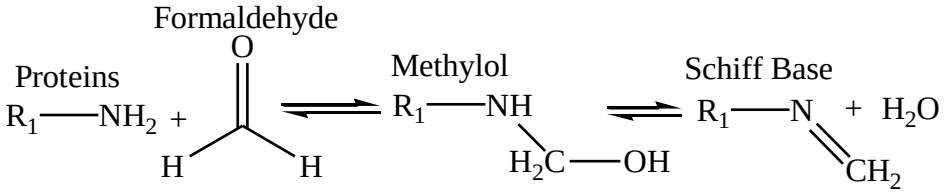

2.46

Schiff base formed reacts with DNA to form crosslinked products (Lu *et al*., 2010) as shown in equation 2.47

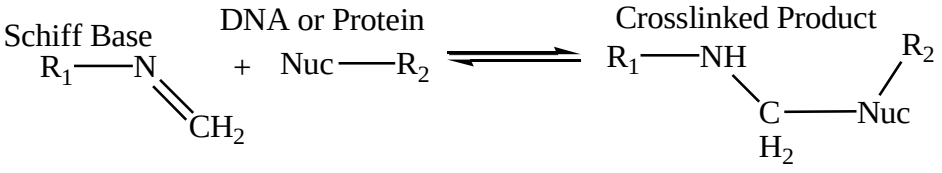

2.47

Formaldehyde acts as a crosslink between proteins with DNA (Lu *et al*., 2010) as shown in Figure 2-15.

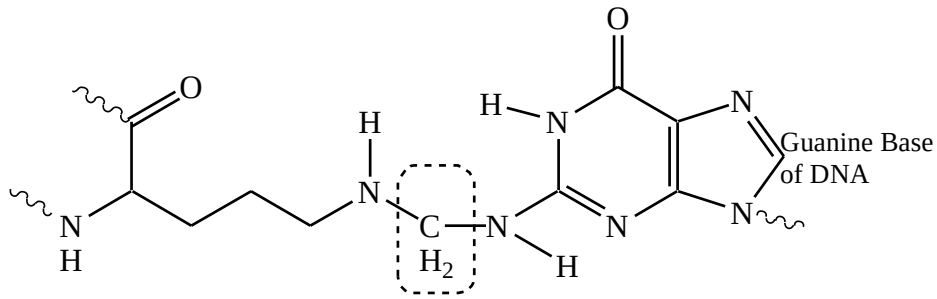

Figure 2-15. Formaldehyde crossling proteins and DNA

Formaldehyde causes irritation, lacrimation, sneezing, cough, dyspnea and nausea (Paiman *et al*., 2019; Tohmura *et al*., 2000; Myers, 1985). Due to its carcinogenic nature, regulations of formaldehyde concentration in fiber and board panels were put in place to reduce the emission of formaldehyde into the environment. Engineered wood products, natural material panels and product emissions are less than 1% w/w of free formaldehyde in glues. Internationally accepted test method EN 120 for particle and MDF boards have emission limits of < 9 mg/100g (Awaluddin *et al.*, 2017; Kelley *et al.*, 2010).

Formaldehyde based boards in countries are produced with strict environmental controls, one of the measures include a decrease in the use of formaldehyde-urea

ratios (Boran *et al*., 2011). Lowering resin ratios has respectively been reflected in the decrease of the strength of commercial products. This issue has made industries to consider their replacement with alternative binders that do not contain formaldehyde (Paiman *et al*., 2019; Khanjanzadeh *et al*., 2013; Saffari, 2011; Tohmura *et al*., 2000).

2.14 Mechanical Tests for the Particleboards

2.14.1 Modulus of Rupture (MOR) and Modulus of Elasticity (MOE)

MOE measures flexural strength where the stress of samples is determined before it is deformed (Stark *et al*., 2010). Three points flexural test technique is used where the specimen is bent until it breaks. The MOR, on the other hand, measures the stress within the test material at the breaking point. MOE measures the resistance of the test material to be deformed when pulled. Therefore MOE is the slope of a curve at its stress-strain deformation region. The higher MOE the material has the more it becomes stiffer (Akinyemi *et al.*, 2016b).

Particleboards formulated in this study were tested for MOR and MOE as set by American Standards for Testing Material (ASTM). ASTM regulate the quality of materials. They also coordinate with international standards so that products are used worldwide. The standard in this project is the (American National Standards Institute) ANSI-particleboard standard. Materials used to make paticleboards in this study were regulated by ASTM standard. The MOR and MOE of various grades are provided in this standard, and they are classified by the density and grade of boards.

2.14.2 Internal Bond (IB) Strength

IB measures tensile strength perpendicular to the surface of the test material (Kowaluk *et al*., 2019). IB provides a quantification of the bonding amongst the particles perpendicular to the board plane. Particleboard normally fails when stressed in tension perpendicular to sample surface at the middle of the thickness, and that higher density particleboards will have higher IB (Kowaluk *et al*., 2019; Li *et al*., 2014). Internal bond is the tensile strength of particleboards perpendicular to the particleboard plane. A fully cured particleboard fails when tension stress is applied at an angle of 90 ^{o} in the middle of the test board where the density is lowest. The lowest density represents part of the particleboard with the least particle interactions

and lowest consolidation. Density is directly proportional to IB. An increase in density correspond increase in IB whereas low density reduces IB of particleboard (Kowaluk *et al.*, 2019). The low density is a result of low pressing that causes high moisture content of the matrix. Moisture trapped within composite material causes spring-back which results in breakage of bonds between the particles thus causing lower density (Jonoobi *et al*., 2016a; Koubaa and Koran, 1995). IB increases with a decrease in moisture content as lower moisture is trapped after pressing.

Tensile strength improves with the configuration of the core particle. The use of wood shaving as an alternative to flakes improved the IB (Mirski *et al*., 2019). Particleboards made with coarse particles at the center and flakes at the surface have been used in the optimization of the three-layer board properties (Ayrilmis *et al*., 2012). Studies also have shown that IB increases with an increase in the amount of wood dust. Further increase in the amount of wood dust beyond 20 % results in a decrease in IB (Nemli *et al*., 2007). The size of particles affects the contact between materials. Research findings showed that the smaller the particle size the more contact is between the blended materials (Nemli *et al.*, 2009). Small particles fill gaps in the core of the composite material which increases tensile strength resistance applied perpendicular to board surface (Koubaa and Koran, 1995).

Wood species highly influence the IB of the formulated particleboard. A decrease in wood species density results in a decrease in IB (Melo *et al*., 2014). A study on an admixture of rubberwood and Mahang showed IB of particleboards formulated was affected by the density of wood particles as an increase of low-density wood particles decreases IB (Lee *et al.*, 2010). Other ways of improving IB include the addition of wax.

2.15 Particleboards Standards and Certification

Particleboard undergoes a different set of testing for strength, hardness and flex following ANSI A208.1, using the standard test methods outlined in ASTM D1037-12 and JIS A-5908 using Japanese standards for material testing, EN 312 using European standards for material testing and KS 2226:2010 using Kenyan standards for material testing. Particleboards control experts perform the following physical tests: WA, TS, MC and density. Particleboards are categorized based on their

densities. Different standards set certain requirements for certification as summarized in Table 2. High, medium and low-density particleboards are represented by HD, MD and LD respectively.

Table 2-2. Different standard requirements for high density, medium density and low-density particleboards used for certification

Property	Density	American standards *ANSI* A208.1	European standards EN 312	Japanese standards JIS A-5908	Kenyan standards
Density (g/cm^3)	LD	<0.60	<640	0.30-0.50	<0.60
	MD	0.64-0.80	640-800	0.60-0.90	0.60-0.780
	HD	>0.85	>800	>0.9.	>0.780
Moisture content (%)	LD	8 to 13	8-15	<13	4-15
	MD	8 to 13	8-15	5.00 – 13.00	4-15
	HD	8 to 13	8-15	<13	4-15
Water absorption (%)	LD	<77	<50	35	<50
	MD	<77	<50	35	<50
	HD	<77	<50	35	<50
Thickness swelling (%)	LD	18±3	<13	<12	<15
	MD	18±3	< 13	<12	<15
	HD	18±3	<13	<12	<15
MOR (N/mm^2)	LD	2.8-5	8-13	>18	22<
	MD	7.6-16.5	8-13	>18	22-27
	HD	14.9-21.5	8-13	>18	>27
MOE (N/mm^2)	LD	500-1025	1000-2000	<2000	<2500
	MD	1380-2750	1600-1800	2000-3000	2500-2700
	HD	2160-2475	>1800	>3000	>2700
IB (N/mm^2)	LD	0.1-0.4	<0.35	>0.3	<0.60
	MD	0.31-0.55	0.35	>0.3	0.60-0.9
	HD	0.81-1	>0.9	>0.3	>0.9

Conventional methods of using formaldehyde-based resin all cause formaldehyde emmision. Formaldehyde is carcinogenic and harmful. Use of alternative biobased binders such as cassava peel starch become an alternative source of adhesive. Use of wood as a lignocellulose material has led to decrease in tree cover. Due to this, this material has become scarce leading to high cost of conventional particleboards. The aim of the study is to make prototype formaldehyde free particleboards.

CHAPTER THREE

3 MATERIALS AND METHODS

3.1 Samples

Maize stalk, sugarcane bagasse and rice husks were used in the study as lignocellulose source. These materials pose environmental challenges as they require large space to be disposed. These materials were choosen as lignocellulose material as they are mainly disposed off through burning. Maize stalk was sampled from Nakuru, an agricultural area, after harvesting season. Sugarcane bagasse was collected from Kisumu where there is largescale production of sugarcane plant. Rice husks was collected from Kirinyaga County where rice is grown in large scale and cassava tubers sampled at random in Thika. All samples were collected at random where they were in plently during research period.

3.2 Sampling Sites and Sampling Design

Sampling of raw materials was done randomly from selected sites. Lignin source materials were obtained from three geographical areas and starch source from one geographical area. Maize stalks were obtained from Arahuka Farm in Nakuru County, Kenya (0^o 18’ S, 36^o 4’ E), Sugarcane bagasse was obtained from Muhoroni Sugar Company in Kisumu County, Kenya (0^o 5’ S, 34^o 46' E) while rice husks were obtained from Mwea Rice Millers (0^o 37’S, 37^o 20' E), Kirinyaga county. Cassava tubers were obtained from Thika in Kiambu County (1^o 3’ S, 37^o 5’ E). Multistage design was used during the sample collection where three samples were obtained from each site. Experimental design was used in the study. Each sample was homogenized and analyzed separately in triplicate.

3.3 Cleaning of Apparatus

All glassware was soaked in nitric acid (AR grade reagent) mixed in the ratio of 1:1 to deionized water for 8 hours and then cleaned using detergent, rinsed with deionized water and oven-dried at 105 ^oC for 10 minutes. Plastic containers were washed with 1:1 of nitric acid (AR grade reagent) to water, washed with appropriate detergents and rinsed four times with deionized water. They were then oven-dried at 60 ^oC.

3.4 Preparation of Reagent

All reagents used were of analytical grade prepared in deionized water unless otherwise stated.

3.5 Sample Treatment

Maize stalk was chopped with an electric chaff cutter with motor and 2 blades (Model Phagwara PB National Foundry 2010) rotating at 2 revolutions per second, to smaller size. The largest choppings were measured with verneer calipers and found to be less than 10 mm. No further pretreatment was done to sugarcane bagasse. It was used as obtained from the sampling site. Rice husks were pulverized to pass through 1.5 mm sieve. Cassava tubers were washed with tap water, periderm removed, rinsed with distilled water and peeled. Cassava peels were rinsed with deionized water and then sun-dried. Rice grains, maize corn, cassava tubers, wheat grains, millet grains and sorghum grains, cassava peel starch, maize stalk and sugarcane bagasse were dried in an oven at 105 ^{o}C to a constant mass. The samples were then removed allowed to cool and packed in 2 kg khaki paper bags and placed in desiccators for three hours. Cassava peel starch, rice husks and maize stalk were then ground using a pulverizer (5E-PCM1x100 Pulverizer) and sieved to pass through 300 microns standard gauge sieve.

3.6 Starch Characterization

3.6.1 Determination of Starch Content

Starch content in rice grains, maize corn, cassava tubers, wheat grains, cassava peels, millet grains and sorghum grains was determined using spectrometric titration (Nielsen, 1943). 2.0 g of oven-dried starch samples were placed separately in a 500.0 ml beaker placed on a magnetic stirrer. Into the same beaker, 2 ml of deionized water and 2.7 ml 7.2 M perchloric acid were added and the resultant mixture stirred for 10 minutes. Deionized water was then added to the resulting mixture to make a total volume of 50 ml. 1.0 ml of the resulting solution was placed in 100 ml Pyrex glass beaker, followed by 6 ml of deionized water, then one drop of phenolphthalein indicator and 0.6 mL of 6.0 M NaOH while stirring. The resultant mixture was titrated with standardized acetic acid until the pink color of the solution disappeared. 2.5 ml of 0.4 M NaOH was then added to the resultant mixture. 5.0 ml of 0.6 M KI and 5.0 ml of 0.01 M KIO_3 was added to the resultant mixture while stirring. The

resultant mixture was analyzed using UV–vis spectrophotometer (Spectrometer, Model: UV1700, AC240V/50 HZ, SN: VD01181803015) for absorbance at 650 nm wavelength after 3 minutes of addition of KIO_3. Laboratory starch was analyzed using the same procedures as a control.

3.6.2 Determination of Starch pH

The pH of the starch was determined in accordance to Chen, *et al.,* (2016). 5.0 g of starch sample was put into 500 ml Pyrex beaker. 15 ml of deionized water then added and stirred for 30 seconds using a stirrer. 85 ml of boiling deionized water was added to the resulting mixture while stirring to make a slurry. The resulting mixture was allowed to cool to room temperature and pH measured using a pH Meter (HI 2211 Microprocessor-based pH/mV/^{o}C Bench Meters) (Chen *et al.*, 2016).

3.6.3 Determination of Starch Ash Content

Starch ash content was determined using a procedure described by Aloko and Adebayo, (2007). 2.0 g of starch sample was weighed and placed in a porcelain crucible. The crucible with starch was placed over a hot water bath and dried to a constant mass. Over-water dried samples were placed in a preheated muffle furnace at 900 °C for 1 hour. The porcelain crucible and residue was placed in a desiccator and allowed to cool to room temperature. The crucible and residue were re-weighed. Starch ash content was determined using equation 3.1.

$$\text{Percentage ash content} = \frac{W_o - W_{ash}}{W_o} \times 100 \qquad 3.1$$

Where W_o represents the sample dry weight and W_{ash} represents mass after heating.

3.6.4 Pre-Treatment of Starch

Oxidized starch was prepared using a method adopted from Opara, *et al*., (2017). 17.50 g of ground starch and 5.00 g Na_2CO_3 were put in 200 ml beaker. 40.0 ml of 20 % H_2O_2 was added and the resultant mixture stirred for 30 minutes using a magnetic stirrer. The resulting mixture was dried to a constant mass at 60 °C. The resultant solid was pulverized to pass through a 100 microns standard sieve. The process was done in triplicate.

Dextinization of cassava peel starch was done following the preparation of cassava-based adhesive (Opara *et* al., 2017). 12.5 ml of 0.1 M HCl was placed in a 500 ml Pyrex beaker. 17.5 g cassava peel starch was put into the same beaker and the mixture heated to dryness. The resulting mixture was further dried in an oven at 105 ^{o}C to a constant mass. The oven-dried mixture was allowed to cool to room temperature and placed in a desiccator. Dextrinized starch was pulverized to pass through 100 microns sieve. The process was done in triplicate.

3.6.4.1 Preparation of Urea-Oxidized Starch

Urea-oxidized starch was prepared in accordance with a procedure adopted from Opara *et al.*, (2017), with slight modifications. 17.5 g of ground cassava peel starch, 2.5 ml of 20 % H_2O_2, 1.25 g of sodium carbonate, and 5.00 g of urea was mixed in 500 ml clean beaker and the resultant mixture analyzed.

3.7 Preparation of lignocellulose material

Lignocellulose materials used in the study were prepared in accordance with Sluiter *et al.,* (2016). 70.0 g of dried lignocellulose samples were separately soaked in 1400 ml of 20% hydrogen peroxide (H_2O_2) in a 2000 ml plastic beaker at pH 11.5 maintained using sodium hydroxide. The resultant mixture was stirred at room temperature for 15 min, after which the resultant mixture was filtered with a Buchner funnel. The residue was rinsed using deionized water and oven-dried at 105 °C to a constant mass.

3.8 Lignin Content Determination

Lignin content in lignocellulose material was determined using the Klason method (Fagerstedt *et al*., 2015). 10.00 g of the ground lignocellulose material was weighed in a 500 ml beaker. 14 ml of 13.4 M sulphuric acid at 25 ^{o}C was then added to the resulting mixture while stirring for 30 minutes. The resultant mixture was allowed to cool for 2 hours. The mixture was placed in a conical flask and 450 ml deionized water added into the mixture. The resultant mixture was boiled for 4 hours under reflux then filtered using a Buchner funnel. The residue was washed with 250 mL of deionized water. The residue was dried in an oven at 105˚C to constant mass. The residue was then cooled to room temperature and weighed as insoluble substance. The ercentage of lignin content was calculated using equation 3.2.

$$\text{Percentage ash content} = {}^{L_2}/_{L_1} \times w \times 100 \quad 3.2$$

Where L_1 represents mass of lignocellulose material, L_2 represent the residue after acid treatment and w is the mass of lignocellulose used.

3.9 Formulation of Particleboards

Particleboards were formulated using an approach adopted in the synthesis of starch-lignin copolymer preparation (Vengal and Manu, 2016; Vengal and Srikumar, 2015; Srikumar and Vengal, 2015) with slight modifications. 250 mL of 0.4 M NaOH was transferred into a 500 mL Pyrex beaker and pre-heated to 40 ^{o}C using an electric heater. To the pre-heated 0.4 M NaOH, 17.5 g of the cassava peels starch was added and the temperature gradually raised to between 55 ^{o}C and 60 ^{o}C while stirring the mixture for 15 minutes. To the resulting mixture, 2.0 g of sodium borate was added and stirring continued for 15 minutes. The hot mixture was put in a 1000 ml plastic beaker and 70 g of prepared maize stalk added while stirring with a clean wood for 5 minutes. The composite material was allowed to cure at 25.0 ^{o}C for 8 hours. The resulting composite material was transferred into 300 mm by 150 mm by 30 mm mild steel fabricated moulds with an internal lining of polyethylene sheet. The moulded composite material was compressed using 6.5 Nmm^{-2} mechanical compressor for 6 minutes at 30 ^{o}C. The moulded composites were air-dried under a shade and further dried at 60 ^{o}C for 3 hours. The procedure was repeated for the formulation of composite materials with sugarcane bagasse and rice husks. Labeling of the particleboards formulated was done according to lignocellulose material and treated cassava peels starch. Particleboards made from sugarcane bagasse with hydrolyzed starch, dextrinized starch, oxidized cassava peel starch and urea-oxidized cassava peel starch were labeled as PBS-HS, PBR-DS, PBR-OS and PBR-U-OS respectively. Particleboards formulated with rice husks with hydrolyzed starch cassava peel, dextrinized starch cassava peel, oxidized cassava peel starch and urea-oxidized cassava peel starch are PBR-HS, PBR-DS, PBR-OS and PBR-U-OS respectively. Particleboards formulated from maize stalks with hydrolyzed cassava peel starch, dextrinized cassava peel starch, oxidized starch and urea-oxidized starch were labelled as PBM-HS, PBM-DS, PBM-OS and PBM-U-OS respectively. Samples of prototype formulated particleboards from maize stalk, sugarcane bagasse and rice husks with oxidized cassava peel starch are shown in Plate 3-1.

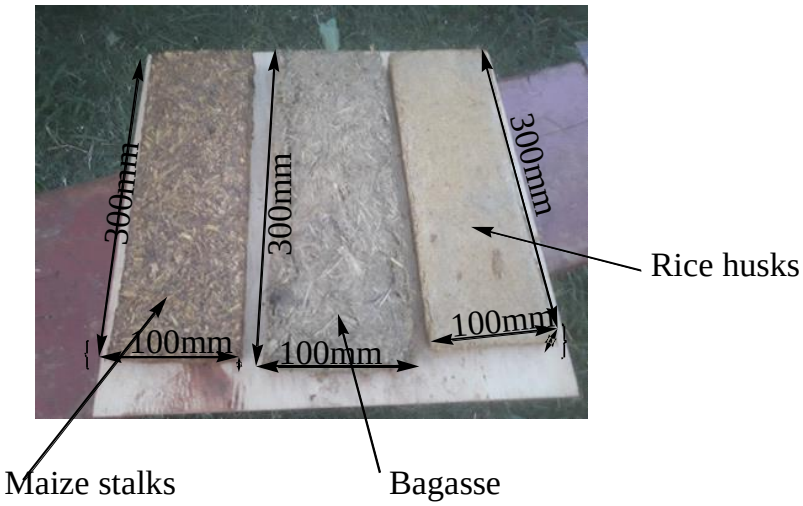

Plate 3-1. Sample prototype particleboards

3.10 Optimization of Starch to Lignocellulose Ratio in Particleboard Formulation

The treated cassava peel starch was mixed separately with sugarcane bagasse, rice husks and maize stalk at a ratio of 2:20 to 8:20 in increments of 0.05 in clean 500 ml plastic beakers. The mixture was then covered with aluminium foil for 8 hours. The cooled composite materials were put in the fabricated mould (Appendix II) and compressed using 6.5 Nmm^{-2} mechanical compressor. Models were sun-dried for 48 hours.

3.11 Time-Temperatures Optimization for Gelatinization of Sodium Hydroxide-Starch

12.5 g of starch was put in a 250 mL of a glass beaker. 100 cm^3 of 0.1 M NaOH was added to the starch and the resultant mixture heated at temperatures of 25 ^oC. The time taken for the starch to gelatinize was recorded. The same procedure was separately repeated but the heating temperature was changed to 30 ^oC, 35 ^oC, 40 ^oC, 45 ^oC, 50 ^oC, 55 ^oC, or 60 ^oC. In all cases the time taken for the starch to gelatinize was recorded. Time taken to gelatinize was plotted against temperature. The graph was used to determine the optimum time-temperature for starch to gelatinize. The optimal condition was adopted in this study.

3.12 Characterization and Testing of Particleboard

3.12.1 Sample Preparation for AAS Analysis

AAS sample analysis was determined using an approach adopted from standards used in water and effluent analysis (Ademoroti, 1996; Rantala and Loring, 1992; Allen, 1974). 0.10 g of lignocellulose material was transferred into 125 ml plastic beaker followed by 1 ml of aquaregia (concentrated HNO_3 and HCl in the ratio 1:3). To the resulting mixture, 3.0 ml hydrofluoric acid was added onto the mixture and stirred for 1 minute. The mixture was allowed to cool for 8 hours after which 50.0 ml of concentrated H_3BO_3 was added into the mixture and allowed to settle for 1.5 hours. The resultant mixture was transferred to a 100 ml volumetric flask and topped up to the mark using deionized water. AAS Standards were prepared using Mount Royal Gabbro (MRG) rock and Syenite (SY-3) (Abbey and Gladney, 2005). 5 ml of the standard solutions prepared were ransferred separately into a 100 ml volumetric flask topped up with deionized water. Standard and sample solutions were run in SpectrAA.10 Model SEANAC Company in the usual procedure.

3.12.2 Sample Preparation for XRFS Analyses

XRF analysis was carried out using a procedure described by Inkrod *et* al., (2018) that was used to characterize lignocellulose materials (Inkrod *et al*., 2018). 10.0 grams of ground starch was pulverized to pass through 100 micron sieve. The ground starch was mixed with 5.0 g analytical grade starch flux then made into pellets. Pellets were then put into the XRF machine for analysis. 100 ml of 0.2 M oxalic acid was added to 20.00 g of the sugarcane bagasse, maize stalk and rice husks in a 250 ml conical flask placed on a hot plate and agitated at 80 ^{o}C to 90 ^{o}C for 2 hours while covered with a watch glass. The mixture was then filtered and the residue washed and dried at 105 ^{o}C in an oven for 2 hours. Chemical analyses in each sample were determined using the XRF.

3.12.3 Mineralogical Analysis Using X-ray Diffraction (XRD)

10.0 g of ground samples of lignocellulose materials and starch were placed in six cell holders. Sample holders were tapped carefully to ensure the particles are parked to avoid displacement which affects peak shifts. The cell holders containing the samples were loaded in Bruker D_2 phaser diffractometer for analysis installed with data collector software. Data was shown in single-phase collection of XRD patterns

for most intense 3D values in form of interplanar spacings (D) tables, mineral name and relative intensities ($^{I}/_{I_o}$) (Zhou *et al*., 2010). Sample spectra were related to literature reference spectra to identify the mineral.

3.12.4 Fourier Transform Infra-Red (FTIR) Analysis of Samples

FTIR spectroscopy was done using direct transmittance with attenuated total reflectance (ATR) accessory (IRT Laser-100 SHIMADZU). Sample spectrum was scanned as a resolution of 4 cm^{-1} between 400 cm^{-1} to 4000 cm^{-1}. The background spectrum for each test sample was collected before sampling. All the infra-red spectra were obtained with an FTIR spectrometer by use of the KBr disk. Spectra recording were obtained using 32 scans at an average using a resolution of 4 cm^{-1}. Particleboard samples were conditioned to 102 ^{o}C for 24 hours in an oven. Raw samples and particleboard samples were homogenized using a Universal disintegrator (Model FW80-1) to pass through 100 micron sieve. 200 mg of samples were placed in an oven set at 60 ^{o}C for 8 hours. Ground samples were made into a ball and placed in a desiccator with phosphorus pentoxide (P_2O_5). Heat-treated samples were used for obtaining the spectra. Each treatment-time-species combination gave one spectrum. All spectra were obtained with 1.50 mg to 1.55 mg of sample materials using ATR. The spectra were identified using literature reference spectra to identify major functional groups (Ouhaddouch *et al*., 2019).

3.12.5 Solid-Nuclear Magnetic Resonance (NMR) Analysis of Samples

All NMR measurements were performed on a Bruker AV400 spectrometer in NMR facility at ICMM-CSIC Spain operating at a 100.61 MHz frequency, using a 4 mm wide-line MAS probe. Raw materials and particleboard samples were spun at 10 kHz in zirconia rotors to obtain spectra utilizing a CP-MAS pulse sequence equipped with 1 microsecond contact time and a 5 second recycle delay. The spectra were obtained by averaging 1800–4000 scans. All chemical shifts (δ) were identified with reference to standard deuterochloroform ($CDCl_3$). Sample spectra were determined using literature reference spectra to identify main molecular groups.

3.12.6 Scanning Electron Microscopy (SEM) Analysis

Surface analysis was determined using SEM using a high-resolution machine model JSM-5300LV emitting 47 μA current at an accelerating voltage of 15 kV in operation. Samples were coated with 50 nm Au/Pb and data magnified by 200x (Tay *et al.*, 2016). Interfacial interaction between lignocellulose materials and cassava peel starch was determined.

3.12.7 Thermal Conductivity Determination

Thermal conductivity of the particleboard was determined in accordance to the ASTM C518-98 method for material testing (ASTM, 2000). Thermal conductivity was determined using a guarded hot plate apparatus model HFS-4 heat flux sensor (Omega Engineering, Stamford, CT). Particleboard specimens were cut into sizes of 150 x 150 mm and 11 to 12.5 mm thick. The hot plate was set at 117.0 ^{o}C and the cold plate 77.0 ^{o}C with a temperature gradient of 3.5 ^{o}C mm^{-1}. Thermal equilibrium was reached and five successive observations were made at 5 min intervals.

3.12.8 Determination of Formaldehyde Emission

Formaldehyde emission was determined according to ASTM D 5582-00 (ASTM 2006), using the desiccator method. Samples of formulated particleboards were were cut into 5 cm by 15 cm and placed in a desiccator at 20.0 °C for 24 hours with deionized water. Formaldehyde emitted from samples dissolved in distilled water and the resultant solution analyzed for absorbance at 412 nm wavelength. Deionized water was used as a control using a UV-vis spectrophotometer (Spectrophotometer, Model: UV1700, AC240V/50 HZ, SN: VD01181803015). Formaldehyde standard solution was used in calibration and the graph of absorbance against the concentration of formaldehyde in mg/L plotted.

3.13 Particleboard Physical and Mechanical Evaluation

Evaluation of particleboards was carried out according to ASTM D 1037 (ASTM, 2002). Physical properties evaluated include density, thickness swelling (TS) and water absorption (WA) and mechanical properties evaluated include modulus of Rupture (MOR), Modulus of Elasticity (MOE) and Internal bond (IB).

3.13.1 Determination of Density

Square samples of length and width dimensions of 50 mm by 50 mm by 20 mm respectively were cut and placed on a weighing balance to an accuracy of 0.01 g. The density (ρ) of the samples was calculated by dividing mass in grams with volume in square millimeters.

3.13.2 Determination of Moisture Content

Determination of Mositure content in starch was done in accordance to procedure adopted from Darkwa and Sekyere (2003). 5.0 g of starch sample was placed in a clean porcelain dish and placed over a hot water-bath and dried to a constant mass. Over-water dried samples were further dried at 105 °C in an oven set for 1 hour and then placed in a desiccator to cool. The samples were then weighed using analytical balance Model Mettler AJ150 GWB. Moisture content in starch was expressed as a percentage as shown in equation 3.3.

$$\frac{M_2 - M_1}{M_1} \times 100 \qquad 3.3$$

Where M_1 represents mass of starch samples dried over water bath and M_2 represents oven dried starch samples.

3.13.3 Determination of Thickness Swelling (TS) and Water Absorption (WA) of Particleboard Formulated

Particleboard specimen was cut into 152 mm by 152 mm by 20 mm in size and the four edges trimmed and smoothened. The test specimen was placed at 65 % relative humidity set at 20 ^{o}C. The moisture content after conditioning was recorded. After conditioning, the samples were weighed and measurement for width, length, and thickness made using a micrometer screw gauge. The volume of the specimen was calculated in the normal way using these measurements. The thickness of specimens was made as an average of TS in four points at the middle that is 25 mm away from edges of specimens. The WA and TS were converted into a percentage for all specimen soaked after 24 hours (ASTM, 2002).

3.13.4 Static Bending Test

Particleboard samples were cut into 50 mm width and length was 20 times the thickness plus 50 mm. The width was measured at the mid-length and thickness was

measured at the intersection of the diagonals. The samples were placed on the supports with a longitudinal axis set at 90 ^{o} to the supports with the center point under the load. The load was applied at a constant rate of crosshead movement through the sample. The loading rate was adjusted to 60 ± 30 seconds at a speed of 10 mm/min. The deflection was measured in the middle of the test sample to an accuracy of 0.1 mm. The test speed was applied continuously at a uniform motion rate of movable cross-head of the machine used for testing calculated using equation 3.4.

$$N = \frac{zL^2}{6d} \qquad 3.4$$

Where N represents the rate of movement the head in mm/min, z represents the rate of fiber strain in mm/min, L represents span radius mm and d represents the thickness of tested material in mm (ASTM, 2002).

3.13.4.1 Modulus of Rupture (MOR) and Modulus of Elasticity (MOE)

Samples size 152 mm in length and 76 mm width were cut from formulated particleboards made in this study. The samples were placed in the flexural unit-model Dkz-5000 shown in Plate 3-2.

Plate 3-2. Instrument Used to Measure Modulus of Rupture

A load was applied continuously at a rate of 12 mm $(min)^{-1}$ until definite failure occurred. The maximum load of the testing machine was noted and MOR in N/mm^2 calculated using equation 3.5 (Muruganandam *et al.*, 2016).

$$MOR = \frac{3PL}{2bd^2} \quad 3.5$$

Where P represents the largest load in kg, L represents the length of the span in mm, d represents the specimen thickness in mm and b represents specimen width in mm.

MOE was calculated using equation 3.6 (Muruganandam *et al.*, 2016).

$$MOE = \frac{PL^3}{4bh^3Y} \quad 3.6$$

Where P represents load at the proportionality limit, L represents the span length, measured in mm, b represents the width of the specimen, in mm and Y, represents the deflection corresponding to P, in mm.

3.13.5 Internal Bonding (IB) Strength

IB was determined according to ASTM D1037 procedure (Stark *et al.*, 2010)., samples were cut into 50 mm x 50mm x 10 mm that were stuck onto steel loading blocks with hot melt adhesive. The temperature in which the hot melt adhesive was applied to the loading blocks and samples was around 170 °C (±10 °C). The cross-head spin at a speed of 0.8 mm $(min)^{-1}$. Three replicate of each particleboard was used. The IB strength was obtained in Nmm^{-2}, by the quotient of maximum load (Newtons) with the surface (mm^2) of the samples. IB was determined using a compression machine model YAW-300 shown in Plate 3-3.

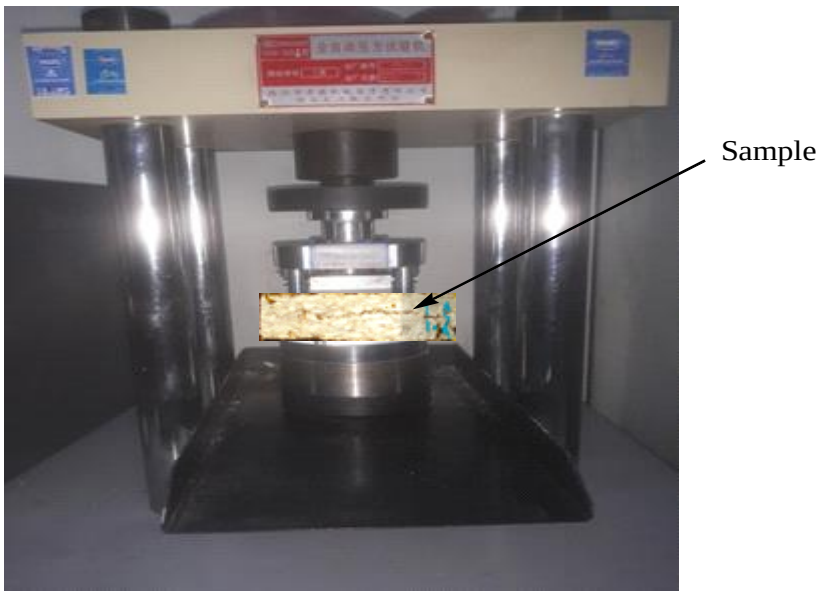

Plate 3-3. Instrument Used to Measure Internal Bonding of Particleboard

IB was calculated (Koubaa and Koran, 1995) using equation 3.7.

$$\sigma t = Wtb \times t \qquad 3.7$$

Where: σt represents the tensile stress in N/mm^2, Wt represents tensile load at failure in N, b represents the specimen breadth in mm and t represents the specimen thickness.

3.14 Data Analysis

Samples were analyzed in triplicate and their means calculated using equation 3.8.

$$\bar{x} = \sum_i \frac{x_i}{n} \qquad 3.8$$

Where: $\bar{x}$ represent sample mean, x_i represents several measurements and n represents the sample population.

Results of WA, TS, MOE, MOR, IB and thermal conductivity were presented graphically with use of error bars to represent standard deviation. Standard errors were calculated using equation 3.9.

$$sd = S.E.\sqrt{n} \qquad 3.9$$

Where sd represents the standard deviation, S.E. represents the standard error and n represents the population.

The t-test was used to compare experimental means obtained from AAS for significance difference and Tukey one way ANOVA (Harvey, 2000; Miller and Miller, 1988). The standard deviation of the means was calculated using equation 3.10 shown below (Miller and Miller, 1988).

$$s = \sqrt{\sum_i (x_i - \bar{x})^2 / (n-1)} \qquad 3.10$$

t – Calculated was given by equation 3.11.

$$t_{cal} = \frac{\left(\bar{x}_1 - \bar{x}_2\right)}{\sqrt{\frac{s_1^2}{n_1} + \frac{s_2^2}{n_2}}} \qquad 3.11$$

Bar graphs were used for the representation of data obtained in this study. The analyzed data are in the form of diffractograms, tables, and bar graphs. Comparative

statistical analysis was used where appropriate to test for the significant difference using Tukey one way ANOVA was used.

CHAPTER FOUR

4 RESULTS AND DISCUSSION

4.1 Results Overview

The study investigated the use of agricultural crop residues bound with modified cassava peel starch in the formulation of particleboards. This chapter gives a detailed discussion of the results obtained in this study. The physical-chemical properties of the resultant materials have also been presented in this chapter.

4.2 Starch Characterization

4.2.1 Starch Content of Various Sources

Results for various test starch samples are presented in figure 4-1.

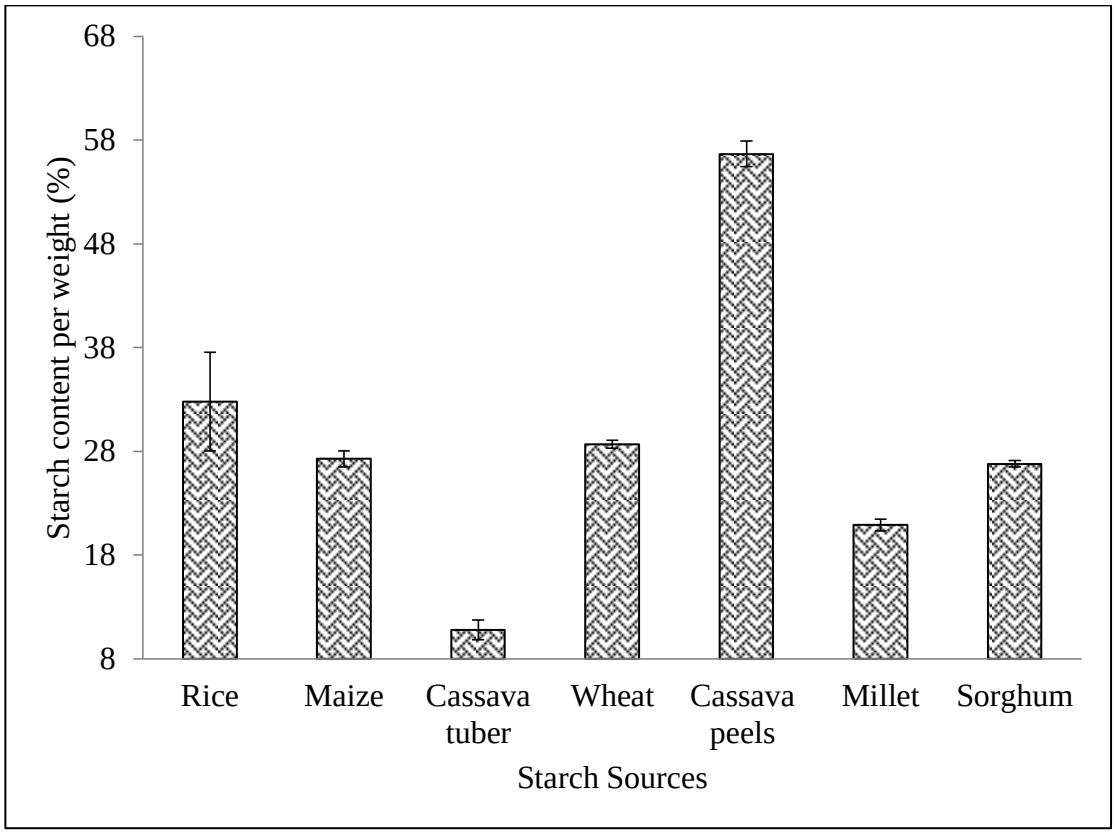

Figure 4-1. Percentage of starch content in various sources

From the results, all sample materials exhibited different starch contents with cassava peels exhibiting the highest content. Rice grains, maize corn, cassava tubers, wheat grains, millet grains and sorghum grains are mainly used as a source of starch for human consumption. This reduces their industrial applications. High starch content of cassava peel makes it an alternative source of starch for industrial applications.

Cassava peels constitute 15 to 20 % of the tuber (Onyimonyi and Ugwu, 2007; Obadina *et al.*, 2006) thus cassava peel is a good source of the starch. Cassava peels contain high carbon content thus used in the preparation of activated carbon (Sudaryanto *et al*., 2006). Studies have shown that cassava peels are rich in starch which makes them raw materials for industrial production of ethanol (Oparaku *et al.*, 2013). Cassava peels have been used as a binder in production of concrete (Salau *et al*., 2012). Cassava peel therefore remains one of the best alterative source of biobased adhesive for particleboard formulation.

Cassava peels starch contains high levels of cyanogenic glucosides (Bayitse *et al.*, 2015; Kongkiattikajorn and Sornvoraweat, 2011). Cyanogenic glucosides contain ammine functional groups that undergo a condensation reaction with carboxylic and hydroxyl groups from lignocellulose material which makes particleboards better. Cyanogenic glucoside reduces soil microbial activities and increases soil acidity. This makes it unsuitable for crop production thus considered as a waste. Utilization of cassava peels as a source of starch provides an alternative waste disposal of the cassava peels.

Cassava peels contain large numbers of carboxyl, amino acid and hydroxyl groups. The functional groups make cassava peels useful in formulation of adhesives (Cumpstey, 2013; Crini, 2006). Hydroxyl and ammine groups act as a connecting point between lignocellulose material and cassava peels starch (Oladele *et al*., 2020). Free hydroxyl groups from starch react with free hydroxyl groups in lignocellulose material through etherification to form covalent bonding. Amine groups from cassava peel react with carboxylic and hydroxyl groups from lignocellulose material through condensation reaction to produce peptide bonds. This results in the production of composite material used in the formulation of particleboard in this study.

From the results, cassava peels can be utilized as a source of starch for formulating particleboards. This is because of its high starch content and limited alternative use of the peels. The limited use of the peels as food material is due to the high cyanoglucoside content which is very important in preventing attack of the peels

product by termites. (Bhandari *et al*., 2014). This provides inherent protection against termites hence particleboards last longer.

4.2.2 Statistical Analysis for Various Starch Materials

Statistical analysis for significant difference between starch sources is presented in table 4-1.

Table 4-1. Statistical analysis for significance difference in starch contents from different sources with superscript showing signifiance difference

Starch sources	Rice grains	Maize corn	Cassava tubers	Wheat grains	Cassava peels	Millet grains	Sorghum grains
Starch content	$32.79^{a}\pm$ 4.756	$27.27^{a}\pm$ 0.777	$10.79^{b}\pm$ 0.951	$28.69^{c}\pm$ 0.378	$56.66^{d}\pm$ 1.245	$32.62^{a}\pm$ 2.822	$26.82^{f}\pm$ 0.275

Tukey one way ANOVA at 95 % confidence level showed statistical differences within the means across the samples. Mean samples concentrations of rice grain and maize corn showed no significant difference where t_{cal} =1.99 < t_{crit} = 4.3027 (P>0.05). Comparative analysis between the mean starch contents between rice grains and millet grains showed no significant difference where t_{cal} = 4.3024 < t_{crit} =4.3027. Comparatively, there was a significance difference between the starch content means between cassava peel starch and rice grains where t_{cal} = 8.41 > t_{cal} = 4.03 (P < 0.05).

Bayitse *et al* (2015) observed a starch content of 47.16 % while Moresco *et al*., (2014) observed 32.1 % and 20.13 % in maize and wheat respectively (Moresco *et al.*, 2014). Cassava tubers have a starch content of between 20 to 30 % (Ascheri *et al*., 2014). Wankhede *et al* (1979) observed that millet contain starch content that ranges from 35.28 % to 39.2% (Wankhede *et al.*, 1979). Starch content in sorghum has been documented as 30.48 % (Sattlera *et al*., 2010) and rice grains contain 28.7 % (Kaur *et al.*, 2016), due to high glucose content. High glucode content provide more ydroxyl groups that are crucial during esterification process. A process utilized in this study for formulating particleboards. Therefore, cassava peel provides this functional groups adequately hence an alternative source of starch for particleboard formulation.

4.2.3 Ash Content for Starch Sources

Results for ash content in various starch materials are presented in figure 4-2.

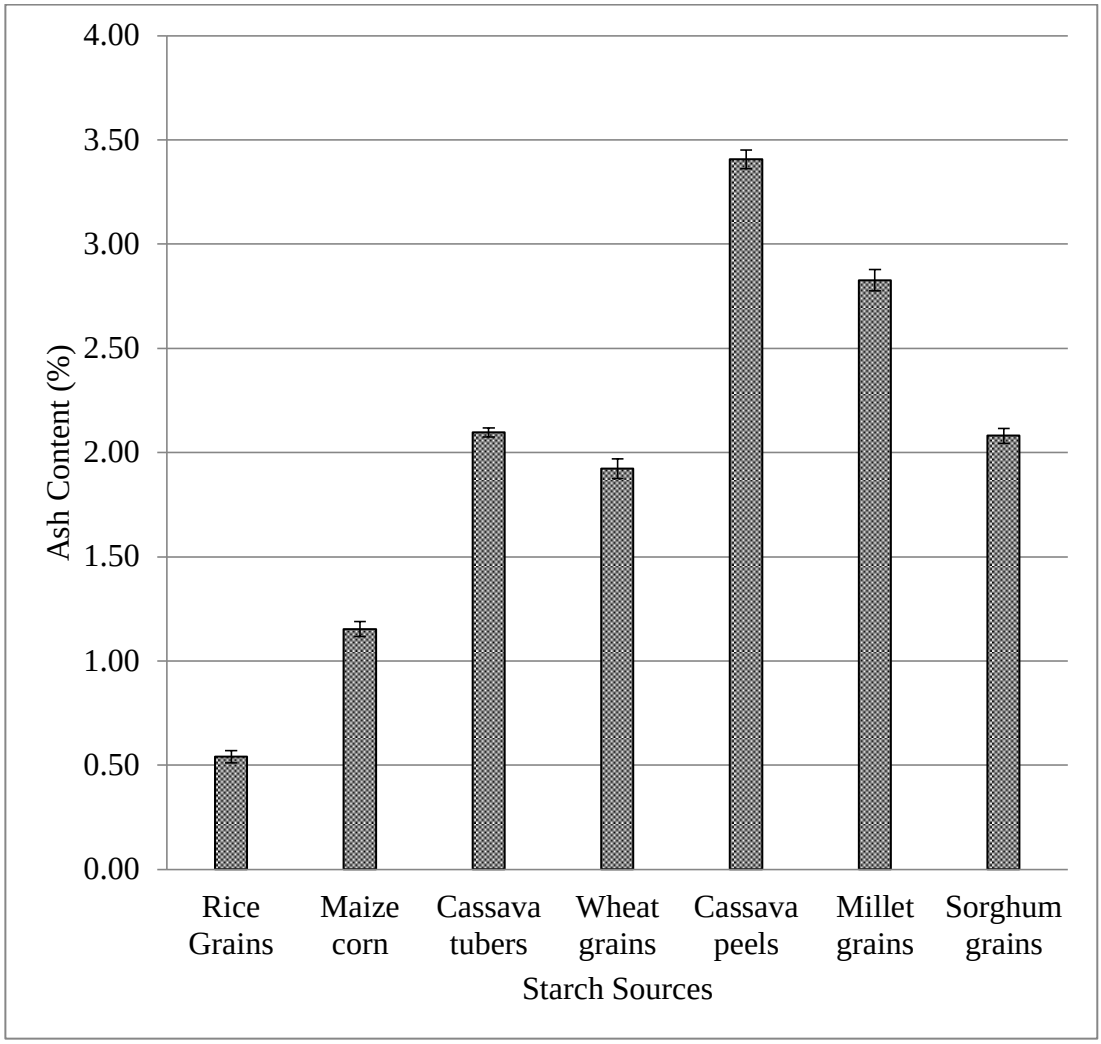

Figure 4-2. Ash content in starch sources

Cassava peel starch contain the highest ash content of 3.41 %. High ash content is as a result of high levels of inorganic substances that is mainly silica (Kartini, 2014b; Habeeb and Mahmud, 2010). High silica content provides the raw material for making sodium silicate after treatment with NaOH (Bakar *et al*., 2016). Study has shown treatment of ash with sodium hydroxide is used as a substitute for sodium silicate (Kamseu *et al*., 2017). Na_2SiO_3 is an inorganic adhesive that combines with starch through the silication process to form a crosslink (Zuo *et al*., 2015).

Sodium silicate undergoes hydrolysis to form silicic acid (Zhang *et al*., 2020). Silicic acid contains mainly hydroxyl groups (Chen *et al*., 2020). This implies that high concentration of silica in lignocellulose material will result in a large number of

hydroxyl groups. Hydroxyl groups in silicic acid undergo condensation reaction with amine and hydroxyl (Annenkov *et al*., 2017). Cassava peel starch contains cyano glucosides that have amine and hydroxyl groups. Reaction between amine and hydroxyl groups forms peptide bond. Hydroxyl groups from other materials such as lignocellulose material form ethers when combined with hydroxyk groups from starch. These bonds increase the interaction between the lignocellulose material and cassava peel starch. Ng *et al* (2018) observed that high sodium silicate concentration and its distribution within fibers determine the mechanical properties of particleboard (Ng *et al*., 2018).

Cassava peel ash contain a high concentration of calcium oxide (Raheem *et al*., 2015). Calcium oxide is one of the main binding components in inorganic adhesives. Calcium oxide reacts with water to form calcium hydroxide. Calcium hydroxide reacts with silica in lignocellulose material to form calcium silicate, an inorganic adhesive. Calcium silicate is also the main chemical composition in cement. Cement has been used as a binder in particleboard formulation (Tittelein *et al*., 2012). Calcium oxide is a flame-retardant additive in composite materials (Hamdani-Devarennes *et al*., 2013).

4.2.4 Chemical Analysis of Raw Starch

Results for Na, Zn, Ca and Mg from various starch sources are presented in table 4-2.

Table 4-2. XRF analysis in cassava peels starch with same superscript

Starch Sources	Na	Zn	Ca	Mg
Cassava Tubers	$0.00133^{a}\pm$ 0.00058	$0.03433^{a}\pm$ 0.00473	$9.99633^{b}\pm$ 0.0953	$0.00167^{a}\pm$ 0.00058
Wheat Four	$0.002^{a}\pm$ 0.0001	$0.12333^{a}\pm$ 0.00513	$7.755^{b}\pm$ 0.03568	$6.55333^{bc}\pm$ 0.01124
Maize Corn	$0.00133^{a}\pm$ 0.00058	$0.132^{a}\pm$ 0.00361	$4.55367^{a}\pm$ 0.00945	$0.14387^{a}\pm$ 0.00184
Sorghum Grains	$0.00133^{a}\pm$ 0.00058	$0.21733^{a}\pm$ 0.00586	$5.21433^{c}\pm$ 0.01756	$6.24067^{cd}\pm$ 0.01343
Millet Grains	$0.00167^{a}\pm$ 0.00058	$0.23733^{a}\pm$ 0.0185	$5.62533^{b}\pm$ 0.00586	$5.953^{bc}\pm$ 0.01082
Cassava Peel Starch	$0.00467^{a}\pm$ 0.000577	$0.06333^{a}\pm$ 0.00635	$13.4633^{b}\pm$ 0.10017	$0.1270^{a}\pm$ 0.00781

Analyses for Na, Zn, Ca and Mg in starch sources in this study showed that major ions were present. The results show that there is no significant difference in the

presence of Na, Zn and Mg across the starch sources, especially in cassava tubers, maize corn and cassava peel. In all starches, sodium ions (Na^+) were of low concentrations. Na^+ enables the curing process of the biobased adhesive such as cassava peel starch. Sodium hydroxide used in this study provided more Na^+, a crucial ion for the curing process (Li *et al*., 2018).

Zn level was low in all the starch resources. The level was highest in millet grains at 0.23733 % and lowest in cassava tubers at 0.03433 %. Compounds containing zinc and magnesium increases bond strength in particleboards (Zuo *et al.*, 2015). Zn^{2+} improves starch granules dissolution as it allows percolation into the starch structure which weakens the intra-molecular and inter-molecular bond which breaks down the crystalline nature of the starch (Garcia and Gonzalez, 2019). ZnO in aqueous sodium hydroxide forms a complex radical of zincate $[Zn(OH)_4]^{2-}$. Zincate ion improves cellulose dissolution through the formation of strong hydrogen bonding (Kanga *et al.*, 2016). Zinc ions coordination with amino and carboxylic groups strengthens and toughen the adhesive formulated from cassava (Bai *et al*., 2020).

Calcium level was the highest element in all starch sources ranging from 4.55 to 13.46 %. Cassava peel starch showed highest levels calcium with 13.463 % and maize corn with the lowest at 4.5536 %. The chemical and physical properties of starch granules are affected by Ca^{2+} ions. It also changes morphological, mechanical and pasting properties of adhesive (Garcia *et al.*, 2017). Ca^{2+} determines plastic and elastic parts of the hydrogel. Ca^{2+} increases the hydrophobic nature of the lignocellulose material and increases the repellant of water in the particleboards. This also helps in the reduction of TS by up to 25 % (Halvarsson *et al.*, 2004). Calcium ions gel the adhesives that provide cohesion force that makes network structure more compact (Bai *et al.*, 2020).

Levels of magnesium were highest in wheat flour at 6.55 %. Cassava peels starch showed the lowest levels among the starch sources at 0.00167 %. Mg^{2+} as a plasticizer increases swelling as well as solubility index (Garcia and Gonzalez, 2019). $Mg(OH)_2$ and MgO reduces the concentration of the acid in a reacting mixture. Magnesium oxide has been used as inert filler during the preparation of plywood (Du *et al.*, 1995). Mineral fillers increase board performance compared to

those with no filler or with the filler of starch. This is because filler prevents over permeation of adhesive to the wood substrate. This results in the reduction of internal stress attributed to the shrinkage of the glue line (Koubaa and Koran, 1995).

4.3 Characterization of Lignocellulose Materials

4.3.1 Lignin Content in Various Lignocellulose Materials

Results for lignin content in various lignocellulose materials are presented in figure 4-3.

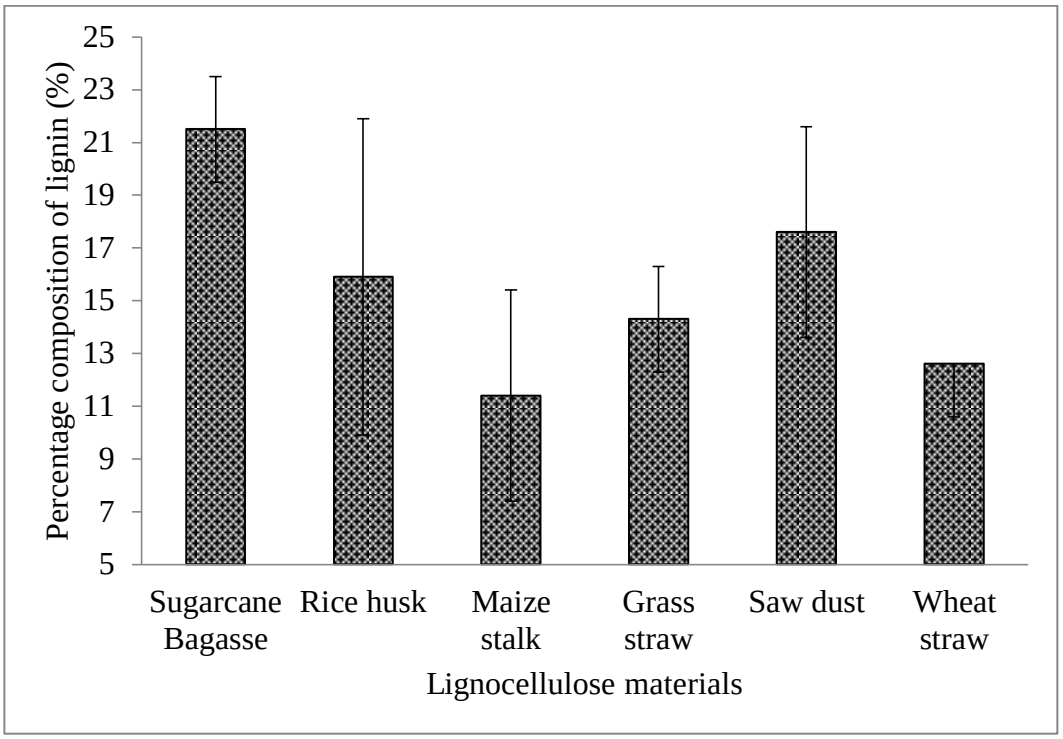

Figure 4-3. Lignin content in crop residues

Percentage of lignin in sugarcane bagasse was highest compared to the other lignocellulose materials used in this study whereas maize stalk had the lowest lignin content. High lignin content in sugarcane bagasse is attributed to degradration of cellulose and hemicellulose (Perez *et al*., 2002). Lignin has high molecular mass compared to cellulose and hemicellulose which makes them to undergo slow biodegradation (Perez *et al*., 2002). Cellulose has been found to constitute the highest part of maize stalk with up to 50 % and lignin of content less than 30 % (Cao *et al*., 2014). Rice husks are mainly composed of cellulose and silica (Bakar *et al*., 2016). Silica reduces biodegradation of rice husks. This makes rice husks have high lignin content compared to maize stalk.

Lignin has phenolic hydroxyl groups which react with polyols such as starch to form ethers (Laurichesse and Averous, 2014). Lignin content determines water absorption (WA) and thickness swelling (TS) of particleboard (Zarifa *et al.*, 2018). Low lignin content results in high WA (Achyuthan *et al.*, 2010). Lignin-starch composites have low WA and TS (Welker *et al*., 2015; Baumberger *et al*., 2010). Higher lignin content in sugarcane bagasse has been observed to lower WA and TS of formulated particleboard (Atiqah *et al*., 2017).

The test crop residues can be used as a source of lignocellulose material for making particleboards. This is because the test sample residues have been observed to have adequate lignin components. The lignin component plays a vital role in particleboard formulation since they affect WA and TS of particleboards. Lignin content determines the physical characteristics of particleboards. An increase in lignin content lowers WA and TS, a characteristic that is required for particleboards used in making furniture. The test crop residues can be used in the formulation of particleboards for interior applications like making furniture, doors and partitioning of rooms. Lignin has been observed to undergo slow biodegradation. It is therefore expected that particleboards formulated with such crop residues would show reasonable service life.

4.3.2 Chemical Analysis of Lignocellulose Material

The Results on XRF for Na, Zn, Ca and Mg from various lignocellulose materials used in particleboards formulated are presented in table 4-3.

Table 4-3. Chemical analysis of lignocellulose materials

Lignocellulose material	Na_2O	ZnO	CaO	MgO
Sugarcane bagasse	0.010±0.0001	0.012±0.002	3.867±0.024	12.86±0.074
Rice husk	0.002±0.0001	0.005±0.001	1.037±0.009	0.010±0.0001
Maize stalk	0.003±0.001	0.054±0.008	7.958±0.063	17.006±0.069
Grass straw	0.013±0.003	0.017±0.002	7.457±0.030	0.010±0.001
Saw dust	0.014±0.003	0.457±0.007	1.702±0.006	0.828±0.008
Wheat straw	0.002±0.001	0.051±0.0046	3.315±0.015	10.570±0.053

Table 4-3 shows that maize stalk contains the highest amount of CaO and MgO of 7.958 and 17.00 respectively. The main source of these ions in lignocellulose

material is mainly from the fertilizers used. The presence of calcium in lignocellulose material is CaO and MgO dissolves in water to form an alkaline medium. The presence of Ca ions extensively cross-links lignin molecules under alkaline conditions. An alkaline solution such as $Ca(OH)_2$ and $Mg(OH)_2$ is used in breaking up of lignocellulose material to obtain free lignin and acetyl groups from hemicellulose, thus increasing biomass porosity (Grimaldi *et al*., 2015).

4.4 Optimization of Starch to Lignocellulose Ratio in Particleboard Formulation

The particleboards were formulated with varying the starch to lignocellulose ratio and the results obtained are indicated in figure 4-4. Comparison of various ratios showed that increase in the starch to rice husks ratio reduces moisture content MC steadily up to the ratio of 4:20. This ratio was adopted for the formulation of the particleboard between rice husks and cassava peel starch.

Different lignocellulose material have been observed to give varied moisture content of the resultant particleboards. Formulation of particleboard using 20 % (w/w) of cassava starch with maize stalk as lignocellulose material, for example, gave moisture content of 12 % (Ye *et al*., 2018). Particleboards formulated with 15 % (w/w) of wheat starch as a binder and oil palm starch with rubberwood as lignocellulose material gave MC of 10 % (Salleh *et al*., 2014). Particleboard formulated with wood and bound with starch in a mixture of 1:1 gave moisture content of between 15.1 % and 15.5 % (Monteiro *et al*., 2019). Higher moisture content was attributed to the heterogeneity in the particleboards formulated due to unreacted starch materials.

Results from the comparison of various ratios showed that an increase in the ratio increases the density of the particleboards up to ratio of a 5:20. Densities of particleboard formulated with ratios 3:20 and 4:20 were significantly different where $t_{cal} = 12.26 > t_{crit} = 3.18$. Comparatively, there was significant difference between the densities obtained at a ration of 4:20 and 5:20, the $t_{cal} = 2.789 <$ t crit = 3.18 ($p<0.05$, one way ANOVA). Increase in density is attributed to the interaction between cassava peels starch and lignocellulose material through esterification.

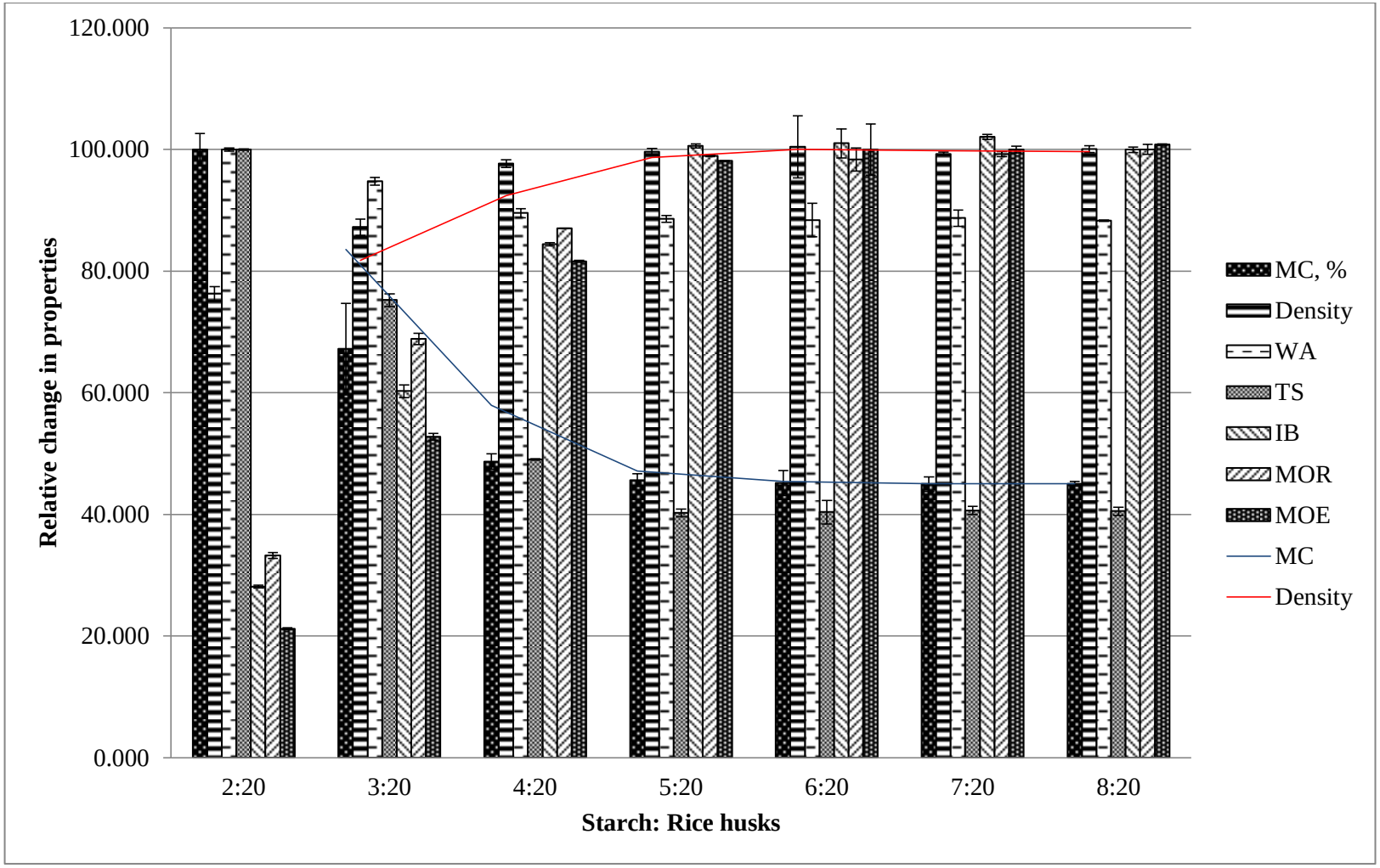

Figure 4-4. Optimization of starch-rice husks material for formulation of particleboard

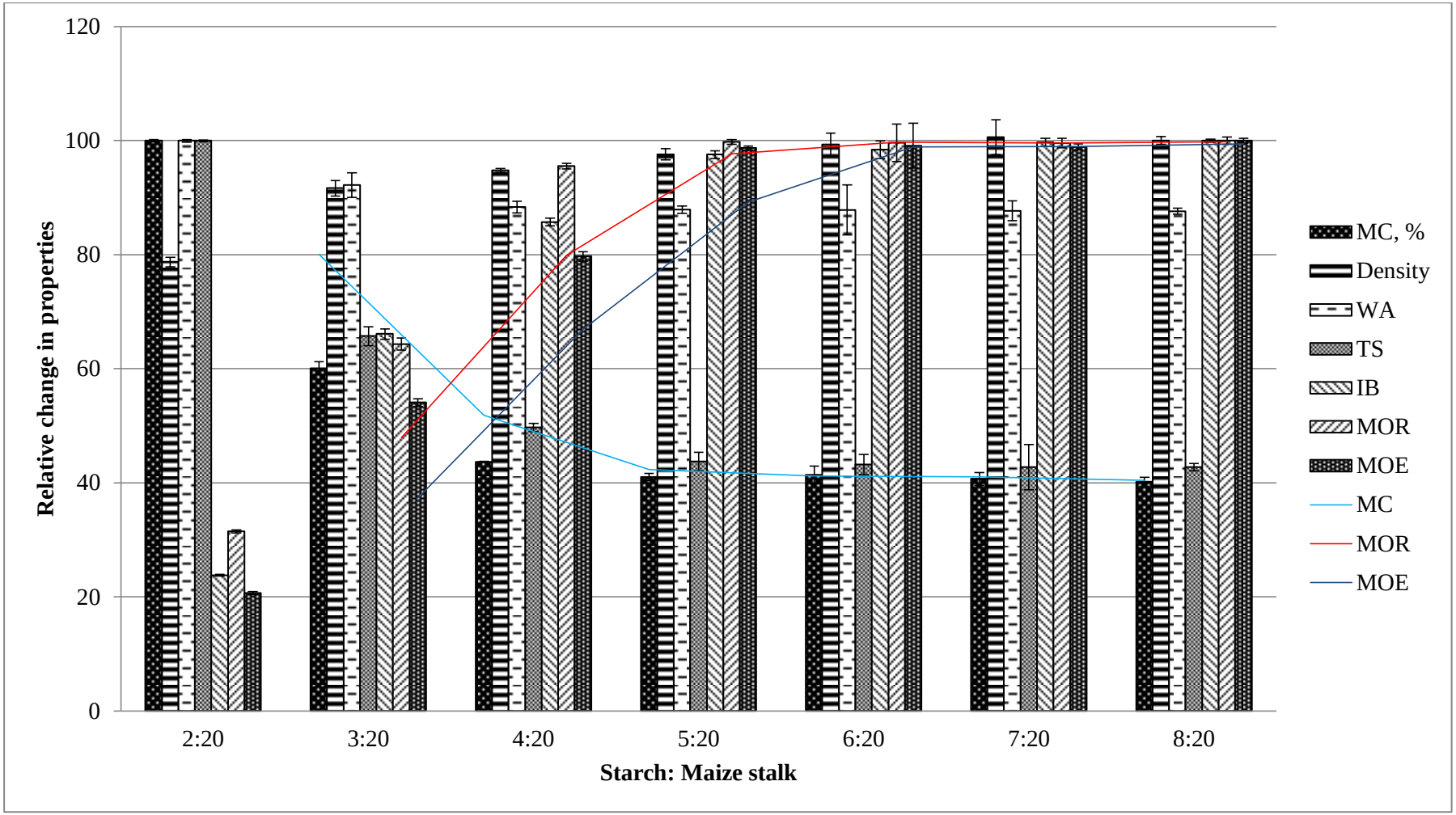

Figure 4-5. Optimization of starch-maize stalk material for formulation of particleboard

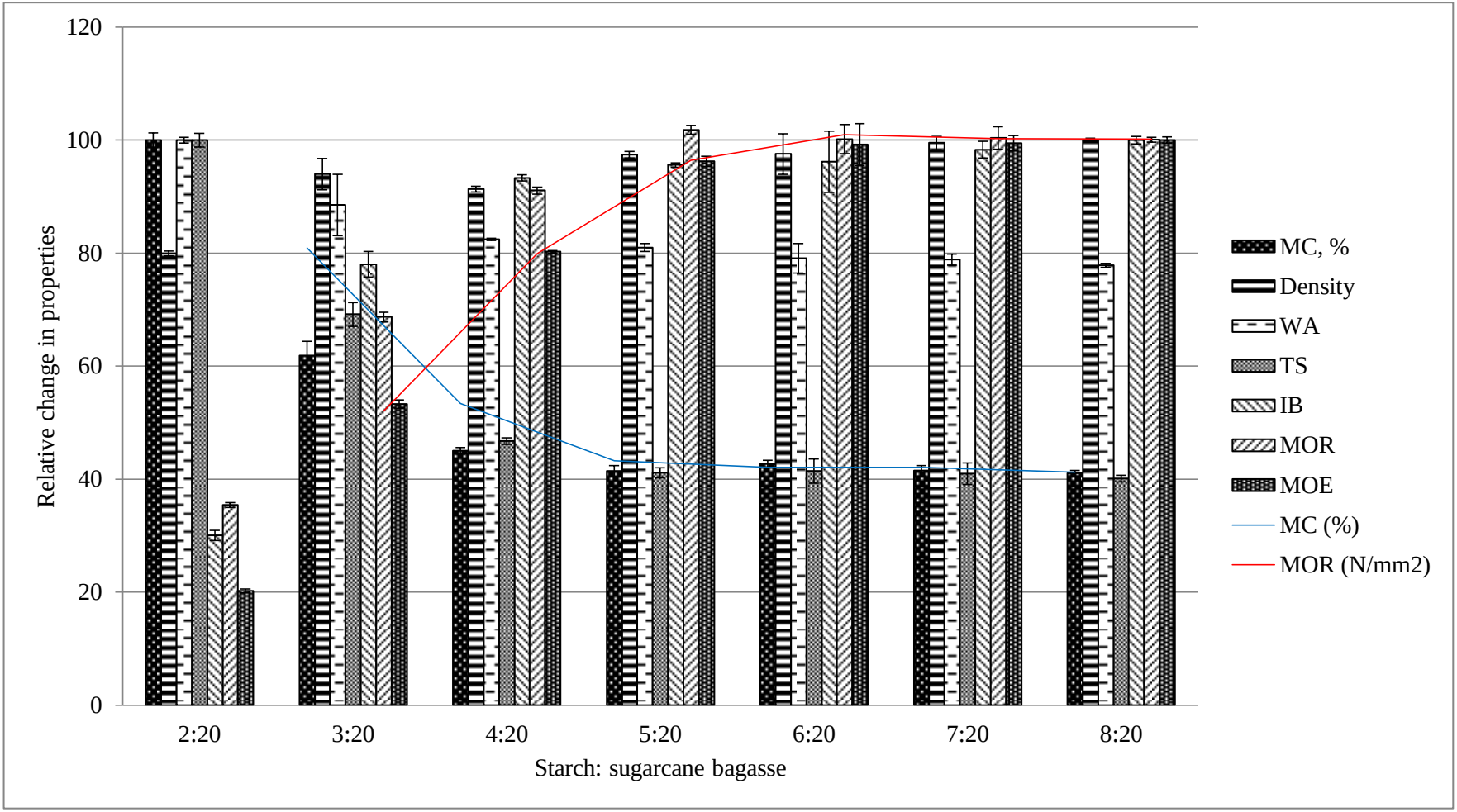

Figure 4-6. Optimization of starch-sugarcane bagasse for formulation of particleboard

Montero *et al* (2020) observed that increase of potato starch to wood ratio increases the density of the particleboard (Monteiro *et al*., 2020). Starch/wood dry mass ratio increase from 0.6 to 1.2 resulted to increase in density from 0.290 g/cm^3 to 0.372 g/cm^3. Particleboards formulated from 20 % wheat flour by mass to wood gave the highest density of 0.65±0.02 g/cm^3 (Ferreira *et al*., 2018).

Results in figure 4-4 showed a gradual decrease in water absorption up to a starch to lignocellulose ratio of 4:20. Comparison between the ratios 4:20 and 5:20 showed significant difference where t_{cal} =143.0> t_{crit} = 3.18. Further comparison of the ratios 5:20 and 6:20 showed no significance difference where t_{cal} =1.22< t_{crit}=3.18. This implies that starch to lignocellulose ratio of 5:20 left fewest hydroxyl groups which determine water absorption. Unreacted starch determines water absorption in composite materials (Kale *et al*., 2007) that is higher starch content results to higher WA. Increase in starch content more than of 50 % to lignocellulose material increased water absorption in particleboard formulated from rice husks and cassava starch by over 60 % (Ameh *et al.*, 2019).

Salleh *et al* (2014) observed that particleboards formulated with wheat starch to wood ratio of 15 % gave WA of 96.6 % (Salleh *et al*., 2014). This value is higher compared to the ones obtained in this study. This can be attributed to the initial pretreatment of the raw materials especially lignocellulose materials with sodium hydroxide. Study has also shown particleboards made from rubberwood were optimized at 15 % corn starch as a binder content gave water absorption of 87.35 % (Amini *et al.*, 2013). Study has also shown that increase of tapioca starch from 10 to 20 % (w/w) improved WA from 112.5 to 93.4 % (Homkhiew *et al*., 2020).

Results in figure 4-4 show that a ratio 5:20 gave the optimum combinations of cassava peel starch to rice husks for particleboard formulation. The high water absorption is reduced further by chemical modification of cassava starch. Chemical modification of corn starch with glutaldehyde reduced WA in particleboards formulated from rubberwood by 10 %. Initial chemical treatment with sodium hydroxide and borax reduces the number of hydroxyl groups (Ali *et al*., 2012) that

intern reduces the overall performance of WA in particleboard (Murphy and Mitchell, 2009).

Results in figure 4-4 show a gradual decrease of thickness swelling (TS) up to 5:20 which is attributed to the size of voids in the particleboards. Voids are attributed to the interaction between cassava peel starch and lignocellulose material. Gradual decrease signifies interaction between the functional groups in starch and those in lignocellulose material. Comparative analysis shows a significant difference between starch to lignocellulose material ratios of 4:20 and 5:20 where t_{cal} =18.08 > t_{crit}=2.776. Further comparison between the starch to lignocellulose material ratios of 5:20 and 6:20 showed no significance different where t_{cal} =0.268 <t_{crit} = 3.18. Unreacted starch increases the hydrophilic properties in composite materials (Amini *et al*., 2013) thus starch content influences water uptake that affects the TS. Slight increase in water absorption is therefore attributed to excess unreacted starch.

Particleboards formulated with tapioca starch optimized at 25 % starch (w/w) showed stabilization of thickness swelling at 26.55 % (Liew *et al*., 2018). A study showed use of additional tapioca starch decrease to a minimum of 8.45 % when 25% of starch was used (Liew *et al*., 2018). These results were similar to the TS obtained in this study.

Result from figure 4-4 shows a gradual increase in internal bonding with an increase in starch to lignocellulose ratio from 2:20 to 5:20. Comparative analysis of the IB using ratios 4:20 and 5:20 showed a significance difference where t_{cal} = 8.35>t_{crit} = 2.77. Comparison of the results using the ratios 5:20 and 6:20 showed no significant difference where t_{cal} = 0.237 < t_{cric} = 2.77. Optimum starch to lignocellulose ratio combination therefore is 5:20. This implies that a combination of starch to lignocellulose ratio at 5:20 gave the optimal interaction through condensation reactions to form covalent bonding. Excess starch content affects the interaction between starch and lignocellulose material resulting in weaker IB.

Increase in tapioca starch to sawdust ratio from 10 and 20 % result to change in internal bonding of particleboard from 0.69 N/mm^2, 0.93 N/mm^2 and then to 0.50

N/mm^2 (Homkhiew *et al*., 2020). Increase in starch content to lignocellulose material increases the adhesion between wood and starch. Starch improves the interaction with lignocellulose material that fills the voids in composite material hence act as a filler material (Boon *et al*., 2019). Results obtained in this study were in line with results obtained by other researchers.

Results in figure 4-4 showed a gradual increase in modulus of rupture (MOR) with an increase in starch to lignocellulose ratio up to 5:20. Comparative analysis of the starch to lignocellulose ratios of 4:20 and 5:20 showed no significant difference where t_{cal} =13.86 < t_{crit} = 3.18. Further comparison between starch to lignocellulose materials for 5:20 and 6:20 showed no significance difference where t_{cal} =1.38 < t_{crit} = 2.78. This implies an increase in starch content in formulation of the composite material to 6:20 did not increase the interaction of the starch with lignocellulose material. Excess starch reduces the rigidity of composite material formulated using starch and lignocellulose materials (Ye *et al*., 2018).

Study has shown that increase in tapioca starch increase from 10, 15 and 20% (w/w) changed MOR from 6.7 N/mm^2, 9.0 N/mm^2 and then dropped to 8.5 N/mm^2 (Homkhiew *et al*., 2020). This shows that excess starch content lowers the overall MOR of the particleboards. Results obtained in this study are in line with results obtained in other research. Particleboards formulated met the minimum requirements required for medium density particleboards accordind to ASTM.

Results obtained in figure 4-4 show a gradual increase in modulus of elasticity with an increase in starch to lignocellulose ratio. Comparatively, starch to lignocellulose ratios of 4:20 and 5:20 showed significant difference in MOE where t_{cal} = 40.19 > tcric = 4.30. Further comparison of MOE obtained using starch to lignocellulose ratios of 5:20 and 6:20 showed a significance difference where t_{cal} = 3.9>t_{crit} =3.18. Comparison between MOR using starch to lignocellulose ratio of 6:20 and 7:20 showed no significant difference where t_{cal} = 0 < tcric = 3.18. This implies that a combination of starch to lignocellulose ratio of 6:20 gave the optimum interaction between starch and lignocellulose material to form a composite material.

Researchers such as Homkhiew *et al*., (2020) optimized tapioca starch to sawdust ratios jointly using the maximum MOR, IBS and minimum WA. Properties of the particleboards increased with the ratio of cassava peel starch-lignocellulose. Optimum combination was achieved at a ratio of starch-rice husks of 4:20. Particleboard whose density is 0.638 g/cm^3 and at a moisture content of 9.61 % and a compression pressure of 6.5 Nmm^{-2}. The particleboard showed WA and TS of 78.55 % and 19.08 %. The IB, MOR and MOE were 1.597 Nmm^{-2}, 13.63 Nmm^{-2} and 2599 Nmm^{-2} respectively. The high percentage of WA and TS indicates the presence of an unmodified hydroxyl group. Hydroxyl groups in composite materials interact through hydrogen bonding with water molecules. Similar trends in physical and mechanical properties were shown with other lignocellulose materials such as maize stalk and sugarcane bagasse as shown in figure 4-5 and figure 4-6 respectively. The optimum combination of starch-lignocellulose materials adopted for his study was starch to lignocellulose material of 5:20.

4.4.1 Time-Temperatures Dependent Optimization for the Gelatinization of Starch using Sodium Hydroxide

Optimisation results on time-temperature taken for starch to gelatinize against change in concentration are presented in figure 4-7.

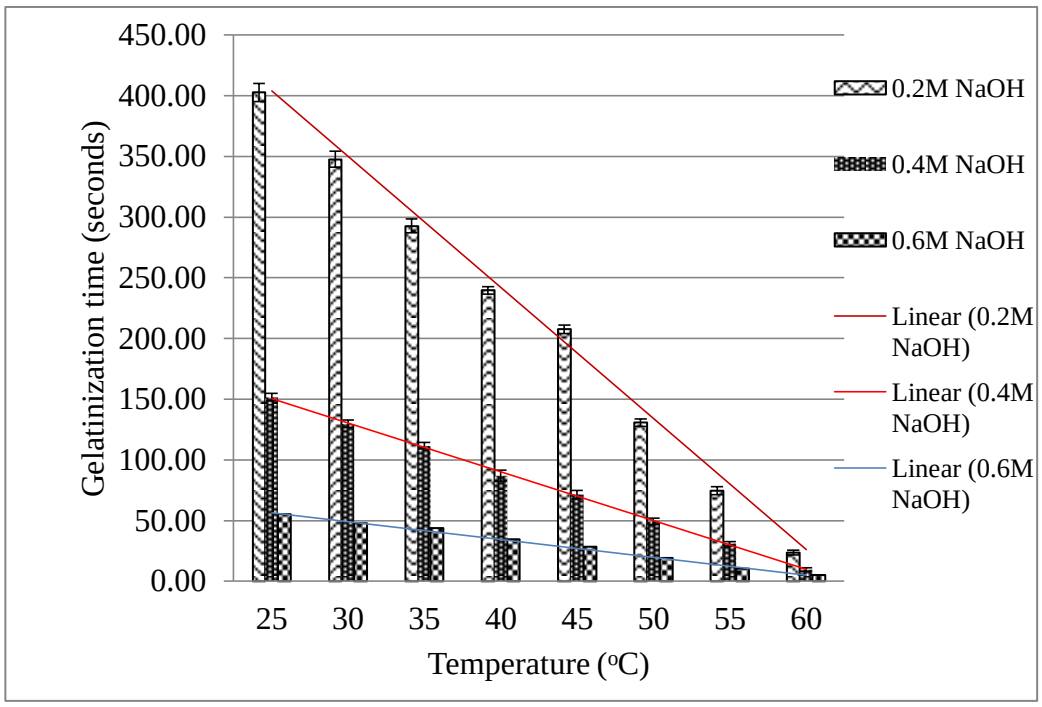

Figure 4-7. Effect of variation of concentrated sodium hydroxide on cassava peels starch gelatinization

Increase in sodium hydroxide concentration result in lower gelatinization time. Sodium hydroxide concentration determined the time taken for cassava peels to gelatinize. An increase in sodium hydroxide concentration results in a reduction of the time taken for cassava starch to be clear. Sodium hydroxide increased the swelling of cassava peel starch due to the rapid breaking of intramolecular hydrogen bonding as a result of interaction with water.

Sodium hydroxide concentration reduces gelatinization time using potato as a starch source as was ivestigated by Roberts and Cameron, (2007). The researchers found that starch treated with 2M sodium hydroxide gelatinized almost instantly at room temperature (Roberts and Cameron, 2002). Similar results were obtained during the gelatinization of carboxymethyl starch using rice as a starch source and using sodium hydroxide by Rachtanapun *et al.*,(2012). Researchers observed that increase in sodium hydroxide concentration increases breaking down of starch structure. During gelatinization of starch, St-OH, sodium hydroxide reacts with starch to produce an alkoxide, St-ONa (Rachtanapun *et al*., 2012).

Sodium hydroxide breaks hydrogen bonding leading to the formation of free hydroxyl groups in cassava peels starch (Awaluddin *et al*., 2017; Ragheb *et al*., 1995). Hydroxyl groups, -C-OH, are converted to -COOH. The resultant -COOH groups react with hydroxyl groups in lignocellulose material to form the composite material. Sodium hydroxide increases the rate at which hydrogen bonding are broken thus resulting in formation of free hydroxyl groups. This reduces the time taken for the cassava-based adhesive to be formulated and used to bind the lignocellulose material.

4.5 Mineralogical Composition of Starch, Lignocellulose and Composite Material Formed

Results from XRD analysis for the cassava peel starch, maize stalk, sugarcane bagasse, rice husks, and laboratory starch are shown in figure 4-8.

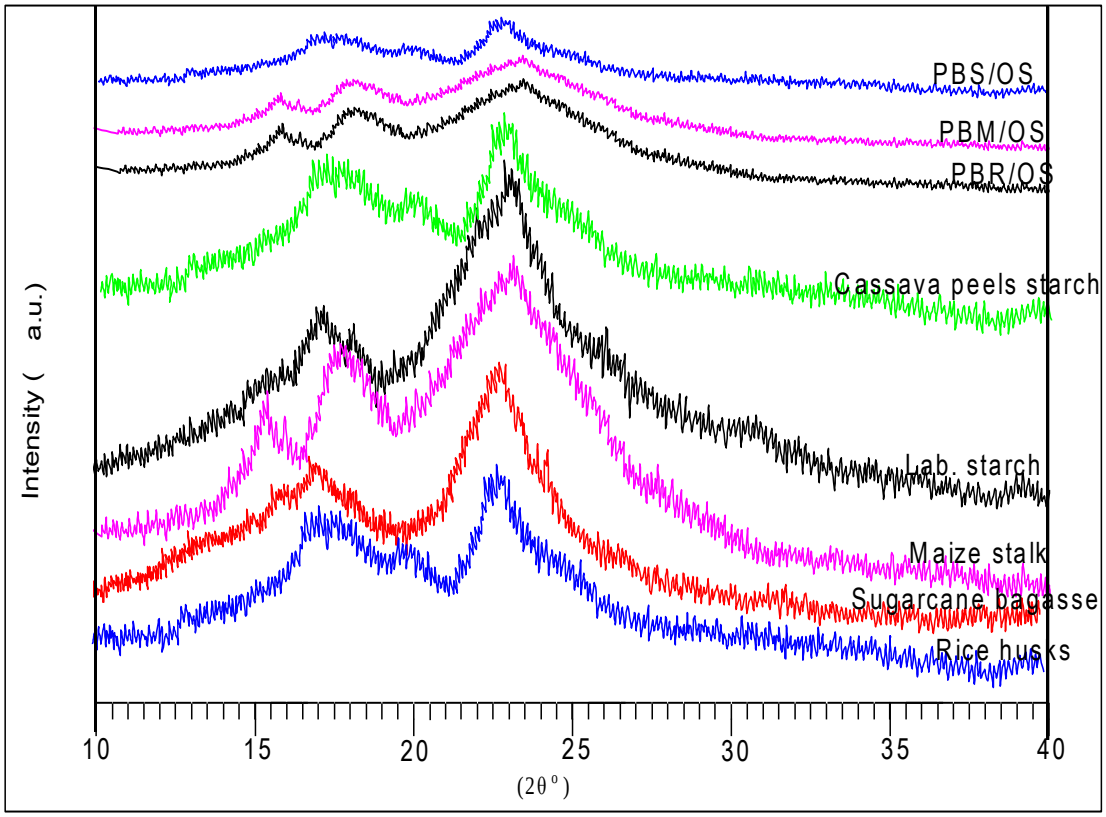

Figure 4-8. X-ray diffraction of rice husks, sugarcane bagasse, maize stalk, and lab starch

XRD patterns of untreated Sugarcane bagasse, rice husks, and maize stalk had peaks (2θ) at 15.3 °, 17.5 °, and 23.1° which are a typical identity of cellulose that cause crystallinity in biomass. Large peaks in cassava peels starch, laboratory starch and maize stalk are attributed to high contents of carbohydrates and cellulose (Rahman and Netravali, 2018a; Cengiz *et al*., 2016). Smaller peaks on rice husks and sugarcane bagasse are attributed to low cellulose content (Akhtar *et al*., 2016a; Wu *et al*., 2009a).

Crystallinity is attributed to hydrogen bonding in cellulose that combine with starch and lignocellulose materials. Decrease in the peak size shows the transformation after reaction between the cassava peel starch and lignocellulose materials. This is attributed to the incorporation of lignin from lignocellulose material to cassava peel starch and cellulose to form a composite material. Crystallinity is also attributed to amide linkages through covalent and hydrogen bonding in amino groups and -OH of cassava peel starch and -OH in cellulose. The intensity of the crystallinity depends

on the amount of cellulose. Change in the peaks size showed the coexistence of cellulose in both starch and lignocellulose material (Mandal and Chakrabarty, 2011).

Cassava peel starch showed a C-type crystalline structure. The cassava peel starch analysis showed a major peak of 2θ at 17.5°. The peak was attributed to the presence of amylopectin recrystallization (B-type crystallization) (Lemos *et al*., 2019). Amylose diffraction spectra were observed at 2θ = 23.1° denoted as V_H-type (Lemos *et al*., 2019; Obiro *et al*., 2012). Addition of lignocellulose material to cassava peel starch reduced the V_H –type peak due to lignin present (Sun *et al*., 2014). The reduction of the B-type crystalline form index was observed in all samples due to addition of the amorphous lignin content. The partial decrease in peak size due to the introduction of amorphous lignin in starch shows partial interaction between cassava peel starch and lignocellulose materials (Rahman and Netravali, 2018b). The above results were observed by Uthumporn, *et al.*,(2012) who were working on hydrolysis of cereal starch granules using sodium hydroxide (Uthumporn *et al.*, 2012).

XRD spectra for rice husks showed extra spectra at 2θ = 22^o which is attributed to silica in the form of SiO_2 and 25.23 ^{o} attributed to sodium silicate (Zhang *et al*., 2020; Ng *et al*., 2018; Zuo *et al*., 2015). Rice husks are known to have high ash content than the other materials under study. Further, the ash is documented to have a high silica content (Bakar *et al*., 2016). The same results were observed by Fernandes, *et al* (2017) while characterizing SiO_2 from RHA. Same results were observed during evaluation of amorphous SiO_2 from RHA which produced similar results (Paranhos and Santana Costa, 2018). Silica can be utilized in bonding by converting it to silicic acid. Silicic acid has been utilized as an adhesive and can be crosslinked with organic molecules through biomineralization (Zhou *et al.*, 2019).

The results above shows a reduction in crystallinity in cassava peels starch with the addition of lignocellulose material through copolymerization. Copolymerization through etherification and esterification between cassava peels starch and lignocellulose material form a covalent bond. This is attributed to the etherification of -OH groups from cassava peel starch and hydroxyl groups from phenolic groups in lignin from lignocellulose material. Covalent bonding is one of the major molecular bonds in the formulation of particleboards.

4.6 Chemical Characterization of Starch, Lignocellulose Material and Particleboards Using Fourier Transform Infrared Spectroscopy (FTIR)

FTIR results for raw cassava peel starch, oxidized cassava peel starch, lignocellulose materials sources, PBM/OS, PBR/OS and PBS/OS are shown in figure 4-9.

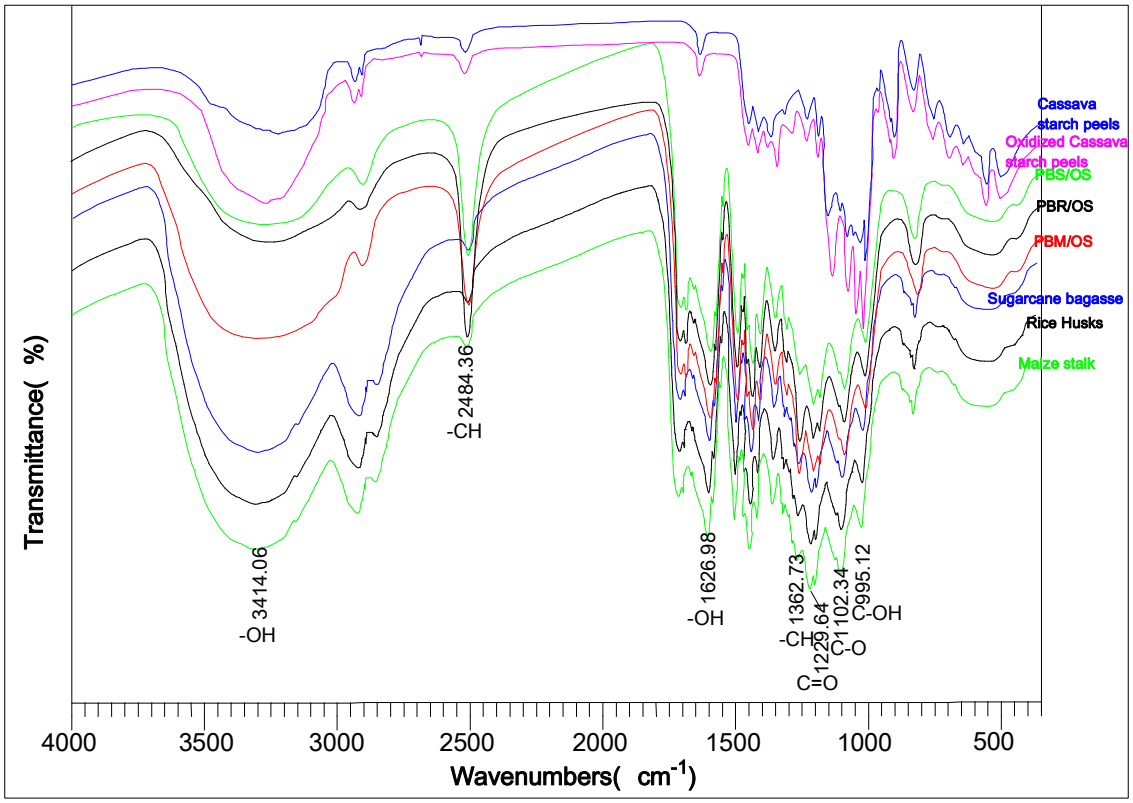

Figure 4-9. FTIR spectra for raw starch and lignocellulose sources and PBM/OS board

An interpretation of the FT-IR spectra from cassava peels, sugarcane bagasse and maize stalk, and rice husks particleboards formulated in this study are shown in Table 4-4.

Table 4-4. FTIR Analysis

Agricultural Waste Material/ particleboard	Wavelength range(cm^{-1})	Identified groups
Cassava peel	3500-3200	-O-H free groups and chemically bonded compounds such as alcohol, phenols, carboxylic acids
	3000-2850	Symmetric or asymmetric stretching of CH, CH_2, of aliphatic acids
	1750-1680	C=O stretching vibration of carboxylic groups
	1375-1300	C=O Stretching of carboxylic
	1300-1000	C-O of carboxylic acid (COOH)
Sugarcane Bagasse	3300	-OH from Polysaccharides
	2885	-CH symmetrical stretching Polysaccharides
	1732	-C=O stretching Xylans
	1650-1630	-OH water
	1335	-C-O in Cellulose
	1162	-C-O-C asymmetrical stretching Cellulose
	670	-C-OH bending Cellulose
Maize stalk	1724	C=O stretching vibrations
	1325-1031	SiO_2 stretching vibrations
Rice Husks	3300	-OH broad band
	2925	C-H vibration
	1738	The vibration of carbonyl from carboxylic groups in ester link
	1839	Carbonyl
	1217	-Si-O
Particleboards	3414.06	-OH Bending
	2484.36 and 1362.73	-CH bending
	1229.64	C=O stretching
	1102.34	C-O
	1150 and 950	B-OH

The peak attributed to the hydroxyl group is observed at 3414.06 cm^{-1}. Hydroxyl forms hydrogen bonding with water in a single bridge (Nishida and Fayer, 2017) and another major peak associated with the hydroxyl group was also observed at 1626.98 cm^{-1}. Peaks attributed to a C-H bond were observed at 2484.36 cm^{-1} and 1362.73 cm^{-1}. At a wavenumber 1229.64 cm^{-1} a peak was associated with the vibration of C=O and another peak at a wavelength of 1102.34 cm^{-1} attributed to stretching of C-O. The condensation reaction between carboxylic groups in cassava peels starch and hydroxyl groups from lignocellulose materials (Yamada *et al*., 2001). This reaction

leads to a reduction of OH peaks at 3414.06 cm^{-1} and at 1626.98 cm^{-1} and an increase of C-O at 2484.36 cm^{-1}.

Ester formation results in the reduction of -OH as the peak is attributed to the formation of esters that is mainly that of C-O in C-O-C. The –OH peak that remained is associated with hydroxyl groups from sodium hydroxide that was used during the treatment of lignocellulose material and cassava peel starch and water produced during condensation reaction of lignocellulose material, cassava peels starch and boric acid. Increase of the C-H peak results from a combination of C-H in cassava peel starch and lignocellulose materials. Peaks for B-OH from hydrolyzed sodium borate were observed at 1150 cm^{-1} and 950 cm^{-1} (Altan *et al.,* 2019).

Borax hydrolyzes in deionized water to form the equilibrium of boric acid and borate ion solution , as shown in equation 4.1 to 4.3 (Altan *et al.*, 2019).

$$B_4O_{7(aq)}^{2-} + H_2O_{(l)} \rightarrow HB_4O_{7(aq)}^{-} + OH_{(aq)}^{-} \quad 4.1$$

$$B_4O_{7(aq)}^{2-} + H_2O_{(l)} + 2H_{(aq)}^{+} \rightarrow 4B(OH)_{3(aq)} \quad 4.2$$

$$B(OH)_{3(aq)} + H_2O_{(l)} \rightarrow H_{(aq)}^{+} + B(OH)_{4(aq)}^{-} \quad 4.3$$

Starch reacts with borax as shown in equation 4.4 (Ali *et al*., 2012).

$$(C_6H_{12}O_6)_n + NaB_4O_7.10H_2O \rightarrow C_6H_{12}B_4O_{11} + \tfrac{1}{2}O_2 + (Na_2O + 10H_2O) \quad 4.4$$

The peak formed at 1075 cm^{-1} and 725 cm^{-1} is associated with Si-O. Si-O is produced from the reaction between silica in rice husks and sodium hydroxide. The reaction is shown in equation 4.5 and 4.6 (Kamseu *et al*., 2017; Jendoubi *et al*., 1997).

$$NaOH_{(aq)} + SiO_{2(s)} \rightarrow Na_2O.SiO_{2(aq)} + H_2O_{(l)} \quad 4.5$$

$$Na_2O.SiO_{2(aq)} + 3H_2O_{(l)} \rightarrow 2NaOH_{(aq)} + H_4SiO_{4(aq)} \quad 4.6$$

Silicic acid undergoes polycondensation reaction in the following ways, as shown in equations 4.7 and 4.8 (Zhang *et al*., 2020; Annenkov *et al.*, 2017).

$$OH_{(aq)}^{-} + (OH)_3Si - OH_{(aq)} \rightarrow (OH)_3Si - O_{(aq)}^{-} + H_2O_{(l)} \quad 4.7$$

$$(OH)_3Si - OH_{(aq)} + (OH)_3Si - O_{(aq)}^{-} \rightarrow OH_{(aq)}^{-} + (OH)_3Si - O - Si(OH)_{3(aq)} + OH_{(aq)}^{-} \quad 4.8$$

NaOH shifts -OH group stretching vibrations from low frequencies to higher frequencies. Higher frequencies are related to free –OH groups which does not take

part in hydrogen bonding. Silication has been used to combine cellulose from the cotton fiber with hydrolyzed silica during cotton fabric processing (Shateri-Khalilabad *et al.*, 2017).

FTIR analysis of soy-lignin adhesive showed results similar to those observed in particleboards formulated on major functional groups in the bio-based adhesive (Nasir *et al.*, 2014). Peak due to –OH was observed between 3300 and 3500cm^{-1} reduced considerably during particleboard formulation in the study. This observation is related to the transformation of –OH during a chemical reaction. Reduction in peak size is due to ester formation. Peaks observed between 1420 cm^{-1} to 1430 cm^{-1} were related to C-OH which explains the existence of crystals over the amorphous nature structure of molecules (Oh *et al.*, 2005). Peak intensity and peak position of –OH around 3400cm^{-1} changed due to the formation of an ester (Umemura *et al*., 2012).

The above results show bond formation as a result of esterification between carboxylic groups from cassava peels starch and hydroxyl groups from lignocellulose material. Silication process refer to the reaction between hydroxyl groups from silicic acid with carboxylic groups from cassava peels starch. Crosslinking of starch with hydrolyzed borax through condensation reaction between hydroxyl groups from borate and lignocellulose material form ether linkage. These are the major bond formation that resulted in particleboard formulation.

4.7 NMR Analysis Results for Raw Materials and Formulated Particleboard

Results of NMR analysis for maize stalk, sugarcane bagasse, rice husks, and formulated particle boards are presented in figure 4-10.

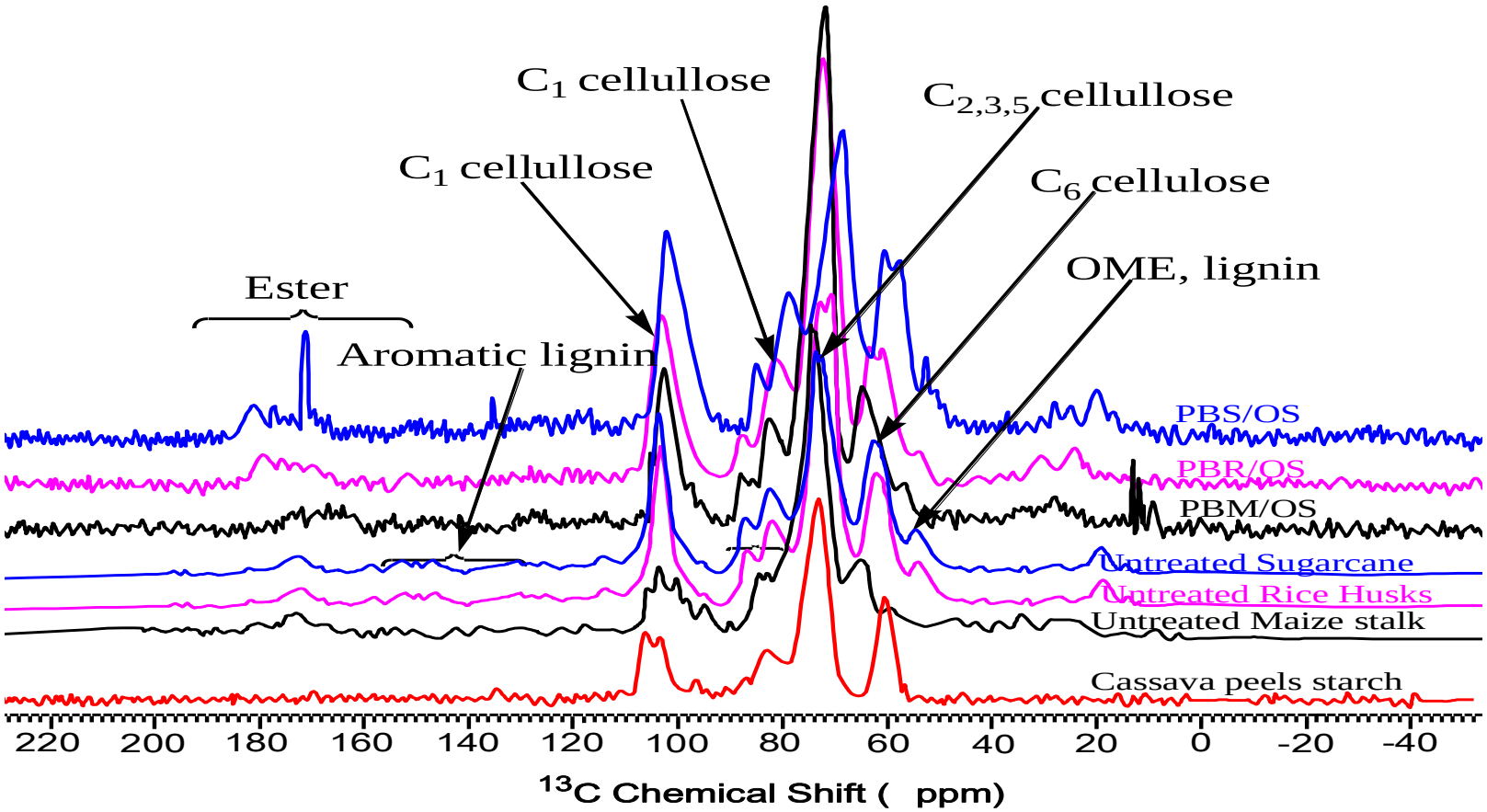

Figure 4-10. NMR spectra of lignocellulose material, starch and formulated particleboards

The major chemical shifts in NMR spectra are shown in table 4-5.

Table 4-5. MAS ^{13}C NMR chemical shifts and attributed functional groups

^{13}C chemical shift (ppm)	Chemical group
11.5	RCH_3
24.7	CH_3, C in R_2CH_2
25.4	C in R_2CH_2
32.9	C in CH_3CO
42.3	C in RCH_2NH_2
46.9	C in R_2CH_2
46.9	Ethoxy (CH_3CO), hydroxylamine, oximes, hydroxamic acid
57.4	C in RCH_2OH of C6 carbon of crystalline cellulose
64.6	C in RCH_2OH
72.4	C_2, C_3, and C_5 of cellulose and hemicellulose and hemicellulose and $OC_\alpha H_2$ carbons of lignin
82.0	Alkynes and hemicelluloses $OC_\alpha H_2$ carbons of lignin
88.6	C in RCH_2O
104.8 and 119.4	C in alkene
116.0 and 146.0	C_1 and C_6 associated with aromatic and carbon of double bonds
128.8, 137.0, 145.3, and 150.8	Alkene and aromatic in lignin and its derivative
131.0	Alkene
172.0 and 176.0	Carbonyl in ester and acid and carbonyl
128.8, 137.0, 145.3, 150.8	C in alkene aromatic
167.8, 170.3, 171.8, 172.8, 177.2 and 181.4	carbonyls in ester and carboxylic acid

Particleboards formulated from sugarcane bagasse showed a peak at 24.7 ppm associated with CH_3 in acetyl groups of hemicelluloses and lignin. This peak is associated with CH_3CO, hydroxylamines, oximes and hydroxamic acids. At 46.0 ppm, a peak was observed that is related to disilene. At 64.0 ppm a peak associated with CH_2- in RCH_2OH was also observed from C_6 carbon of crystalline cellulose. Peaks between at 60 to 105 ppm were due to carbohydrates from starch, cellulose, and hemicellulose. An increase in the peak size is as a result from the combination of starch, cellulose, lignin and hemicellulose molecules (Nordqvist, 2012). Other peaks observed were at 72.0 ppm

associated with C_2, C_3 and C_5 of cellulose and hemicellulose. Spectra between 60.0 to 80.0 ppm are attributed to the etherification of aromatic rings (Yuan *et al.*, 2011). A peak at 82.0 ppm associated with alkynes, 116.0 ppm and 146.0 for C_1 and C_6 associated with aromatic and carbon of double bonds on the side chain. A peak at 131.0 ppm is associated with an alkene, 172.0 and 176.0 ppm were observed for carbonyl in ester and acid and carbonyl. NMR peaks around 170.0 ppm are a result of aliphatic esters and aliphatic carbonyls (El Hage *et al.*, 2009).

Particleboards formulated with rice husks and modified starch showed prominent peaks at 11.5 which is associated with RCH_3. A peak at 25.4 ppm is attributed to C in R_2CH_2. A peak observed at 32.9 ppm was attributed to CH_3CO- whereas at 42.3 ppm associated with C in RCH_2NH_2. A peak at 57.4 ppm is associated with C in the methoxy group (Capanema *et al.*, 2005) and 64.6 ppm associated with C in RCH_2OH of C_6 carbon of crystalline cellulose, 72.3 and 82.4 ppm associated with C in alkynes and hemicelluloses (Hult *et al.*, 2002). A peak was observed at 88.6 ppm is associated with the presence of C in RCH_2O-, 104.8 and 119.4 ppm associated with C in alkene, 128.8, 137.0, 145.3, and 150.8 ppm associated with aromatic rings of lignin (Hazwan *et al.*, 2019). Spectral lines observed at 167.8, 170.3, 171.8, 172.8, 177.2 and 181.4 ppm are associated with carbonyls in ester and carboxylic acid.

Particleboards formulated with maize stalk major spectra peaks at 24.7 ppm associated with R_2CH_2, 46.9 ppm for C in RCH_2NH_2, 64.6 ppm for C in RCH_2OH. The strong peak at 58.0 to 68.0 ppm is associated with C_6 (Tan *et al.*, 2007), 72.4 ppm from C_2 C_3, C_5 of cellulose. Peaks between 68.0 to 78.0 ppm are brought about by the interaction of C_2, C_3, C_5 during the reaction between hydrolyzed starch and high amylose starch (Qin *et al.*, 2019). A peak at 82.5 ppm was observed and is associated with C in alkynes, 104.6 ppm associated with C_1 of single helix part in starch granules, 116.6, 131.7 and 146.1 ppm are attributed to the presence of aromatic rings of lignin. 172.7 and 176.5 ppm are identified with carbonyls in ester and carboxylic acid.

Spectrum observed on sugarcane bagasse, rice husks and maize stalk showed the presence of signals at 21.6 ppm and 173.7 ppm evident that hemicellulose is present. The spectra observed at 50.0 ppm to 120.0 ppm attributed to hemicellulose and cellulose carbons (Spaccini *et al.*, 2016). There were slightly changed due to delignification during sodium hydroxide treatment. Cellulose extracted from sugarcane was identified with the following peaks: 64.8 ppm. 62.4 ppm, 72.5 to 74.8 ppm, 82.3 to 83.7 ppm, 88.8 ppm and 104.7 ppm (Sun *et al*., 2004a). Signals at 62.5 ppm, 64.8 ppm, 83.5 ppm and 87.9 ppm were attributed to carbons in cellulose. Peaks related to lignin are observed from 100.0 ppm to 200.0 ppm. Signals at 21.5 ppm and 173.6 ppm were associated with hemicellulose and that observed at 56.3 ppm was due to $-OCH_3$ found in the lignin molecule (Rezende *et al.*, 2011).

The appearance of peaks related to carbonyl groups in esters and polypeptide bonds is attributed to the reaction between cassava peels starch and lignocellulose material. Carbonyl groups are produced through the reaction between carboxylic acid groups from starch and hydroxyl groups from aromatic groups of lignin, cellulose and hemicellulose through a condensation reaction. Polypeptide bond is formed from the reaction between amine groups from crude proteins in cassava peels starch and hydroxyl groups from lignocellulose material through a condensation reaction. Condensation reaction results in copolymerization between natural polymers in lignocellulose material and cassava peel starch that was used in the formulation of the particleboards. Results above shows esterification as one of the major processes of combining cassava peel starch and lignocellulose materials. Esterification led to formation of strong covalent bonds between starch and lignocellulose materials.

4.8 Morphological Analysis of Starch and Particleboards

Results on morphological analysis of untreated cassava peel starch are shown in figure 4-11.

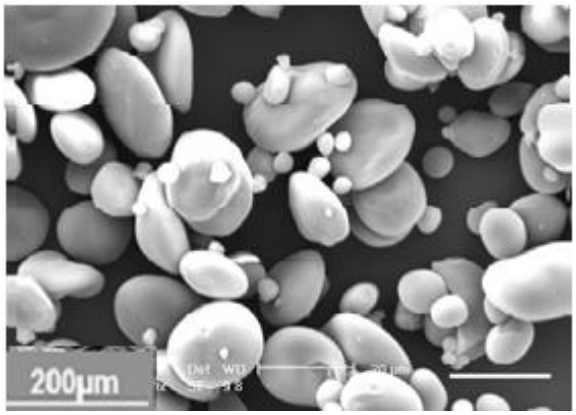

Figure 4-11. SEM analysis of raw Starch from cassava peels

Cassava peels starch exists in mixed patterns of elliptical-shape, round crystalline form and amorphous parts. Different shapes are related to hydrogen bonding in amylose molecules and amylopectin molecules. Hydrogen bonding exists between O-3 and OH-3 of D-glucosyl of amylopectin. Hydrogen bonding also exists between amylose and amylopectin. Pores increase the surface area where the chemical reaction occurs. Porosity significantly influences starch chemical reactivity (Sujka and Jamroz, 2010). Microscopic pores make the surface of cassava peel starch appear smooth. Molecules in the starch granules and amorphous region contain hydroxyl groups that are required during the chemical reaction. Break down of the crystalline nature of the granules increases the surface area of starch molecules.

Results on morphological analysis of gelatinized starch is shown in figure 4-12.

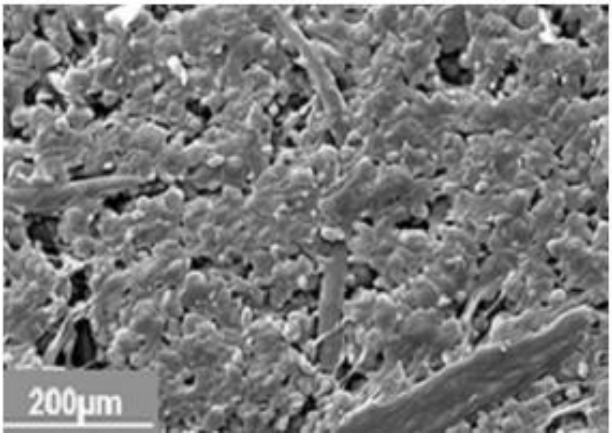

Figure 4-12. SEM image for gelatinized starch

Figure 4-12 shows the dispersion of starch granules in sodium hydroxide solution. Sodium hydroxide promotes swelling and dispersion of starch granules. Chemical treatment of starch with sodium hydroxide was utilized to form a gel that exposes the -OH groups used during copolymerization. NaOH reacts with cassava peel starch to form sodium salts. The formation of sodium salts breaks up the hydrogen bonding between starch molecules leading to exposure of more hydroxyl groups (Yamamoto *et al.*, 2006; Tako and Hizukuri, 2002). Morphological changes are attributed to the transformation of some OH to $O^{-}Na^{+}$ and alkali hydrolysis of some glycoside bonds. NaOH reduce the rigidity of cassava peel starch and stability. The mobility of cassava peels starch leads to loss of granule nature (Cardoso, 2007). Gelatinized starch was used as a binder in this study.

Results for SEM analysis of formulated particleboards with sugarcane bagasse, maize stalk and rice husks bound with oxidized starch are given in figure 4-13.

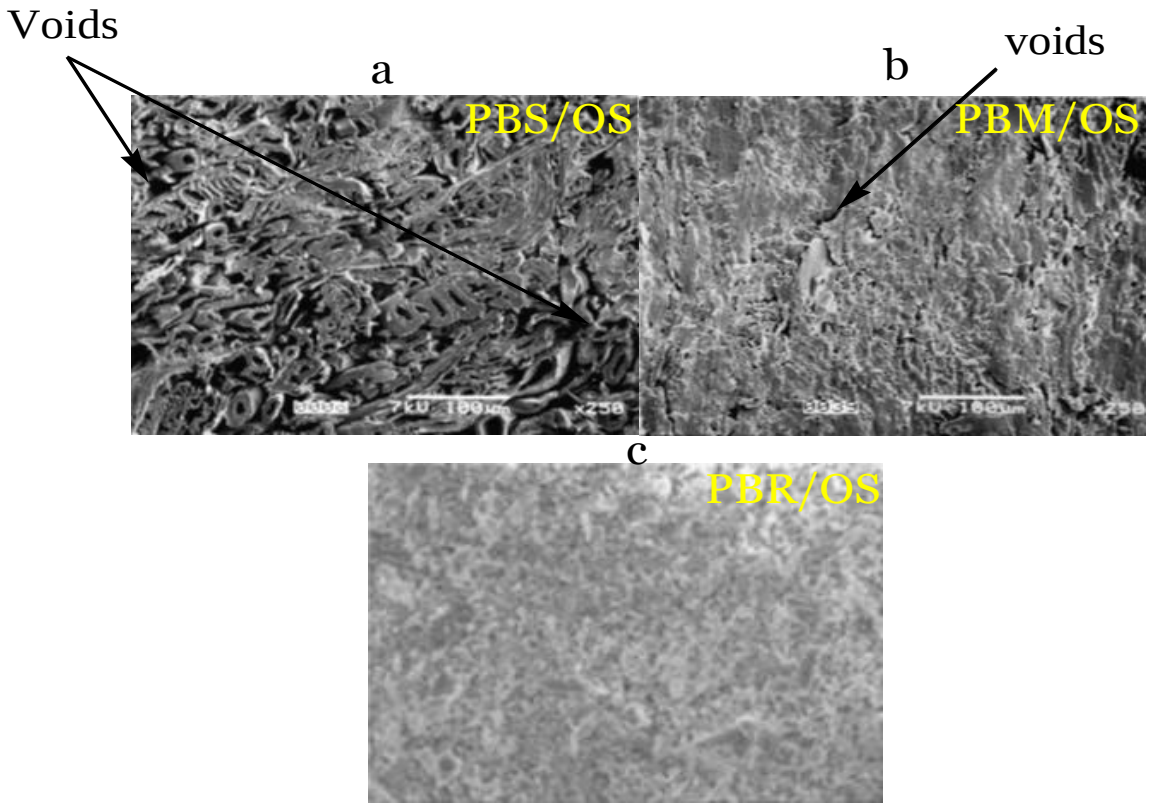

Figure 4-13. Analysis of the formulated particleboards

SEM analysis of surfaces of the particleboards formulated in this study is given in figure 4-13 (a-c). All particleboards showed an interaction between gelatinized starch and the lignocellulose materials. The variation in density is attributed to the reaction between starch and the lignocellulose material. SEM analysis for the particleboards showed larger voids between the sugarcane bagasse fiber materials and cassava peels adhesive. Voids are formed due to insufficient interaction between lignocellulose material and the adhesive. Sugarcane bagasse had the highest lignin content among the three lignocellulose material. Lignin is hydrophobic with few hydroxyl groups that are used in bonding with starch molecules. Low cellulose content reduces the binding area of adhesive. Particleboards formulated with sugarcane bagasse appeared rough due to protrusions roughness of the lignocellulose material used. Carboxylic groups in oxidized starch react with –OH of the lignocellulose material. Starch hydrolysis with sodium hydroxide only broke the hydrogen bonding. Gelatinized starch was trapped in the sugarcane bagasse matrix resulting in a lower degree of penetration. Interaction between two polymers reduces the mobility of an adhesive (Mokhena *et al.*, 2018).

SEM micrographs of particleboards formulated with maize stalk showed smaller voids between lignocellulose material and adhesive. The presence of cellulose and hemicellulose fillers provided extra interaction sites between lignocellulose material and the adhesive. Cellulose content increases fiber tensile properties through oxidation (Williams *et al.*, 2011). Carboxylic groups from cassava peel starch (Warui *et al*., 2019; Potthast *et al*., 2006) react with hydroxyl groups in lignocellulose materials to form covalent bondage by esterification. Particleboards formulated from maize stalk showed smooth surfaces due to cementation from hemicellulose and lignin. Similar studies of the rice husks treatment using sodium hydroxide were obtained (Ciannamea *et al*., 2010)

SEM analysis of particleboards formulated with rice husks showed an undulated surface due to regularly spaced conical-shaped protrusion and bright spots of treated silica. This is due to the treatment of silica with sodium hydroxide to form sodium silicate. Small pores are associated with the cementing of cellulose and hemicellulose. Sodium silicate acts as an adhesive and filler for voids to make the surface have a smoother appearance.

Images in SEM analysis explain the different spectral lines in NMR analysis. The reaction between the cassava peel adhesive and lignocellulose material relates to the difference in appearances on the surface of the particleboard formulated. The peak at 72.3 ppm increased from those of raw materials to those of particleboards. The change is associated with the combination of cellulose and starch materials. The interaction between maize stalk and cassava peel starch showed the highest peak. The interaction between lignocellulose material and the modified cassava peel starch determines the mechanical properties of the formulated particleboards. Higher compatibility results in a higher MOR. The reaction between rice husks and cassava peels starch as clearly indicated in NMR spectra, gave the highest MOR and IB. MOR is determined by bonding strength in composite material (Singha and Thakur, 2010).

The results shown in figure 4-13 suggests the interaction between cassava peel starch and lignocellulose material. Voids are attributed to reaction between carboxylic groups in cassava peel starch with hydroxyl groups of cellulose, lignin and hemicellulose (Dai *et al*., 2005). Voids present in particleboards can be used to explain the levels of interaction between the lignocellulose materials and cassava peels starch (Boon *et al*., 2019). Boards formulated using rice husks were observed to have smaller voids compared to other particleboards formulated from sugarcane bagasse, maize stalk bound with oxidized starch. This was attributed to the reaction between carboxylic and hydroxyl groups from starch with hydroxyl groups from silicic acid, lignin, cellulose and hemicellulose (Zhang *et al*., 2020; Annenkov *et al*., 2017; Alessandra *et al*., 2015). Maize stalk consists of hydroxyl groups from cellulose, hemicellulose and lignin that reacted with carboxylic and hydroxyl groups in starch molecules (Mtibe *et al*., 2015). Sugarcane bagasse had a higher content of lignin which implies that few hydroxyl groups were available for reaction with carboxylic and hydroxyl groups in cassava starch (Jonglertjunya *et al*., 2014). Hydrolyzed rice husk has more reaction sites compared with maize stalk and sugarcane bagasse.

4.9 Thermal Conductivity Analysis

Results on thermal conductivity for the particleboards formulated are shown in figure 4-14.

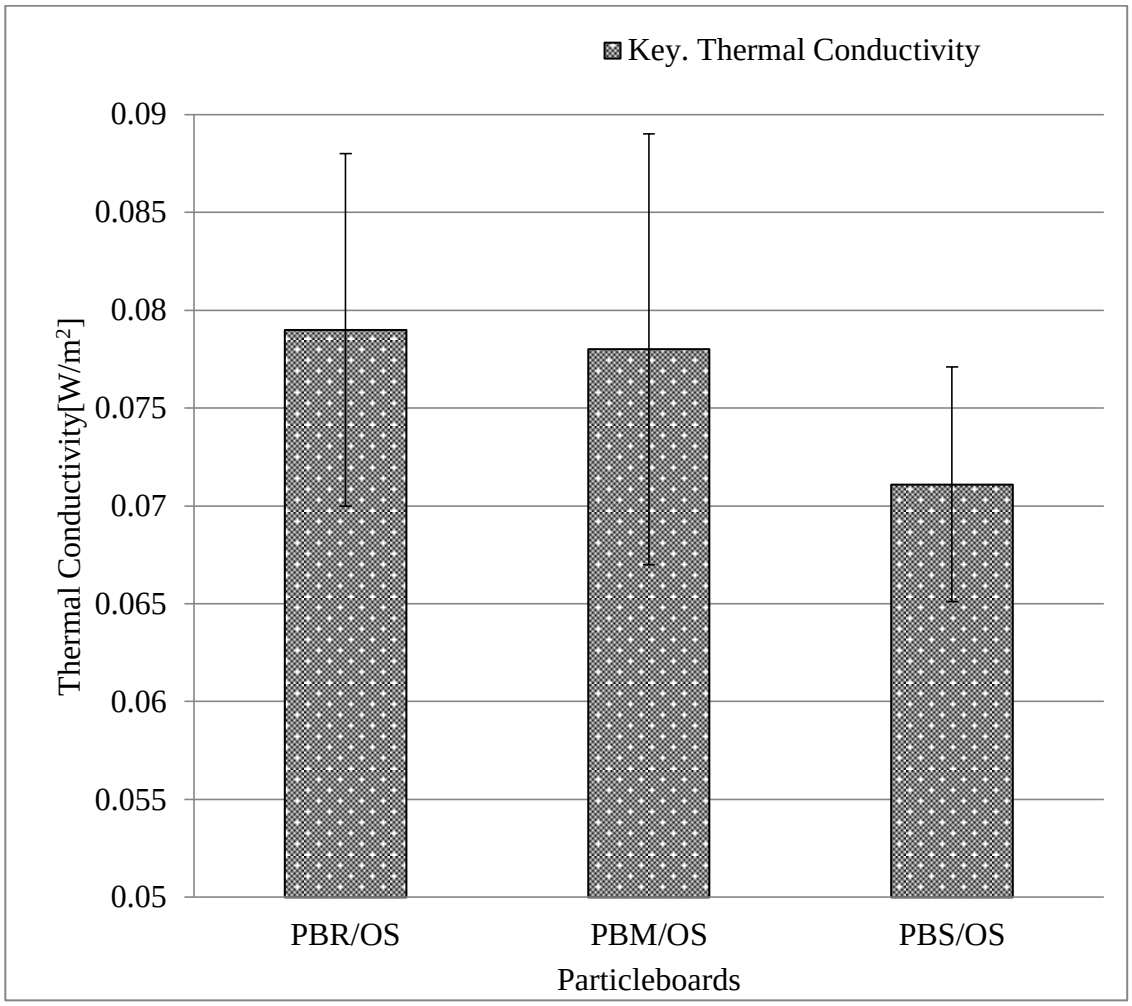

Figure 4-14. Thermal conductivity for the particleboards

Thermal conductivity for PBR/OS was highest with 0.079 W/m^2 and PBS/OS with lowest with 0.071 W/m^2. This is attributed to the differences in densities. The density of PBR/OS was higher than those of PBS/OS. Thermal conductivity is affected by the number of voids in the particleboard. Decrease in voids results into increase in thermal conductivity (Khedari *et al*., 2003). Similar results on the study of wood-gypsum boards showed lower thermal conductivity for particleboards with large voids.

Khedari *et al.* (2003) observed that different lignocellulose materials affect thermal conductivity of the particleboard. This observation was attributed to size of the voids in the particleboards (Khedari *et al*., 2003). Thermal conductivity of medium density particleboards range from 0.054 $Wm^{-1}K^{-1}$ to 0.13 $Wm^{-1}K^{-1}$ (Ferrandez-Villena *et al*., 2020). Efficiency of particleboards insulation against heat was observed also to be inversely proportion to the density of the particleboards (Aravind *et al*., 2019). Results above suggest that all particleboards can be used for internal room partitioning purposes. Low thermal conductivity makes particleboards formulated in this study suitable for interior heat insulation. Interior applications involve room partitioning and making doors.

4.10 Formaldehyde Emissions from Formulated Particleboard

Results for formaldehyde emissions from formulated particleboards are shown in figure 4-15.

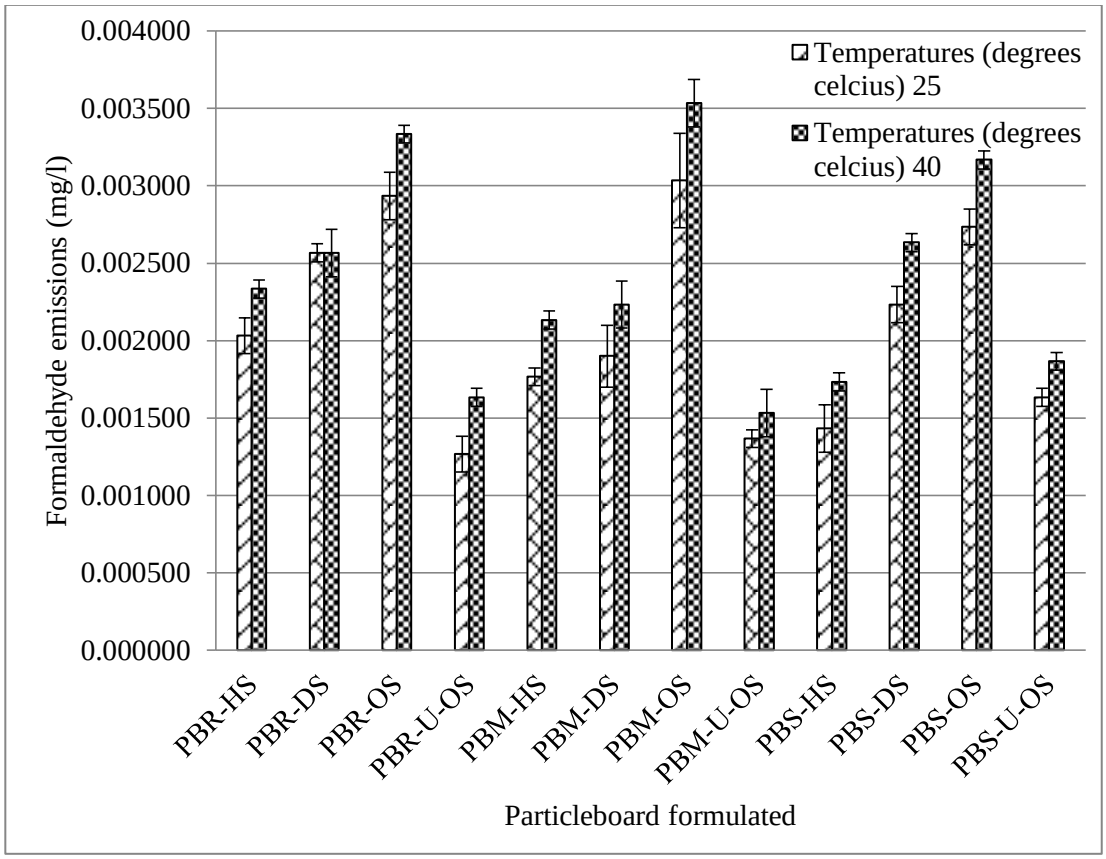

Figure 4-15. Formaldehyde emissions from formulated particleboards

Results on figure 4-15 showed formaldehyde emissions below the maximum allowed which is less than 0.05 mg/l (Bohm *et al*., 2012). Formaldehyde emitted at 40 ^{o}C was higher than those obtained at 25 ^{o}C. Higher temperatures increase formaldehyde emissions (Myers, 1985). Formaldehyde emissions has been observed from flooring materials at 23 and 29 ^{o}C that range from 0.005 to 0.03 mg/l (Bohm *et al*., 2012). Particleboards formulated with urea gave lower formaldehyde emissions compared to other particleboard samples. Urea has been used as a formaldehyde scavenger used to reduce the free formaldehyde to form urea-formaldehyde (Costa *et al*., 2013). Particleboards formulated in this study therefore meet minimum emission requirements and thus may not pause a health risks.

4.11 Physical Properties of Particleboards

Results of density, MC, WA, TS, IB, MOR and MOE for optimized particleboards from the optimized starch-lignocellulose materials are presented in this section.

4.11.1 Densities of Particleboard

Results for densities of formulated particleboards are shown in figure 4-16.

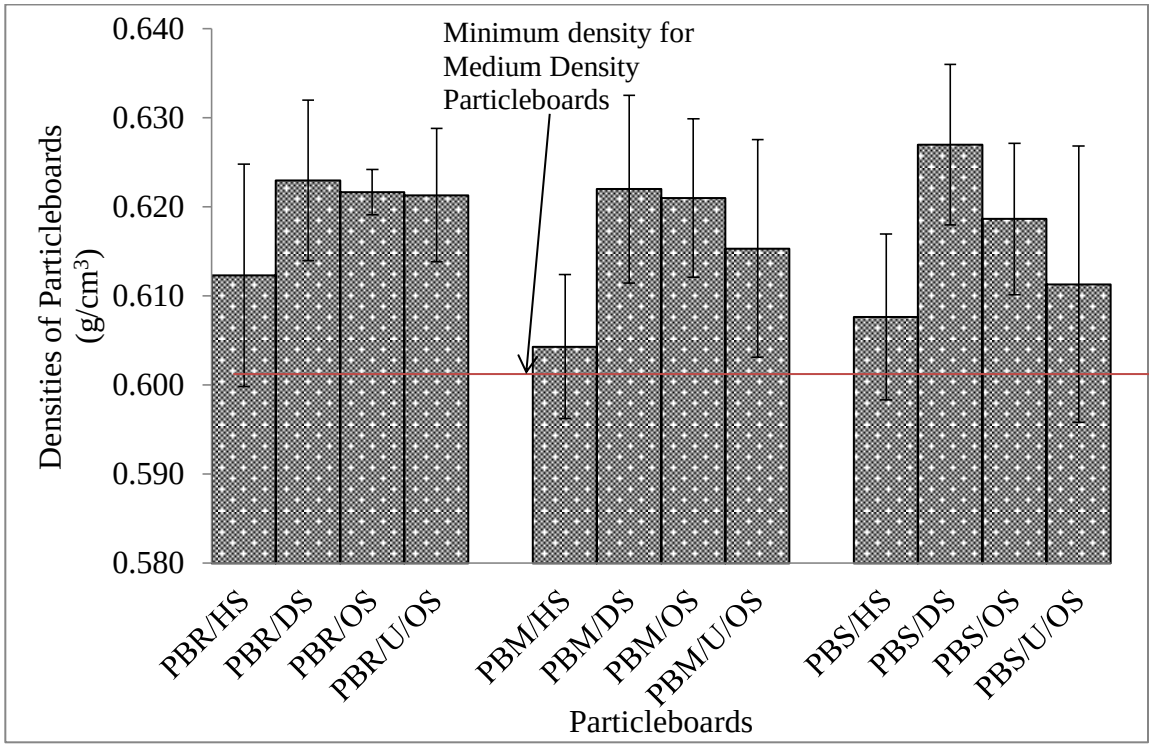

Figure 4-16. Average densities of particleboards

Average densities of the particleboards made using the three lignocellulose materials using different modified cassava peel starch as binders ranged from 0.604 gcm^{-3} to 0.627 gcm^{-3} respectively. Particleboards formulated using dextrinized cassava peel starch showed the highest densities with sugarcane bagasse, maize stalk and rice husks. Densities of the particleboards are dependent on the interaction between cassava peels starch and lignocellulose materials that were used in particleboard formulation. An increase in interaction leads to a reduction of the voids thus increasing the compaction of material hence density increases.

Dextrinized cassava peel starch consists of a large number of free –OH (Srivastava *et al*., 1970). Particleboards formulation involves the esterification process where carboxylic groups in cassava peel starch react with hydroxyl groups in lignocellulose material which results in the formation of covalent bonds. Another source of adhesion involves bondage between the hydroxyl groups in the composite material that is mainly through hydrogen bonding. Adhesion brings cassava peels starch molecules and lignocellulose materials together thus reducing spaces within composite material hence the density increases (Edhirej *et al*., 2017).

Hydrolyzed cassava peels starch has fewer hydroxyl groups. The hydroxyl groups react with sodium hydroxide to form sodium salt (Rachtanapun *et al.*, 2012) as shown in equation 4.9.

$$St - OH + NaOH \longleftrightarrow St - ONa + H_2O \qquad 4.9$$

Reduction in the number of free hydroxyl groups in hydrolyzed cassava peel starch reduces the interaction sites with lignocellulose. Reduction in the interaction increase the size of voids hence reduction in the volume of the formulated particleboards. Interaction between cassava peel starch and rice husks was even more due to the silication process compared to the other lignocellulose materials.

From the results, it is observed that particleboards in this study fall in the category of medium density that ranges between 0.5 to 0.6 gcm^{-3} according to US Standards

ANSI/A208.1 for medium density boards. Razak *et al* (2013) observed that particleboards formulated with oil palm trunks stems gave densities ranging from 0.441 gcm^{-3} to 0.597 gcm^{-3} (Razak *et al.*, 2013). Low variations in density lead to reliability in measuring MC, particleboards specific mass, MOE, MOR and IB. The difference between densities reported in Razak *et al* (2013) study with the ones in this study is brought about by the treatment of lignocellulose material. Alkaline treated lignocellulose materials activate the hydroxyl groups that react with hydroxyl and carboxylic groups thus increasing the interaction between adhesive and lignocellulose material.

4.11.2 Particleboards Moisture Content (MC)

Results for moisture content (MC) for various particleboards formulated are presented in figure 4-17.

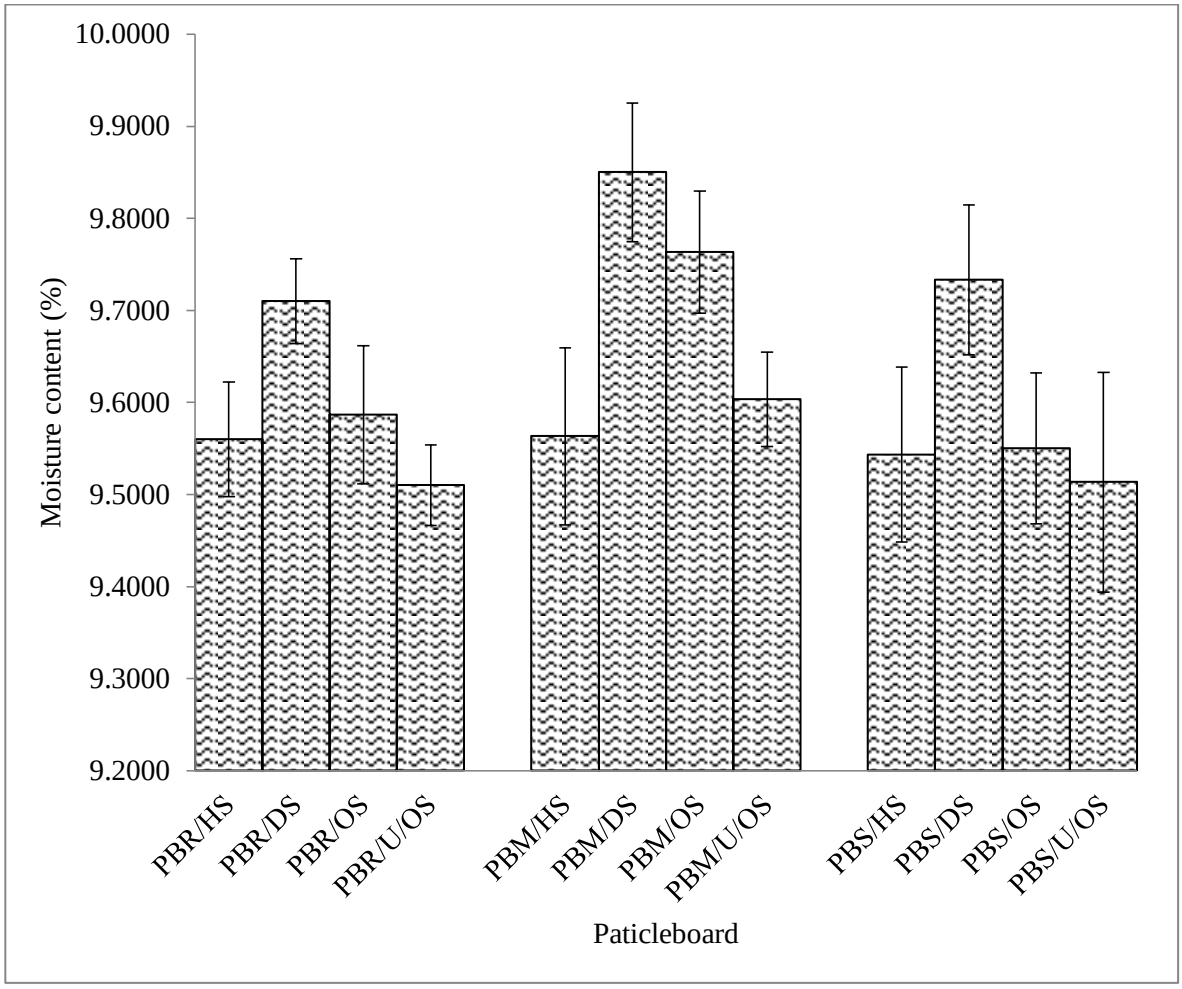

Figure 4-17. Moisture content in the formulated particleboards

PBM/DS showed the highest moisture content of 9.85 % and PBR/U/OS showed the lowest MC with 9.51 %. Lower moisture content is attributed to lower number of free hydroxyl groups. Hydroxyl groups used up during esterification thus reducing their numbers. Moisture content between PBR/HS and PBS/HS showed no significant difference. An increase in moisture in fiber leads to an increase in thickness swelling (TS). An increase in TS results in the weakening of bonding between lignocellulose material and cassava peel starch (Atiqah *et al*., 2017). WA results in the weakening of MOE, MOR and IB of particleboards (Joseph *et al*., 2002).

Heat transfer from composite material helps in the curing of the binder (Sam-Brew and Smith, 2017). Particleboards with high MC were also observed to have high densities. Lowest MOR was recorded from the particleboard with the highest MC. Particleboard made with maize stalk and dextrinized cassava peel starch gave the highest MC. Water absorbed by particleboards results in hydrolysis of ester bondage that holds composite material together. This results to reduction of the interaction between lignocellulose material and starch which weakens the strength of particleboards. Dextrinization of cassava peel starch breaks down molecular chains in the starch granules (Srivastava *et al.*, 1970). The MC in composite materials depends on the free hydroxyl group (Rautkari *et al.*, 2013).

A composite material made with rice husks and oxidized cassava peel starch and urea showed the lowest MC. Urea contain amine groups that react with hydroxyl and carboxylic groups to form covalent bonds. Sodium silicate formed from the reaction between silica with sodium hydroxide undergoes hydrolysis forming silicic acid (H_4SiO_4). H_4SiO_4 reacts with cassava peel starch through silication that enhances cross-linking with cassava peel starch. Particleboard formulated with maize stalk showed higher porosity than in sugarcane bagasse and rice husks due to high number of unused hydroxyl groups (Olumoyewa *et al.*, 2019)

Particleboards formulated from wood, bamboo and rice husks contained moisture content that ranges from 8.3 % to 8.8 % (Diego *et al.*, 2014). Particleboards formulated with sugarcane bagasse- wood particles and UF as an adhesive gave MC that range from 8 % to 12 % (Dahmardehghalehno and Bayatkashkoli, 2013). Boards made from kenaf particles bound with urea-formaldehyde had an MC that ranges from 8 % to 10 % (Allal *et al.*, 2010). The moisture content which ranged from 9.51 % to 9.85 % reported in this study compared well with those obtained from other research done.

4.11.3 Thickness Swelling (TS) of Particleboards

Results on thickness swelling (TS) for various particleboards formulated are as shown in figure 4-18.

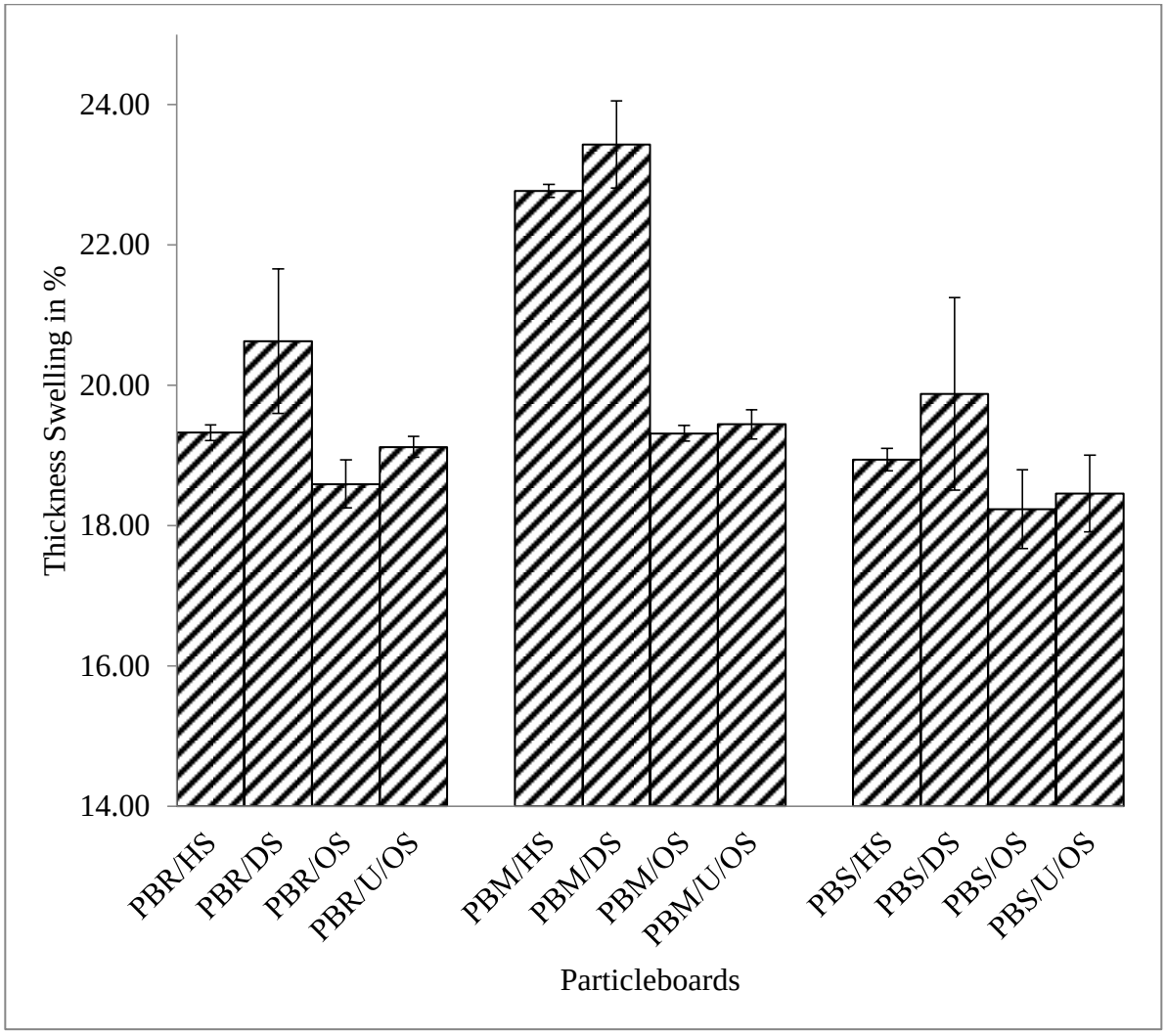

Figure 4-18. Thickness swelling (TS) for the particleboards

Particleboards formulated with maize stalks and dextrinized cassava peel starch gave the highest TS of 23.43 %. Dextrinized cassava peel starch consists of a high number of free -OH that interact with H_2O. This is attributed to the presence of the cellulose material present in maize stalk. Cellulose is a form of carbohydrate that consists of a high number of hydroxyl groups. Particleboards formulated with dextrinized cassava peel starch with maize stalk gave TS of 27.08 % that was the highest whereas those made with sugarcane bagasse and oxidized cassava peel starch showed the lowest TS of 18.23 %.

Dextrinized cassava peel starch involves only the breaking of hydrogen bonding (Srivastava *et al*., 1970). This implies the numbers of free hydroxyl groups are more. This also increases the TS of the resulting particleboards. A combination of dextrinized starch with maize stalk gave the overall highest TS. This is due to cellulose and hemicellulose that consist of a higher percentage compared to lignin content. Cellulose and hemicellulose contain free hydroxyl groups in their molecules, therefore the combination of dextrinized starch and maize stalk contains a higher number of hydroxyl groups that translate to overall high TS. Treatment of starch reduces hydroxyl functional groups thus difference in TS. Hydrolyzed starch gave lower TS as hydrogen in one hydroxyl group is replaced with sodium. The presence of sodium reduces the interaction of starch with water through hydrogen bonding. Oxidation of starch reduces the presence of hydroxyl groups by converting them to carboxylic groups. Carboxylic groups react with hydroxyl groups in maize stalk to form an ester. Esters are hydrophobic in nature. The addition of urea in oxidized starch introduces amine groups that enhance hydrogen bonding between urea and water. This leads to the interaction of water with the particleboards formulated.

Particleboards formulated with sugarcane bagasse with dextrinized cassava peel starch showed similar trends to those made from maize stalk and dextrinized cassava peel starch. Particleboards from sugarcane bagasse and dextrinized cassava peel starch showed the highest TS of 20.63 %. Lignin content in sugarcane bagasse being at 21.5 % implies that cellulose and hemicellulose content is lower compared to that of maize

stalk. Lignin is hydrophobic which explains the low TS. Interaction of sugarcane bagasse with dextrinized starch gave overall lower levels of TS. Chemical treatment of the raw materials reduces the free hydroxyl groups that result to lower interaction of particleboards with water hence lower TS.

Particleboards made with rice husks bound with dextrinized cassava peel starch showed the lowest TS comparatively to other lignocellulose-dextrinized starch matrices. Despite rice consists of 15.9 % lignin content that contributes to the hydrophobic nature of the particleboards. Rice husks have a lower amount of hemicellulose and cellulose content compared to maize stalk (Cengiz *et al*., 2016). In addition to this, rice husks consist of silica as filler material which reduces voids in particleboard formulated (Fernandes *et al*., 2017). Reduction of voids in particleboards reduces water intake (Dai *et al*., 2005) thus minimal interaction exists between particleboards and water leading to lower TS.

Minimum requirements for TS according to ASTM D 1037-99(1999) is set at 25 % for general uses (Abdolzadeh *et al.,* 2010). All particleboards formulated in this study met these minimum requirements. Voids in particleboards accommodate water absorbed which leads to swelling. This results in moisture build-up in maize stalk cell wall and interface of the fiber and adhesive that changes the dimension of particleboards (Dizaj *et al.*, 2015). The moisture build-up is determined by the number of free -OH formed in alkali hydrolysis using NaOH. The number of free -OH varies with the amount of lignin.

Study of particleboard formulated from fiber and soy-lignin showed that biobased adhesives improves adhesion property of MDF (Nasir *et al.*, 2014). Particleboards made from rubberwood particles and wheat starch as a binder gave TS of 50.78 % and 68.79 % (Salleh *et al.*, 2015). These values were higher than those obtained from this study. Research done on particleboards formulated with rubberwood bound with modified corn starch showed TS that ranged between 34.81 % to 47.53 % (Amini *et al*., 2013).

4.11.4 Water Absorption (WA) of Particleboards

Results for water absorption (WA) for various particleboards are presented in figure 4-19.

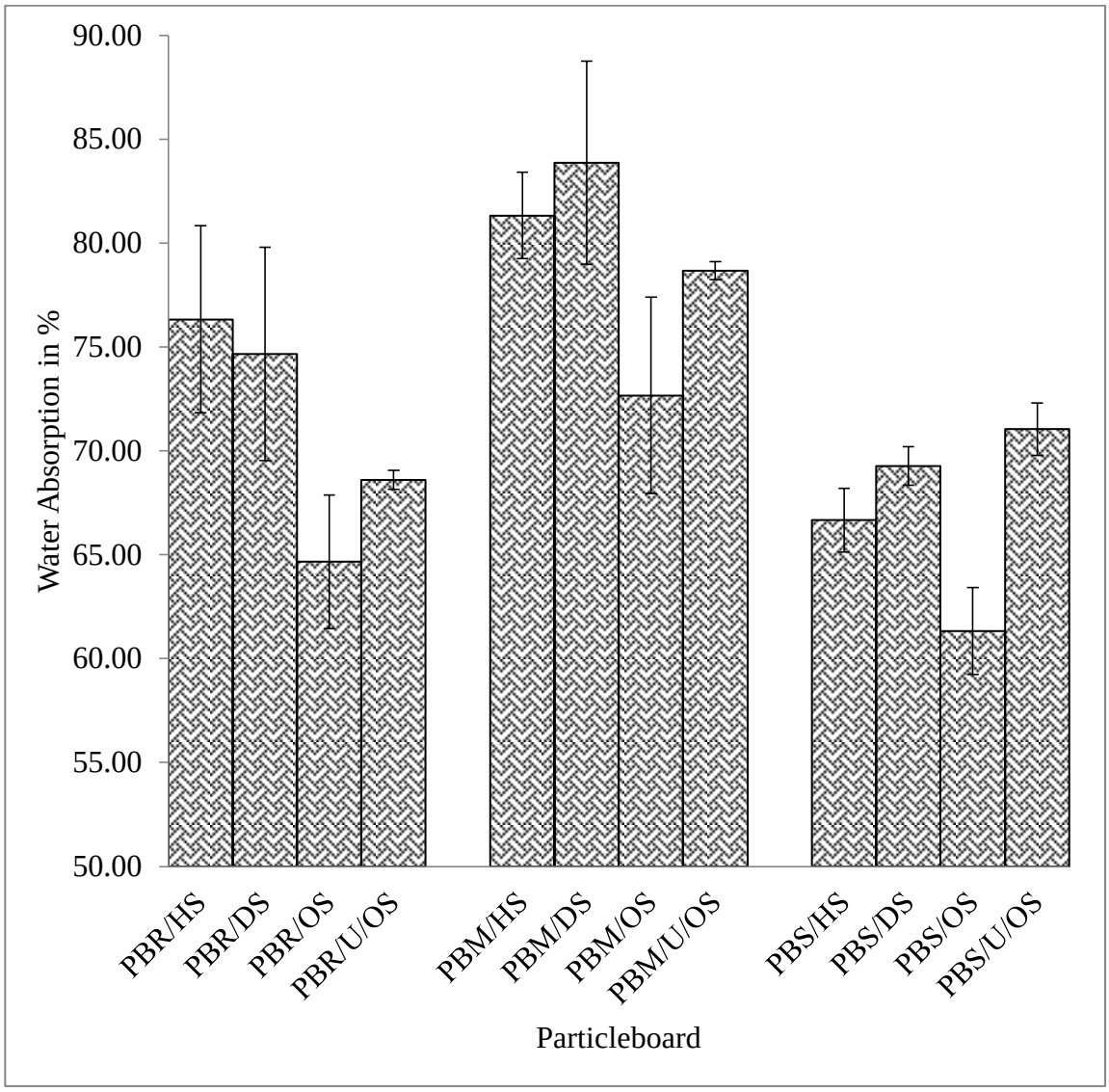

Figure 4-19. WA for particleboards formulated

Maize stalk bound with dextrinized cassava peel starch gave particleboards with WA of 83.87 %. Due to the high content of cellulose and hemicellulose maize stalk consists of large numbers of free hydroxyl groups (Guler *et al*., 2016). Hydroxyl groups combine with water through hydrogen bonding which increases absorption of a high amount of water (Amini *et al*., 2013). Also, maize stalk contains holocellulose with polyose that is hygroscopic hence promote higher WA (Scatolino *et al.*, 2013). Sugarcane bagasse that

contains the highest lignin content showed considerably lower WA. Lignin introduces its hydrophobic nature to the composite material formulated which reduces the overall WA of the particleboards (Zarifa *et al.*, 2018). The initial stages of WA are attributed to the capillarity process as waters move through diffusion.

Movement of water takes place only within the matrix as large cavities enhance water diffusion, especially in maize stalk. WA in maize stalk is higher due to the presence of large cavities whereas in sugarcane bagasse is lower due to the small size of the cavities (Khazaei, 2008). The high amount of the lignocellulose material is required to formulate medium-density particleboard. This brings with them a large number of free hydroxyl groups, hygroscopic sites in water bondage. A maximum requirement of 60 % is recommended for WA for particleboard (ASTM D 1037-99). Particleboards formulated in this study gave higher WA in comparison to highest levels guided by ASTM D 1037-99 standard. The results showed that all particle boards in this study gave higher than 60 % hence did not achieve these standards.

Particleboards formulated from oxidized cassava peel starch showed lower WA and TS. Urea addition increased WA and TS. Urea is a plasticizer with amino groups which increases the hydrophilic nature of the compound. The hydrophilic nature of composite material increases water of relative humidity (Thomas *et al.*, 2013). This is due to the attraction hygroscopic nature of alkali in the urea-based adhesive (Sattayarak *et al.*, 2012).

Research done on particleboards formulated from commercially manufactured particles with wheat starch as a binder had the WA of 96.60 % and 138.82 % (Salleh *et al.*, 2015). Research on formulated composite boards from oil palm trunks exhibited WA range from 63.03 % to 94.33 % (Razak *et al.*, 2013). A study on particleboards formulated with sugarcane bagasse gave 64.2 % for WA (Mendes *et al.*, 2012). In this study, WA in sugarcane bagasse particleboards showed similar results as those in literature, and in other cases showed lower average values. Particleboards formulated with rubberwood and modified corn starch showed WA which ranges from 87.35 % to 107.58 %.

4.12 Analysis of Modulus of Rupture (MOR) and Modulus of Elasticity (MOE) Analysis of Particleboards

Results for modulus of rupture (MOR) tests for various formulated particleboards are presented in figure 4-20.

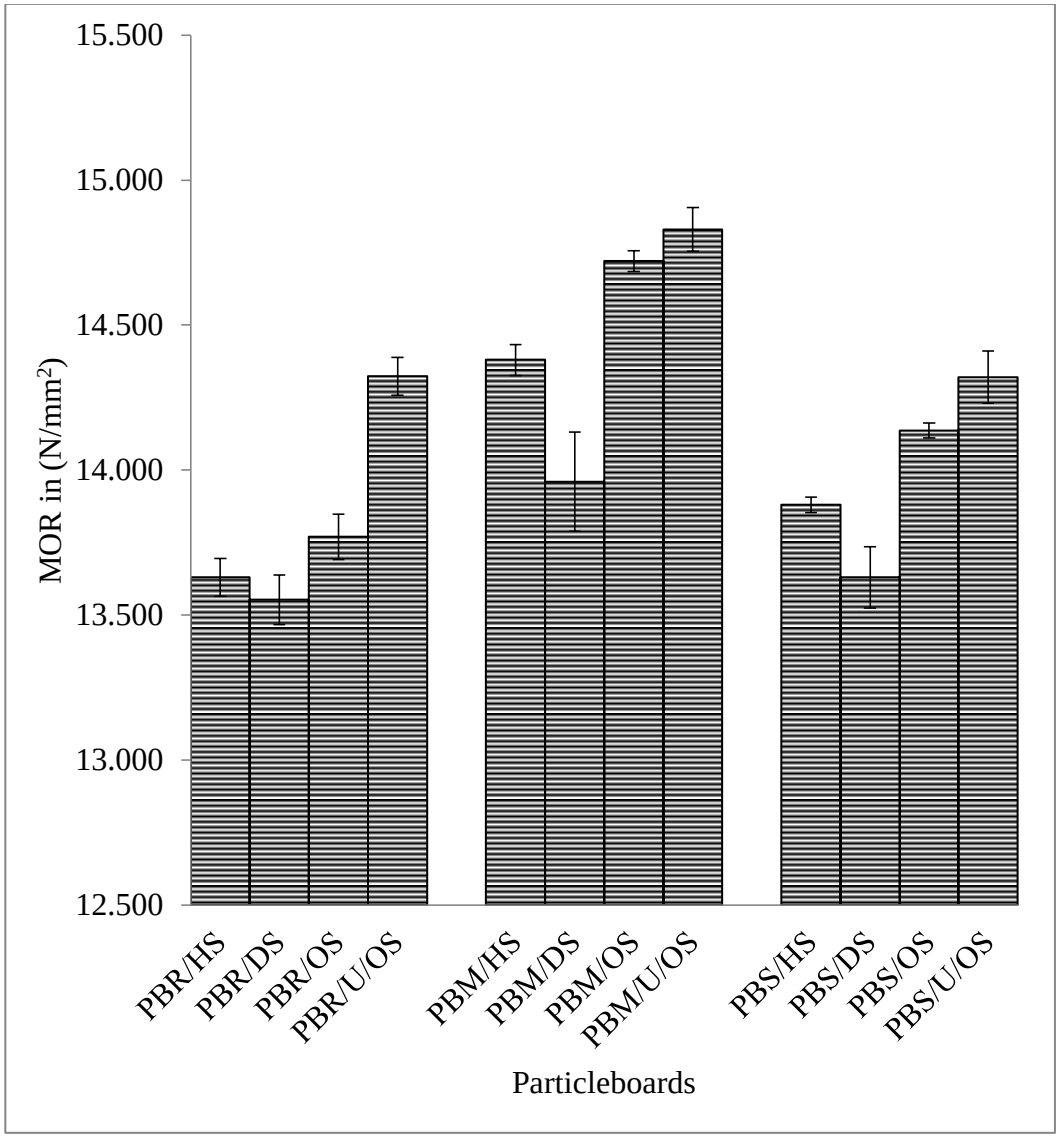

Figure 4-20. MOR for the formulated particleboards

Particleboards were formulated in a random blend between lignocellulose materials with cassava peel starch without consideration of lignocellulose material orientation of any during particleboard formulation. Composite materials in this study were put in a mould with no bias towards the forming direction expected. Tests for the MOR and MOE

properties were taken in a perpendicular and parallel directions of the sample used. Data analysis revealed a significant difference in both directions.

Particleboards formulated with maize stalk gave the highest MOR that was 13.96 Nmm^{-2}. Crosslinking of lignocellulose material with cassava peel bound with increased MOR. Large numbers of free hydroxyl groups in cellulose and hemicellulose of maize stalk react with carboxylic groups from oxidized cassava peels starch through esterification. Esterification results in crosslinking of cassava peel starch and lignocellulose materials thus higher values of MOR as strong covalent bonds are formed. Reddy, *et al.*, (2010) have shown that the reaction of the -OH and –COOH forms cross-linked molecules. Crosslink was formed between hydroxyl groups from starch with a carboxylic group from citric acid which showed improved MOR in the resultant composite materials.

Particleboards formulated in this study surpassed the minimum requirements of ASNI 208.2-2009 medium density used for interior applications of 2.8 Nmm^{-2}. Silica in rice husks provides extra reaction sites with cassava peel starch after hydrolysis with sodium hydroxide. The reaction results in the formation of sodium silicate used as an inorganic adhesive (Guangbao, 2014). Particleboards made from engineered composite materials from palm stems shone lower MOR. MOR ranged from 1.33 to 3.71 Nmm^{-2} (Razak *et al.*, 2013). Similarly, the values were also lower compared to those obtained in this research study.

Sugarcane bagasse produced particleboard with the highest MOR value of 11 Nmm^{-2} (Widyorini *et al.*, 2005). Particleboards formulated from sugarcane bagasse and formaldehyde-based resins showed the highest MO of 11.5 Nmm^{-2} (Mendes *et al.*, 2012). Particleboard made from sugarcane bagasse bound with urea-formaldehyde gave MOR of 20.9 Nmm^{-2} (Mendes *et al.*, 2014). MOR for the particleboards formulated in this study was consistent compared to literature values. All particleboards formulated met the minimum requirements for a medium density of 12.8 Nmm^{-2} (ASTM, 2002). Also, the particleboards met and exceeded the minimum requirement of EN 312 standard (ECS, 1993) standards which gives the lowest value of 13 Nmm^{-2}.

Results for various modulus of elasticity (MOE) tests for various particleboards are presented in figure 4-21.

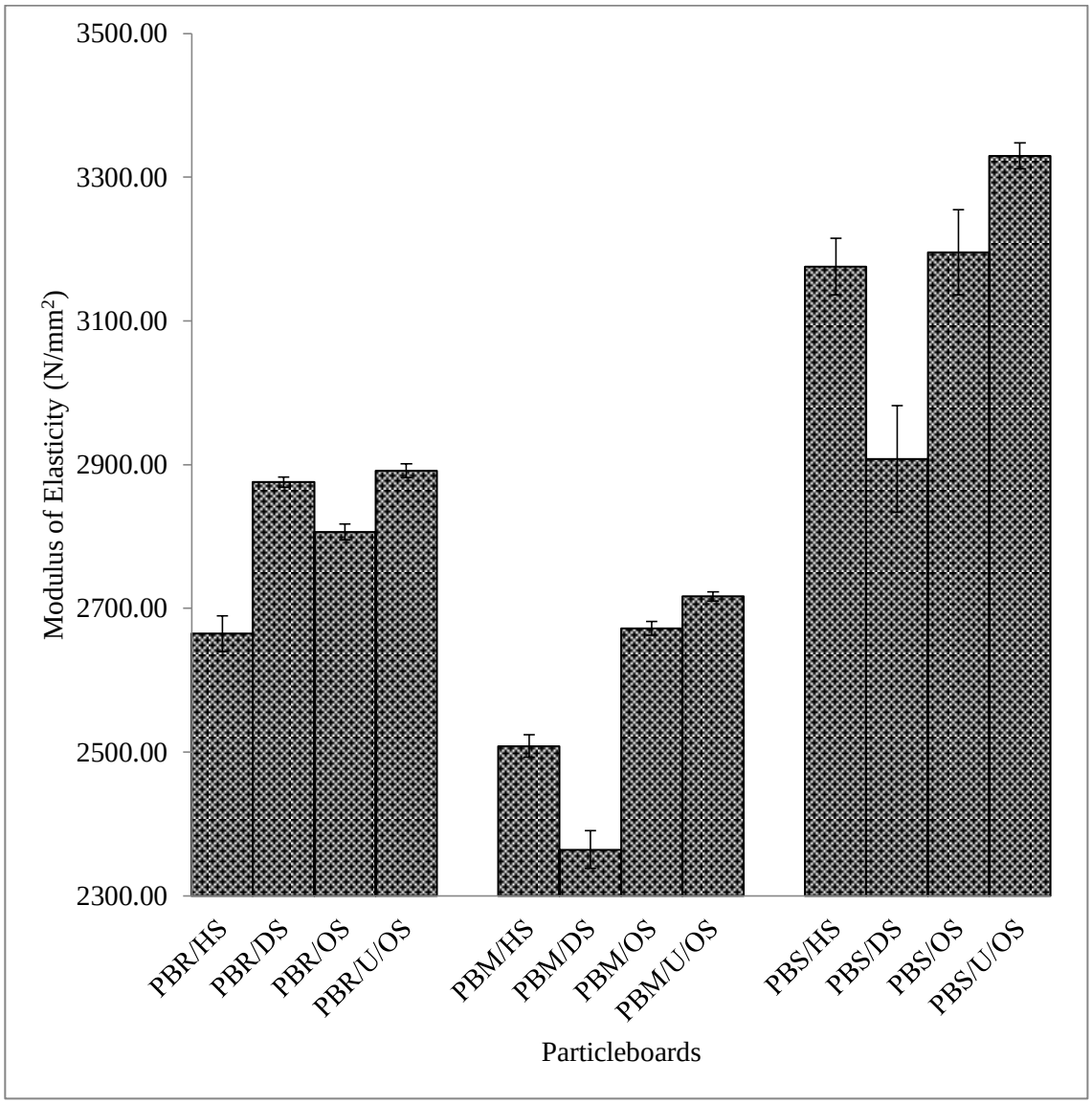

Figure 4-21. MOE for the formulated particleboards

Particleboards formulated with sugarcane bagasse bound with a mixture of oxidized cassava peel starch and urea had highest MOE of 3329.93 Nmm^{-2}, due to presence of fibers that reinforce the structure of the boards (Gilfillan *et al.,* 2012). MOE and MOR showed similar trends where there was no significant difference between particleboards synthesized with rice husks. There was no significant difference when particleboards

formulated with maize stalk were compared to those made with sugarcane bagasse. The particleboards formulated exceeded the minimum MOR for low-density particleboards of 500 Nmm^{-2}.

Particleboards made from palm stems gave MOE that ranged from 109.69 to 304.73 Nmm^{-2} (Amirou *et al.*, 2013) Particleboards made from bagasse mixed with industrial wood particles bound with urea-formaldehyde gave MOE that ranged between 1706 Nmm^{-2} to 2384 Nmm^{-2} (Dahmardehghalehno and Bayatkashkoli, 2013). Boards formulated from a mixture of sugarcane bagasse and wood bound together with urea-formaldehyde mixed with ammonium chloride gave MOE that ranged from 1020 Nmm^{-2} to 2550 Nmm^{-2} (Tabarsa, 2011). Particleboards formulated from wheat straw bound using urea and urearase inhibitor N-(n-butyl) thiophosphoric triamide (nBTPT) gave MOE that ranged from 2601.6 Nmm^{-2} to 3343.2 Nmm^{-2}. Comparatively, particleboards formulated in this research study display characteristics that are within the results obtained from other research work.

Particleboard produced using sugarcane bagasse obtained the highest MOE of 1600 Nmm^{-2} (Widyorini *et al.*, 2005). Particleboards formulated from sugarcane bagasse bound with formaldehyde-based resins obtained highest MOE 1064.7 Nmm^{-2} (Mendes *et al.*, 2012). Particleboard formulated from sugarcane bagasse bound with formaldehyde resin obtained the highest MOE of 1643.2 Nmm^{-2} (Mendes *et al.*, 2014). The MOE result in this study relates to those found in the literature. Particleboards formulated in this study met the minimum MOE requirements for medium density particleboards of 1943.7 Nmm^{-2} (ASTM, 2002). Also, they met the minimum requirements of 1800 Nmm^{-2} for MOE for internal use as per the European standards (EN 312). All particleboards attained the standards for medium density for interior use of 1241 Nmm^{-2} (ASTM, 2002).

4.12.1 Internal Bond (IB) Analysis of Particleboards

Results for various internal bonding (IB) tests for various formulated particleboards are presented in figure 4-22.

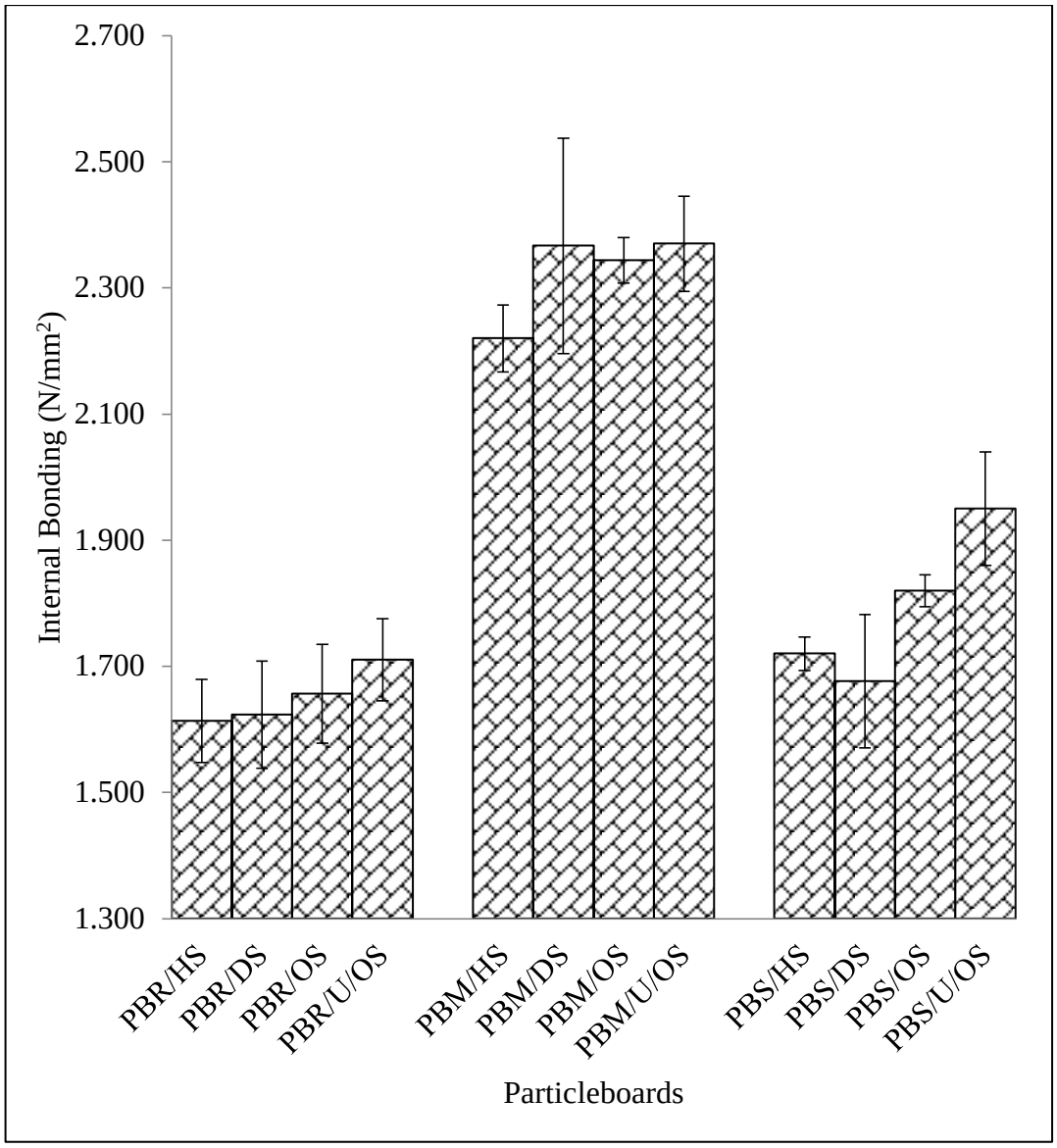

Figure 4-22. IB for the formulated particleboards

Particleboard from maize stalk with dextrinized cassava peel starch as a binder gave highest IB of 2.367 Nmm^{-2}. Maize stalk has high levels of hemicellulose where hemicellulose increases the fiber joint strength. Fiber bondage is explained as the bonded area and the bond strength. Particleboard formulated with maize stalk bound using dextrinized cassava peel starch showed a higher fiber-fiber bond strength which has resulted in improvement of IB (Koubaa and Koran, 1995).

Alkali treatment of maize stalk using NaOH increased its flexibility when compared to other lignocellulose materials which improve the interaction. Sodium hydroxide breaks hydrogen bonding that holds the structure together thus increasing flexibility of lignin in lignocellulose material. Treatment of lignocellulose material changes the morphology of lignin, cellulose and hemicellulose which increases cohesiveness in composite material. Celluloses as a reinforcement material increase the IB composite material (Peng *et al.*, 2010). Cellulose avails more free hydroxyl groups used in chemical reactions with functional groups in cassava peel starch-based binders (Sreekala, 2000).

Particleboard formulated from rice husks bagasse bound with hydrolyzed starch gave the lowest IB of 1.61 Nmm^{-2}. Low amount of hemicellulose and cellulose content in rice husks is attributed to low IB. Hemicelluloses act as reinforcement material that enhances bondage in particleboards. Rice husks have higher lignin content than maize stalk which makes the structure stronger. Low hemicellulose and cellulose content result in a low number of hydroxyl groups which is used in bondage in particleboard formulation.

Particleboards formulated in this study exceeded minimum requirements that range from 0.24 Nmm^{-2} and 0.40 Nmm^{-2} for general use and internal applications such as the manufacture of furniture in accordance with the European standard EN 312:2010 (Taramian *et al.*, 2007). They also met the minimum requirements of 0.60 Nmm^{-2} for ANSI A208 for interior applications. The density of the particleboard increases with increases in IB where particleboards formulated with maize stalk showed the highest IB. Highest IB is attributed to the extent of interactions brought about by crosslinking of cellulose, hemicellulose and lignin with cassava peel starch. At about 40 ^{o}C the density has great improvement to IB (Laemlaksakul, 2010). The higher value of IB can be obtained when more amount of resin is utilized. A study has shown that an increase in the surface area decreases the IB (Rokiah *et al.*, 2010).

IB average values were determined. The industrial panels made from Bagasse, Maize stalk, Rice husks differed in internal bond. Panelboards formed from rice husks were lowest. This is attributed to a low amount of cassava peel starch that interacts with

lignocellulose particles. Particleboards formulated with maize stalk gave the highest IB strength of 3.72 Nmm^{-2}. This is as a result of the presence of more hydroxyl groups for copolymerizing as well as crosslinking. These binding sites are available in cellulose, hemicellulose and also lignin molecules. Particleboards made from bagasse had IB strength of 1.72Nmm^{-2}. Results on IB are as shown in figure 4-22. Significance differences were determined for the IB mean of the particleboards. There was significance difference between PBRHS and PBMS, $t_{cal} = -27.96 < t_{crit} = 4.30$, at P=0.05. comparison of IB means between PBRHS and PBBS showed no significant difference as $t_{cal} = -1.76 < t_{crit} = 4.30$ and IB means between PBMS and PBBS shown significance difference where $t_{cal} = 130.93 > t_{crit} = 4.30$.

Research done on particleboards made from organic waste has shown similar IB. Particleboards made from the ~~a~~ mixture of sugarcane bagasse and wood bound with urea-formaldehyde showed IB ranging from 0.33 Nmm^{-2} to 0.78 Nmm^{-2} (Dahmardehghalehno and Bayatkashkoli, 2013). Ammonium chloride was used to improve the IB from 0.39 Nmm^{-2} to 0.81 Nmm^{-2} (Shahidan and Muhammed, 2011). Boards made from wheat straw bound with urearase inhibitor N-(n-butyl) thiophosphoric triamide (n BTPT) and urea gave IB that range from 3.7 Nmm^{-2} to 5.6 Nmm^{-2} (Sun *et al*., 2004a), which enhance adhesive strength.

Particleboards formulated with sugarcane gave internal bond values of 0.2 Nmm^{-2} (Oliveira *et al.,* 2016). Particleboards made from sugarcane bagasse bound with UF and melamine-formaldehyde showed IB of 0.63 Nmm^{-2} (Mendes *et al*., 2014). A different study has shown that particleboards produced from sugarcane bagasse had IB of 0.85 Nmm^{-2}. Particleboards formulated met the minimum ANSI A208.1 standard for IB of 0.40 Nmm^{-2} and the EN 312 standard of 0.30 Nmm^{-2}. Comparatively the IB obtained in this study showed consistency with those recorded in literature and they met all cited standards.

CHAPTER FIVE

5 CONCLUSION AND RECOMMENDATION

5.1 Conclusion

1. Cassava peels contain 56.66 % (w/w) starch compared to rice grains (32.79 % (w/w)), sorghum grains (26.80 % (w/w)), wheat grains (28.69 % (w/w)) , maize corn (27.27 % (w/w)), millet grains (20.90 % (w/w)) and cassava tubers (10.79 % (w/w)). Cassava peels treated with hydrogen peroxide are alternative source of starch that can be utilized for synthesis of particle board adhesives.
2. Sugarcane bagasse showed highest lignin content of 21.50 % (w/w) compared to sawdust (17.60 % (w/w), rice husks (15.90 % (w/w), grass straw (14.30 % (w/w), wheat straw (12.60 % (w/w) and maize stalks 11.4 % (w/w). All mlignocellulose material have lignin content that was within a range of 11 to 25 % (w/w) compared with wood particle from tree stems, thus, sugarcane bagasse, maize stalk and rice husks can be used as an alternative lignocellulose material for particleboard formulation.
3. X-ray diffraction showed the presence of sodium silicate (Na_2SiO_3), an inorganic adhesive. Absence of $CaSiO_3$ that makes particleboard fragile during installation and readily absorbs moisture, absence of $MgSiO_3$ which reduces adhesion of Na_2SiO_3, absence of zinc silicate that causes mud cracking of particleboard.
4. Esterification is the main bondage in particleboard formulation due to reaction between -C-OH from hydrolyzed lignocellulose material and -COOH oxidized cassava peel starch as shown using FTIR spectroscopy and NMR. Esterification formed the main bondage in composite material.
5. All particleboards showed a density range of 0.60 to 0.80 gcm^{-3} thus all particleboards are classified as medium density particleboard. Water absorption 35 to 50 % and thickness swelling exceeded the minimum standard requirements for particleboards. Particleboards formulated which had thermal conductivity within 0.04 to 0.12 W/m^2 thus can be used as insulators for room partitioning. Mechanical (IB, MOE, MOR) properties of the particleboards exceeded the ASTM standard for MDP, thus can be used to supplement MDF deficits.

5.2 Recommendations

The following recommendations are made from the study:

1. Treating of particleboard surfaces such as the use of undercoat with fillers, pigments with alkyd based paints and nitrocellulose based varnish need to be investigated to improve physical properties.
2. Further investigations on the use of chemical cross-linking of cassava peel adhesive with biodegradable synthetic polyvinyl acetate (PVA) to improve TS, WA and bonding strength.
3. Further investigation by blending sugarcane bagasse, maize stalk and rice husks can be done to ascertain whether individual characteristics improve the overall physical and mechanical properties of particleboards.

REFERENCES

Abbey S., Gladney E.S. (2005) A Re-Evaluation of Three Canadian Reference Rocks. Geo-Standards Newsletter **10**:3-11.

Abdelmouleh M., Boufi S., Belgacem M.N. (2007) Short Natural-Fibre Reinforced Poly-Ethylene and Natural Rubber Composites: Effect of Silane Coupling Agents and Fibresloading. *Journal for Composite Science Technology* **67**:1627-1639. https://doi.org/10.1016/j.compscitech.2006.07.003.

Abdolzadeh H., Doosthoseini K., Karimi A.N., Enayati A.A. (2010) The Effect of Acetylated Particle Distribution and Type of Resin on Physical and Mechanical Properties of Poplar Particleboard. *European Journal of Wood and Wood Products* **69**:3-10.

Achyuthan K.E., Achyuthan A.M., Adams P.D., Dirk S.M., Harper J.C., Simmons B.A., Singh A.K. (2010) Supramolecular Self-Assembled Chaos: Polyphenolic Lignin's Barrier to Cost-Effective Lignocellulosic Biofuels. *Journal for Molecules* **15**:8641-8688.

Ademoroti C.M.A. (1996) Standard Methods for Water and Effluents Analysis. Ibadan: Foludex Press, 121-214.

Adhikary K.B., Pang S., Staiger M.P. (2008) Long-Term Moisture Absorption and Thickness Swelling Behaviour of Recycled Thermoplastics Reinforced with Pinus Radiata Sawdust. *Journal for Chemical Engineering* **142**:190-198. doi:10.1016/j.cej.2007.11.024.

Agarwal U.P. (2019) Analysis of Cellulose and Lignocellulose Materials by Raman Spectroscopy: A Review of the Current Status. *Journal for Molecules* **24**:1659.

Ago M., Jakes E.J., Orlando J.R. (2013) Thermomechanical Properties of Lignin-Based Electrospun Nanofibers and Films Reinforced with Cellulose Nanocrystals: A Dynamic Mechanical and Nanoindentation Study. *ACS Appl. Mater. Interfaces* **5**:11768-11776.

Akgul M., Camlibel O. (2008) Manufacture of Medium Density Fiberboard (MDF) Panels from Rhododendron (R. *ponticum* L.) Biomass. *Journal for Building and Environment* **43**:438-443.

Akhtar M.N., Sulong A.B., Radzi M.K.F., Ismail N.F., Raza M.R., Muhamad N., Khan M.A. (2016a) Influence of Alkaline Treatment and Fiber Loading on the Physical and Mechanical Properties of Kenaf/Polypropylene Composites for Variety of Applications. *Journal on Progress in Natural Science: Materials International* **26**:657-664. https://doi.org/10.1016/j.pnsc.2016.12.004.

Akhtar M.N., Sulong A.B., Radzi M.K.F., Ismail N.F., Raza M.R., Muhamad N., Khan M.A. (2016b) Influence of Alkaline Treatment and Fiber Loading on the Physical and Mechanical Properties of Kenaf/Polypropylene Composites for Variety of Applications. *Progress in Natural Science: Materials International* **26**:657-664. https://doi.org/10.1016/j.pnsc.2016.12.004.

Akhtar T., Lutfullah G., Ullah Z. (2011) Ligonsulfonate-Phenolformaldehyrde Adhesive: A Potenstial Binder for Wood Panel Industries. *Journal on Chem. Soc. Pak.* **33**:535-538. .

Akinyemi A.B., Afolayan J.O., Ogunji O.E. (2016a) Some Properties of Composite Corn Cob and Sawdust Particle Boards. *Construction and Building Materials* **127**:436-441. doi: 10.1016/j.conbuildmat.2016.10.040.

Akinyemi A.B., Afolayan J.O., Ogunji O.E. (2016b) Some Properties of Composite Corn Cob and Sawdust Particle Boards. *Journal on Construction and Building Materials* **127**:436-441. https://doi.org/10.1016/j.conbuildmat.2016.10.040.

Alessandra S.F., Joabel R., Lina B., Caue R., Maria A.M., Manoel J.M., Lourival M.M., Gustavo H.D.T. (2015) Biocomposite of Cassava Starch Reinforced with Cellulose Pulp Fibers Modified with Deposition of Silica (SiO_2) Nanoparticles. *Journal of Nanomaterials* **119**:1-9.

Ali I., Rehman S., Hyder Ali S., Javaid A. (2012) The Effect of Borax-Modified Starch on Wheat Straw-Based Paper Properties. *Journal for Applied Polymer Science* **128**:3672-3677.

Alizadeh A.S., Mousavi M., Labbafi M. (2017) Synthesis and Characterization of Carboxymethyl Cellulose from Sugarcane Bagasse. *Journal for Food Processing & Technology* **8**:1-6.

Allal A., Charrier B., Charrier F., Moubarik A., Pizzi A. (2010) Preparation and Mechanical Characterization of Particleboard Made From Maritime Pine and Glued with Bio-Adhesives Based on Cornstarch and Tannins. Journal Maderas. Cienc. y Tecnol. **12**:189-197.

Allen S.E. (1974) Chemical analysis of ecological materials. Oxford: Black Well, 241-245.

Altan A., Akıncı E., Arca M. (2019) Comparing the Performances of Aqueous Solution of Boric Acid/Borax and Powder Boric Acid/Borax in Corrugated Board Production Process. *Journal for Biological and Chemical Research* **6**:150-154.

Altendorf H., Jeulin D., Willot F. (2014) Influence of the Fiber Geometry on the Macroscopic Elastic and Thermal Properties. *International Journal of Solids and Structures* **51**:3807-3822.

Ameh E.M., Nwogbu C.C., O. A.A. (2019) Production of Ceiling Board Using Local Raw Materials. *Journal for Science, Engineering and Technology* **4**:1-5.

Amini M.H.M., Hashim R., Hiziroglu S., Sulaiman N.S., Sulaiman O. (2013) Properties of Particleboard Made from Rubberwood Using Modified Starch as Binder. *Composite. Part B Engineering* **50**:259-264.

Amirou S., Zerizer A., Pizzi A., Haddadou I., Zhou X. (2013) Particleboards Production from Date Palm Biomass. *Journal for Wood and Wood Products* **71**:717-723.

Anderson T.R., Hawkins E., Jones P.D. (2016) Carbon dioxide the Greenhouse Effect and Global Warming: from the Pioneering Work of Arrhenius and Callendar to today's Earth System Models. *Journal on Endeavour* **40**:178-187.

Angelova L.V., Leskes M., Berrie B.H., Weiss R.G. (2015) Selective Formation of Organo, Organo-Aqueous, and Hydro Gel-Like Materials from Partially Hydrolysed Poly(Vinyl Acetate)s Based on Different Boron-Containing Crosslinkers. *Journal for Soft Matter* **11**:5060-5066. doi:10.1039/c5sm00465a

Annenkov V.V., Danilovtseva E.N., Pal'shin V.A., Verkhozina O.N., Zelinskiy S.N., Krishnan U.M. (2017) Silicic Acid Condensation Under the Influence of Water-Soluble Polymers: from Biology to New Materials. *Journal for RSC Advances* **7**:20995-21027.

Aravind N., Sathyan D., Mini K.M. (2019) Rice Husk Incorporated Foam Concrete Wall Panels as a Thermal Insulating Material in Buildings. *Journal for Indoor and Built Environment* **29**:721-729.

Ascheri J.L.R., Zamudio L.H.B., Carvalho C.W.P., Arevalo M.A., Fontoura L.M. (2014) Extraction and Characterization of Starch Fractions of Five Phenotypes Pachyrhizus Tuberosus (Lam.) Spreng. *Journal for Food and Nutrition Sciences* 5:1875-1885.

Ashori A., Sheykhnazari S., Tabarsa T., Shakeri A., Golalipour M. (2012) Bacterial Cellulose/Silica Nanocomposites: Preparation and Characterization. *Journal for Carbohydrate Polymers* **90**:413-418. doi:10.1016/j.carbpol.2012.05.060.

ASTM. (2000) Standard Test Method for Steady-State Thermal Transmission Properties by Means of the Heat Flow Meter Apparatus. C 518-98. American Society for Testing and Materials, Philadelphia, PA.

ASTM. (2002) American Society for Testing and Materials. ASTM D-1037. Standard Methods of Evaluating of Wood-Base Fiber and Particles Materials. In: Annual Book of ASTM standard. Philadelphia: ASTM; 2002.

Atiqah A., Jawaid M., Ishak M.R., Sapuan S.M. (2017) Moisture Absorption and Thickness Swelling Behaviour of Sugar Palm Fibre Reinforced Thermoplastic Polyurethane. *Journal for Procedia Engineering* **184**:581-586.

Awaluddin R., Prasetya A.W., Nugraha Y., Suweleh M.F., Kusuma A.P., Indrati O. (2017) Physical Modification and Characterization of Starch Using Pregelatinization and Co-Process of Various Tubers from Yogyakarta as an Excipient, International Conference on Chemistry, Chemical Process and Engineering (IC3PE), American Institute of Physics, Yogyakarta, Indonesia.

Ayrilmis N., Kwon J.H., Han T.H. (2012) Improving Core Bond Strength and Dimensional Stability of Particleboard Using Polymer Powder in Core Layer. *Journal for Composites Part B: Engineering* **43**:3462-3466. doi:10.1016/j.compositesb.2012.01.039.

Bai Y., Liu X., Shi S.Q., Li J. (2020) A Tough and Mildew-Proof Soybean-Based Adhesive Inspired by Mussel and Algae. *Journal for Polymers* **12**:756. doi:10.3390/polym12040756.

Bakar R.A., Yahya R., Gan S.N. (2016) Production of High Purity Amorphous Silica from Rice Husk. *Journal for Procedia Chemistry* 19:189-195. doi:10.1016/j.proche.2016.03.092.

Baker J., Kim S. (2012) The Interaction of Radio-Frequency Fields with Dielectric Materials at Macroscopic to Mesoscopic Scales. *Journal of Research of the National Institute of Standards and Technology* 117:1-60. doi:10.6028/jres.117.001

Balakshin M., Capanema E.A. (2015) On the Quantification of Lignin Hydroxyl Groups With 31P and 13C NMR Spectroscopy. *Journal on Chemistry and Technology* **35**:220-327.

Baldan A. (2012) Adhesion Phenomena in Bonded Joints. *Journal for Adhesion and Adhesives* **38**:95-116.

Barikani M., Mohammadi M. (2007) Synthesis and Characterization of Starch-Modified Polyurethane. *Journal for Carbohydrate Polymers* **68**:773-780.

Barrios S.E., Contreras J.M., López-Carrasquero F., Müller A.J. (2012) Chemical Modification of Cassava Starch by Carboxymethylation Reactions Using Sodium Monochloro Acetate as Modifying Agent. *Journal for Revista de la Facultad de Ingenieria* **27**:97-105.

Battegazzore D., Alongi J., Frache A., Wågberg L., Carosio F. (2017) Layer by Layer-Functionalized Rice Husk Particles: A Novel and Sustainable Solution for Particleboard Production. *Materials Today Communications* **13**:92-101. https://doi.org/10.1016/j.mtcomm.2017.09.006.

Baumberger S., Lapierre C., Monties B., Valle G.D. (1998) Use of Kraft Lignin as Filler for Starch Films. *Polymer Degradation and Stability* **59**:273-277. https://doi.org/10.1016/S0141-3910(97)00193-6.

Baumberger S., Lapierre C., Monties B., Valle G.D. (2010) Use of Kraft Lignin as Filler for Starch Films. *Journal on Polymer Degradation and Stability* **59**:273-277. https://doi.org/10.1016/S0141-3910(97)00193-6.

Bayazeed A., Farag S., Shaarawy S., Hebeish A. (1998) Chemical Modification of Starch via Etherification with Methyl Methacrylate. *Journal on Starch - Stärke* **50**:89-93.

Bayitse R., Hou X., Bjerre A.B., Saalia F.K. (2015) Optimisation of Enzymatic Hydrolysis of Cassava Peel to Produce Fermentable Sugars. *Journal for AMB Express* **5**:1-7.

Bec K.B., Grabska J., Ozaki Y., Hawranek J.P., Huck C.W. (2017) Influence of Non-fundamental Modes on Mid-infrared Spectra: Anharmonic DFT Study of Aliphatic Ethers. *Journal for Physical Chemistry* **121**:1412-1424.

Bekhta P., Sedliacik J., Saldan R., Novak I. (2016) Effect of Different Hardeners for Urea-Formaldehyde Resin on Properties of Birch Plywood. *Joirnal for Acta Facultatis Xylologiae Zvolen* **58**:65-72. doi: 10.17423/afx.2016.58.2.07.

Bhandari R.K., Oda R.P., Petrikovics I., Thompson D.E., Brenner M., Mahon S.B., Logue B.A. (2014) Cyanide Toxicokinetics: The Behavior of Cyanide, Thiocyanate and 2-Amino-2-Thiazoline-4-Carboxylic Acid in Multiple Animal Models. *Journal for Analytical Toxicology* **38**:218-225.

Bhattacharjee G., Neogi S., Das S.K. (2014) Phenol–Formaldehyde Runaway Reaction: A Case Study. *Journal of Industrial Chemistry* **5**:1-6. doi:10.1007/s40090-014-0013-9.

Biswas D., Kanti B.S., Mozaffar H.M. (2011) Physical and Mechanical Properties of Urea Formaldehyde-Bonded Particleboard Made from Bamboo Waste. *International Journal of Adhesion and Adhesives* **31**:84-87. https://doi.org/10.1016/j.ijadhadh.2010.11.006.

Bohm M., Salem M.Z.M., Srba J. (2012) Formaldehyde Emission Monitoring from a Variety of Solid Wood, Plywood, Blockboard and Flooring Products Manufactured for Building and Furnishing Materials. *Journal of Hazardous Materials* **221-222**:, 68-79.

Boon G.J., Hashim R., Danish M., Nadhari N.A. (2019) Physical and Mechanical Properties of Binderless Particleboard Made from Steam-Pretreated Oil Palm Trunk Particles. *Journal for Composite Science* **3**:1-6. doi: 10.3390/jcs3020046.

Boonyanopakun K., Pavasant P. (2012) Comparative Evaluation of Industrial and Agricultural Emissions of carbon dioxide and dinitrogen monoxide. *Journal of the Institution of Engeneers* **42**:50 - 56.

Boran S.M., Usta M.E., Gumuskaya E. (2011) Decreasing Formaldehyde Emission from Medium Density Fiberboard Panels Produced by Adding Different Amine Compounds to Urea Formaldehyde Resin. *Journal for Adhes. Adhes.* **31**:674-678.

Borges J., Mano J.F. (2014) Molecular Interactions Driving the Layer-by-Layer Assembly of Multilayers. *Journal for Chemical Reviews* **114**:8883-8942.

Brouwer P.N. (2010) Theory of XRF-Getting Acquainted with the Principles. 3rd ed. The Netherlands, 25: PANAlytical BV; p. 10.

Buleon A., Colonna P., Planchot V., Ball S. (2012) Starch Granules: Structure and Biosynthesis. *Int. J. Biol. Macromol* **23**:85-112.

Cai Y., Bhuiya M.W., Shanklin J., Liu J.C. (2015) Engineering a Monolignol 4-O-Methyltransferase with High Selectivity for the Condensed Lignin Precursor Coniferyl Alcohol. J. Biol. Chem **44**:26715-26724.

Cao C., Yang Z., Han L., Jiang X., Ji G. (2014) Study on *In situ* Analysis of Cellulose, Hemicelluloses and Lignin Distribution Linked to Tissue Structure of Crop Stalk Internodal Transverse Section Based on FTIR Microspectroscopic Imaging. *Journal for Cellulose* **22**:139-149.

Capanema A.E., Balakshin Y.M., Kadla F.J. (2005) Quantitative Characterization of a Hardwood Milled WoodLignin by Nuclear Magnetic Resonance Spectroscopy. *Journal for Agricultural and Food Chemistry* **53**:9639-9649. doi: 10.1021/jf0515330.

Capanema E.A., Balakshin M. (2015) On the Quantification of Lignin Hydroxyl Groups With 31P and 13C NMR Spectroscopy. *Chemistry and Technology* **35**:220-327.

Cardoso M.B. (2007) From Rice Starch to Amylose Crystals: Alkaline Extraction of Rice Starch, Solution Properties of Amylose and Crystal Structure of V-Amylose Inclusion Complexes. Université Joseph Fourier, Grenoble I, France.

Carey F.A. (2003) Organic Chemistry. 5th ed. New York, NY: McGraw-Hill. pp. 638-684.

Cavalcante R., Canabarro B., Viana H., Scholz S., Simão R., de Farias J. (2017) Surface Lignin Removal on Coir Fibers by Plasma Treatment for Improved Adhesion in Thermoplastic Starch Composites. *Carbohydrate Polymers* **165**:429-436. https://doi.org/10.1016/j.carbpol.2017.02.042.

Cengiz G., Halil I.S., Sevcan Y. (2016) The Potential for Using Corn Stalks as a Raw Material for Production Particleboard with Industrial Wood Chips. *Journal on Wood Research* **61**:299-306.

Cetin N.S., Ozmen N. (2002) Use of Organosolv Lignin in Phenol–Formaldehyde Resins for Particleboard Production: I. Organosolv Lignin Modified Resins. *International Journal of Adhesion and Adhesives* **22**:477-480. https://doi.org/10.1016/S0143-7496(02)00058-1.

Chand N., Fahim M. (2008) 1 - Natural Fibers and their Composites, Tribology of Natural Fiber Polymer Composites, Woodhead Publishing. pp. 1-58.

Chang P.R., Yu J., Ma X. (2010) The Preparation and Properties of Dialdehyde Starch and Thermoplastic Dialdehyde Starch. Carbohydrate Polymers **79**:296-300.

Chen J.C., Hsiao Y.R., Liu Y.C., Chen P.Y., Chen K.H. (2019) Polybenzimidazoles Containing Heterocyclic Benzo[c]cinnoline Structure Prepared by Sol-Gel Process and Acid Doping Level Adjustment for High Temperature PEMFC Application. *Journal for Polymer* **182**:121814.

Chen L., Liu S., Wang H., Wang M., yu L. (2016) Relative Significances of pH and Substrate Starch Level to Roles of Streptococcus Bovis S_1 in Rumen Acidosis. *Journal for AMB Express* 6:1.

Chen N., Zhang H., Luo X.D., Sun C.Y. (2020) SiO_2-Decorated Graphite Felt Electrode by Silicic Acid Etching for Iron-Chromium Redox Flow Battery. *Journal for Electrochimica Acta* **336**:135646.

Chen R.Y., Zhang Y.R., Zhang S.D., Wang X., L., Wang Y.Z. (2009) Effect of Carbonyl Content on the Properties of Thermoplastic Oxidized Starch. *Carbohydrate Polymers* **78**:157-161.

Cheng E., Sun X., Karr G.S. (2004) Adhesive properties of modified soybean flour in wheat straw particleboard, Compos. *Composites Part A: Applied Science and Manufacturing* **35**:297-302.

Cho Y.W., Han S.S., Ko S.W. (1999) PVA-Containing Chito-Oligosaccharide Side Chain. *Journal for Polymer* **41**:2033-2039.

Choong F.X., Marcus B., Steiner S.E., Melican K., Nilsson K.P.R., Edlund U., Dahlfors A.R. (2016) Nondestructive, Real-Time Determination and Visualization of Cellulose, Hemicellulose and Lignin by Luminescent Oligothiophenes. *scientific reports* **6**:35578.

Chotipratoom S., Choi S.H., Choi H.W., Kim H.S., Kim B.Y., Baik M.Y. (2014) High Hydrostatic Pressure (HHP)-Assisted Starch Modification: Acid Hydrolysis, Hydroxypropylation, Acetylation, Cross-linking and Cationization. *Journal of Applied Glycoscience* **61**:31-34.

Ciannamea E.M., Stefani P.M., Ruseckaite R.A. (2010) Medium-Density Particleboards from Modified Rice Husks and Soybean Protein concentrate-Based Adhesives. *Journal for Bioresource Technology* **101**:818-825. doi: 10.1016/j.biortech.2009.08.084.

Collinson S.R., Thielemans W. (2010) The Catalytic Oxidation of Biomass to New Materials Focusing on Starch, Cellulose and Lignin. *Coordination Chemistry Reviews* **254**:1854-1870. https://doi.org/10.1016/j.ccr.2010.04.007.

Colussi R., El Halal S.L.M., Pinto V.Z., Bartz J., Gutkoski L.C., da Rosa Zavareze E., Dias A.R.G. (2015) Acetylation of Rice Starch in an Aqueous Medium for Use in Food. *Journal for Food Science and Technology* **62**:1076-1082.

Costa N.A., Pereira J., Ferra J., Cruz P., Martins J., Magalhaes F.D., Mendes A., Carvalho L.H. (2013) Scavengers for Achieving Zero Formaldehyde Emission of Wood-Based Panels. *Journal for Wood Sci. Technol.* **47**:1261-1272.

Crini G. (2006) Non-conventional Low-Cost Adsorbents for Dye Removal: A Review. *Journal for Bioresource Technology* **97**:1061-1085. doi.org/10.1016/j.biortech.2005.05.001.

Cumpstey I. (2013) Chemical Modification of Polysaccharides. *Journal for ISRN Organic Chemistry* **2013**:1-27. https://doi.10.1155/2013/417672.

Dahmardehghalehno M., Bayatkashkoli A. (2013) Experimental Particleboard from Bagasse and Industrial Wood Particles. Journal on Agric. Crop Sci. **5**:1626-1631. DOI: doi:10.1590/1980-5373-mr-2015-0211.

Dai C., Yu C., Zhou X. (2005) Heat and Mass Transfer in Wood Composite Panels During Hot Pressing. Part II. Modeling Void formation and Mat Permeability. *Journal for Wood Fiber Science* **37**:242-257. http://pascal-francis.inist.fr/vibad/index.phpaction=getRecordDetail&idt=16712428.

De Barros Filho R.M., Mendes L.M., Novack K.M., Aprelini L.O., Botaro V.R. (2011) Hybrid Chipboard Panels Based on Sugarcane Bagasse, Urea Formaldehyde and

Melamine Formaldehyde Resin. *Journal for Industrial Crops and Products* **33**:369-373.

Diego M.S., Ricardo R.C., Pedrosa T.D., Rafaelde M.R. (2014) Physical and Mechanical Properties of Particleboard Manufactured from Wood, Bamboo and Rice Husk. Journal on Materials Research **17**:682-686.

Diop C.I.K., Tajvidia M., Bilodeauc M.A., Bousfieldd D.W., Hunte J.F. (2017) Evaluation of the Incorporation of Lignocellulose Nanofibrils as Sustainable Adhesive Replacement in Medium Density Fiberboards. *Journal for Industrial Crops & Products* **109**:27-36.

Diyamandoglu V., Fortuna L.M. (2015) Deconstruction of Wood-Framed Houses: Material Recovery and Environmental impact. *Journal for Resources, Conservation and Recycling* **100**:21-30. https://doi.10.1016/j.resconrec.2015.04.006

Dizaj M.Y., Khazaeiana A., Ashorib A. (2015) Suitability of Sorghum Stalk Fibers for Production of Particleboard. *Journal for Carbohydrate Polymers* **120**:15-21.

Du G.B., Wu L.Z., Yang Q.X. (1995) Development on Mineral Filler for UF Resin. *Journal of Adhesion* **16**:9-12.

Dulie N.W., Woldeyes B., Demsash H.D., Jabasingh A.S. (2020) An Insight into the Valorization of Hemicellulose Fraction of Biomass into Furfural: Catalytic Conversion and Product Separation. *Journal for Waste and Biomass Valorization* **1**:1-22.

Dunky M. (1998) Urea–Formaldehyde (UF) Adhesive Resins for Wood. *Journal of Adhesion and Adhesives* **18**:95-107. doi:10.1016/s0143-7496(97)00054-7

Ebringerova A., Hromadkova Z., Heinze T. (2005) Hemicellulose. *Journal for Advances in Polymer Science* **186**:1-67.

ECS. (1993) European Committee for Standardization. EN 312. Particleboard: specifications. Brussels: European Committee for Standardization.

Edhirej A., Sapuan S.M., Jawaid M., Zahari N.I., Sanyang M.L. (2017) Effect of Cassava Peel and Cassava Bagasse Natural Fillers on Mechanical Properties of Thermoplastic Cassava Starch, AIP Conf. Proc. 1901, 100010-1–100010-6; https://doi.org/10.1063/1.5010532Published by AIP Publishing. 978-0-7354-1589-8/$30.00.

El Hage R., Brosse N., Chrusciel L., Sanchez C., Sannigrahi P., Ragauskas A. (2009) Characterization of milled wood lignin and ethanol organosolv lignin from miscanthus. *Polymer Degradation and Stability* **94**:1632-1638. https://doi.10.1016/j.polymdegradstab.2009.07.007.

EraghiKazzaz A., HosseinPourFeizi Z., Fatehi P. (2019) Grafting Strategies for Hydroxy Groups of Lignin for Producing Materials. *Journal for Green Chemistry* **21**:5714-5752.

Erdocia X., Prado M.R., Corcuera A., Labidi J. (2014) Base Catalyzed Depolymerization of Lignin: Influence of Organosolv Lignin Nature. *Journal of Biomass and Bioenergy* **66**:379-386.

Fagerstedt K., Saranpaa P., Tapanila T., Immanen J., Serra J., Nieminen K. (2015) Determining the Composition of Lignins in Different Tissues of Silver Birch. *Journal for Plants* **4** 183-195. https://doi.10.3390/plants4020183.

Fang J., Sun R., Tomkinson J., Fowler P. (2000) Acetylation of Wheat Straw Hemicellulose B in a New Non-Aqueous Swelling System. *Journal for Carbohydrate Polymers* **41**:379-387.

FAO. (2015) Food and Agriculture Organization of the United Nations. World paddy production. [Accessed 26 December 2014]. Available rom:http://www.fao.org/newsroom/en/news/2008/1000820/index.html.

Fernandes I.J., Calheiro D., Sanchez F.A.L., Camacho A.L.D., Rocha T.L.A.d.C., Moraes C.A.M., Sousa V.C.d. (2017) Characterization of Silica Produced from Rice Husk Ash: Comparison of Purification and Processing Methods. *Journal for Materials Research* **20**:512-518. doi:10.1590/1980-5373-mr-2016-1043.

Ferrandez-Villena M., Ferrandez-Garcia C.E., Garcia-Ortuño T., Ferrandez-Garcia A., Ferrandez-Garcia M.T. (2020) Properties of Cement-Bonded Particleboards Made from Canary Islands Palm (Phoenix canariensis Ch.) Trunks and Different Amounts of Potato Starch. *Forests* **11**:560.

Ferreira A., Pereira J., Almeida M., Ferra J., Paiva N., Martins J., Carvalho L. (2018) Biosourced Binder for Wood Particleboards Based on Spent Sulfite Liquor and Wheat Flour. *Journal for Polymers* **10**:1070.

Ferreira M.S., Oliveira J.C., Miranda C., Magalhaes M.T., Santos W.J., Silva J.B.A., Jose N.M. (2015) Mechanical, Thermal and Barrier Properties of Starch-based Films Plasticized with Glycerol and Lignin and Reinforced with Cellulose Nanocrystals. *Materials Today: Proceedings* **2**:63-69. https://doi.org/10.1016/j.matpr.2015.04.009.

Figueiredo P., Lintinen K., Hirvonen J.T., Kostiainen M.A., Santos H.A. (2018) Properties and Chemical Modifications of Lignin: Towards Lignin-Based Nanomaterials for Biomedical Applications. *Progress in Materials Science* **93**:233-269. https://doi.org/10.1016/j.pmatsci.2017.12.001.

Fischer K., Heinze T. (2005) Hemicelluloses", Macromolecular Symposia-232: Selected contributions from the conference in Wiesbaden (Germany), June 27-30.

Gambus H., Gumul D., Gibiński M. (2014) Air Oxidation of Potato Starch Over Zinc (II) Catalyst. *Carbohydr. Polym.* **8**:45-50.

Gao W., Fatehi P. (2019) Lignin for Polymer and Nanoparticle Production: Current Status and Challenges. *Canadian Journal for Chemical Engineering* **97**:2827-2842.

Gao W., Rigout M., Owens H. (2016) Facile Control of Silica Nanoparticles Using a Novel Solvent Varying Method for the Fabrication of Artificial Opal Photonic Crystals. *Journal of Nanoparticle Research* **18**:3-10.

Gao Z., Li N., Wang Y., Niu W., Yi W. (2020) Pyrolysis Behavior of Xylan-Based Hemicellulose in a Fixed Bed Reactor. *Journal for Analytical and Applied Pyrolysis* **146**:104772.

Garcia R., Lopez A.R., Villegas M.A. (2017) The Effect of Ca^{2+} Ions on the Pasting, Morphological, Structural, Vibrational, and Mechanical Properties of Corn starch–Water System. *Journal of Cereal Science* **79**:174-182.

Garcia R.E.M., Gonzalez N.M. (2019) Effect of the Addition of Potassium and Magnesium Ions on the Thermal, Pasting, and Functional Properties of Plantain Starch (Musa paradisiaca). *journal of Biological Macromolecules* **124**:41-49.

Gayathri V.G., Debnath S., Babu M.N. (2013) Chemically Modified Starches and their Applications in Pharmacy. *Journal for Pharmacy and Nano Science* **2**:332-344.

Ge H., Liu G., Yin R., Sun Z., Chen H., Yu L., Wang S. (2020) An Aldimine Condensation Reaction Based Fluorescence Enhancement Probe for Detection of Gaseous Formaldehyde. *Journal for Microchemical.* pp104793.

Ghaffar S.H., Fan M. (2014) Lignin in Straw and Its Applications as an Adhesive. *International Journal of Adhesion and Adhesives* **48**:92-101. https://doi.org/10.1016/j.ijadhadh.2013.09.001.

Ghanemi K., Nikpour Y., Omidvar O., Maryamabadi A. (2011) Sulfur-Nanoparticle-Based Method for Separation and Preconcentration of Some Heavy Metals in Marine Samples Prior to Flame Atomic Absorption Spectrometry Determination. *J. Talanta* **85**:763-769.

Ghosh I., Jain R.K., Glasser W.G. (2000) Multiphase Materials with Lignin. Part 16. Blends of Biodegradable Thermoplastics with Lignin Esters. ACS Symp. Ser., 742 (Lignin: Historical, Biological, and Materials Perspectives), 331.

Gilfillan W.N., Nguyen D.M.T., Sopade P.A., Doherty W.O.S. (2012) Preparation and Characterisation of Composites from Starch and Sugar Cane Fibre. *Journal on Ind. Crop. Prod.* **40**:45-54.

Giummarella N., Zhang L., Henriksson G., Lawoko M. (2016) Structural features of mildly fractionated lignin carbohydrate complexes (LCC) from spruce. Royal Society of Chemistry **6**:2356-2375.

Gomes H.I., Mayes W.M., Rogerson M., Stewart D.I., Burke I.T. (2016) Alkaline Residues and the Environment: A Review of Impacts, Management Practices and Opportunities. *Journal of Cleaner Production* **112**:3571-3582. https://doi.org/10.1016/j.jclepro.2015.09.111.

Grace M.R. (2012) Cassava Processing, FAO Rome.

Grenier-Loustalot M.F., Larroque S., Grenier P., Bedel D. (1996) Phenolic resins: 4. Self-Condensation of Methylolphenols in Formaldehyde-Free Media *Journal for Polymer* **37**:955-964. doi:10.1016/0032-3861(96)87277-6

Grimaldi M.P., Marques M.P., Laluce C., Cilli E.M., Sponchiado S.R.P. (2015) Evaluation of Lime and Hydrothermal Pretreatments for Efficient Enzymatic Hydrolysis of Raw Sugarcane Bagasse. *Journal for Biotechnology for Biofuels* **8**:2-14. doi:10.1186/s13068-015-0384-y

Gu J., Qiao Z., Lv S., Cao J., Tan H., Zhang Y. (2016) Preparation and Properties of Normal Temperature Cured Starch-Based Wood Adhesive. *BioResources* **11**:4839-4849. doi: 10.15376/biores.11.2.4839-4849.

Gu X., Kanghua C., Ming H., Shi Y., Li Z. (2012) La-Modified SBA-15/H_2O_2 Systems for the Microwave Assisted Oxidation of Organosolv Beech Wood Lignin. *Journal for Ciencia y Tecnología* **14**:31-41.

Guangbao Y. (2014) Synthesis and Characterization of Cellulose fiber-silica nanocomposites, Chemical Engineering, Lappeenranta University of Technology, Faculty of Technology. pp. 54.

Guler C., Sahin H.I., Yeniay S. (2016) The Potential for Using Corn Stalks as a Raw Material for Production Particleboard With Industrial Wood Chips. *Journal for Wood Research* **61**:299-306. http://www.centrumdp.sk/wr/201602/13.

Gürü M., Tekeli S., Bilici İ. (2006) Manufacturing of Urea–Formaldehyde-Based Composite Particleboard from Almond Shell. *Materials & Design* **27**:1148-1151. doi: 10.1016/j.matdes.2005.03.003

Habeeb A.G., Mahmud H.B. (2010) Study on Properties of Rice Husk Ash and Its Use as Cement Replacement Material. *Journal on Materials Research* **13**:185-190.

Halvarsson S., Norgren M., Edlund H. (2004) Manufacturing of Fiber Composite Medium density Fiberboards (MDF) Based on Annual Plant Fiber and Urea Formaldehyde Resin. In: ICEFOP1 1st International Conference on Environmentally—Compatible Forest Products, 22–24 September 2004, Oporto, Portugal, pp. 131–135.

Hamdani-Devarennes S., Longuet C., Sonnier R., Ganachaud F., Lopez-Cuesta J.M. (2013) Calcium and Aluminum-Based Fillers as Flame-Retardant Additives in Silicone Matrices. III. Investigations on Fire Reaction. *Journal for Polymer Degradation and Stability* **98**:2021-2032.

Han Z., Wang J., Zhao H., Tucker M.E., Zhao Y., Wu G., Zhou J., Yin J., Zhang H., Zhang X., Yan H. (2019) Mechanism of Biomineralization Induced by *Bacillus subtilis* J_2 and Characteristics of the Biominerals. *Journal for Minerals* **9**:218.

Hardy K., Radini A., Buckley S., Blasco R., Copeland L., Burjachs F., Girbal J., Riker Y., Carbonell E., Castro M.J. (2017) Diet and Environment 1.2 Million Years Ago Revealed Through Analysis of Dental Calculus from Europe's Oldest Hominin At Sima Del Elefante, Spain. *The Science of Nature* **104**:1-2.

Haroon M., Wang L., Yu H., Abbasi N.M., Zain-ul-Abdin Z.A., Saleem M., Wu J. (2016) Chemical Modification of Starch and Its Application as an Adsorbent Material. *Journal for RSC Advances* **6**:78264-78285.

Harvey D. (2000) Mordern analytical chemistry. International Edition, McGraw-Hill, Singapore. pp 53 - 56.

Hatakeyama H. (2012) Polyurethanes Containing Lignin. In "Chemical, Modification, Properties, and Usage of Lignin" (T. Q. Hu, ed.), pp 41-56. Kluwer Academic/Plenum Publishers, New York.

Haysa M.D., Fineb P.M., Gerona C.G., Kleemanc M.J., Gulletta B.K. (2015) Open Burning of Agricultural Biomass: Physical and Chemical Properties of Particle-Phase Emission. Atmospheric Environment 39: pp. 6747 - 6764.

Hazwan H.M., Aziz A.A., Iqbal A., Ibrahim M.N.M., Latif N.H.A. (2019) Development and Characterization Novel Bio-adhesive for Wood Using Kenaf Core (Hibiscus cannabinus) Lignin and Glyoxal. *Journal for Biological Macromolecules* **122**:713-722. doi:10.1016/j.ijbiomac.2018.11.009.

He W., Gao W., Fatehi P. (2017) Oxidation of Kraft Lignin with Hydrogen Peroxide and its Application as a Dispersant for Kaolin Suspensions. *Journal for ACS Sustainable Chemistry & Engineering* **5**:10597-10605. doi:10.1021/acssuschemeng.7b02582

Hocking M.B., Crow J.P. (1994) On the Mechanism of Alkaline Hydrogen Peroxide Oxidation of the Lignin Model p-Hydroxyacetophenone. *Canadian Journal for Chemistry* **72**:1137-1142.

Homkhiew C., Boonchouytan W., Cheewawuttipong W., Hoysakul N., Kaewkong W., Ratanawilai T. (2020) Measurement in Some Properties of Non-Toxic Particleboard to Optimize the Formulation for Food Containers. *Journal for Measurement* **156**:107617.

Hoong Y.B., Paridah M.T., Loh Y.F., Koh M.P., Luqman C.A., Zaidon A. (2010) Acacia mangium Tannin as Formaldehyde Scavenger for Low Molecular Weight Phenol-Formaldehyde Resin in Bonding Tropical Plywood. *Journal for Adhesion Science and Technology* **24**:1653-1664.

Huang Z., Lu J., Li X., Tong Z. (2017) Effect of Mechanical Activation on Physico-Chemical Properties and Structure of Cassava Starch. Carbohydr. Polym. **68**:128-135.

Hult E.L., Larsson P.T., Iversen T. (2002) A Comparative CP/MAS 13C-NMR Study of the Supermolecular Structure of Polysaccharides in Sulphite and Kraft Pulps. *Journal for Holzforschung* **56**:179-184. https://doi.org/10.1515/HF.2002.030.

Inkrod C., Raita M., Champreda V., Laosiripojana N. (2018) Characteristics of Lignin Extracted from Different Lignocellulosic Materials via Organosolv Fractionation. *Journal for BioEnergy Research* **11**:277-290.

Jablonskis A., Arshanitsa A., Telysheva G. (2016) Solvent Pretreatment of Lignin for Obtaining of Low Viscosity Lignopolyols by Oxypropylation for Synthesis of Polyurethanes. Mater. Sci. and Eng. **111**:1-6.

Jacob M., Varughese K.T., Thomas S. (2004) Hybrid Composites. *J. of Applied Polymer Science* **93** 2305-2312.

Jendoubi F., Mgaidi A., El Maaoui M. (1997) Kinetics of the Dissolution of Silica in aqueous Sodium Hydroxide Solutions at High Pressure and Temperature. *Journal of Chemical Engineering* **75**:721-727. doi:10.1002/cjce.5450750409.

Jones E.R., Childers R.L. (2003) Contemporary College Physics 2nd Edition, Addison Wesley Publishing Co.

Jonglertjunya W., Juntong T., Pakkang N., Srimarut N., Sakdaronnarong C. (2014) Properties of Lignin Extracted from Sugarcane Bagasse and its Efficacy in Maintaining Postharvest Quality of Limes During Storage. *Journal for Food Science and Technology* **57**:116-125.

Jonoobi M., Grami M., Ashori A., Ebrahimi G. (2016a) Effect of Ozone Pretreatment on the Physical and Mechanical Properties of Particleboard Panels Made from Bagasse. *Journal on Measurement* **94**:451-455. https://doi.org/10.1016/j.measurement.2016.08.019.

Jonoobi M., Grami M., Ashori A., Ebrahimi G. (2016b) Effect of Ozone Pretreatment on the Physical and Mechanical Properties of Particleboard Panels Made from Bagasse. *Measurement* **94**:451-455. https://doi.org/10.1016/j.measurement.2016.08.019.

Joseph P.V., Rabello M.S., Mattoso L.H.C., Joseph K., Thomas S. (2002) Environmental Effects on the Degradation Behaviour of Sisal Fibre Reinforced Polypropylene Composites. *Journal for Composites Science and Technology* **62**:1357-1372. doi:10.1016/s0266-3538(02)00080-5

Kaewtatip K., Thongmee J. (2013) Effect of Kraft Lignin and Esterified Lignin on the Properties of Thermoplastic Starch. Materials & Design **49**:701-7040261-3069. https://doi.org/10.1016/j.matdes.2013.02.010.

Kale G., Kijchavengkul T., Auras R., Rubino M., Selke S.E., Singh S.P. (2007) Compostability of Bioplastic Packaging Materials: An Overview. Journal for Macromolecular Bioscience **7**:255-277.

Kalnicky D.J., Singhvi R. (2012) Field portable XRF Analysis for Environmental Samples. *Journal of Hazardous Materials* **83**:149-152.

Kamseu E., Beleuk à Moungam L.M., Cannio M., Billong N., Chaysuwan D., Melo U.C., Leonelli C. (2017) Substitution of Sodium Silicate with Rice Husk Ash-NaOH Solution in Metakaolin Based Geopolymer Cement Concerning Reduction in Global Warming. *Journal for Cleaner Production* **142**:3050-3060.

Kanga X., Kugaa S., Wanga L., Wua M., Huanga Y. (2016) Dissociation of Intra/inter-Molecular Hydrogen Bonds of Cellulose Molecules in the Dissolution Process: A Mini Review. *Journal for Bioresource and Bioproducts* 1:58-63.

Kapelko-Zeberska M., Drozdz W., Gryszkin A., Grzechac M., Golachowski A., Zieba T. (2015) Current research addressing starch acetylation. *Journal for Food Chemistry* **176**:350-356.

Kartini K. (2014a) Rice Husk Ash – Pozzolanic Material for Sustainability. *International Journal of Applied Science And Technology* **1**:266 - 711.

Kartini K. (2014b) Rice Husk Ash – Pozzolanic Material for Sustainability. *Journal on Applied Science and Technology* **1**:266 - 711.

Kasim J., Lias H., Johari N.A.N., Moktar I.L.M. (2014) Influence of Board Density and Particle Sizes on the Homogeneous Particleboard Propperties from Kelempayan (*Neolamarcackia cadamba)*. *International Journal of Latest Research in Science and Technology* **3**:173-176.

Kaur P., Pal P., Virdi A.S., Kaur A., Singh N., Mahajan G. (2016) Protein and starch characteristics of milled rice from different cultivars affected by transplantation date. *Journal for Food Science and Technology* **53**:3186-3196.

Kaushik A., Kumar R., Arya S.K., Nair M., Malhotra B.D., Bhansali S. (2015) Organic–Inorganic Hybrid Nanocomposite-Based Gas Sensors for Environmental Monitoring. *Journal for Chemical Reviews* **115**:4571-4606.

Kelley S.S., Glasser W.G., Ward T.C. (2010) Effect of Soft-Segment Content on the Properties of Lignin-Based Polyurethanes. In "Lignin: Properties and Materials" (W. G. Glasser and S. Sarkanen, eds.), pp 402-413. ACS Symposium Series No. 397. American Chemical Society, Washington, D.C.

Kerns W.D., Pavkov K.L., Donofrio D.J., Gralla E.J., Swenberg J.A. (1983) Carcinogenicity of Formaldehyde in Rats and Mice after Long-Term Inhalation Exposure. *Journal for Cancer Res.* **43**:4382-4392.

Kerschbaumer R.C., Stieger S., Gschwandl M., Hutterer T., Fasching M., Lechner B., Friesenbichler W. (2019) Comparison of Steady-State and Transient Thermal Conductivity Testing Methods Using Different Industrial Rubber Compounds. *Journal for Polymer Testing* **80**:106121. https://doi.10.1016/j.polymertesting.2019.106121.

Khanjanzadeh H., Pirayesh H., Salari A. (2013) Effect of Using Walnut/Almond Shells on the Physical, Mechanical Properties and Formaldehyde Emission of Particleboard. *Journal for Composites Part B: Engineering* **45**:858-863.

Khazaei J. (2008) Water Absorption Characteristics of Three Wood Varieties. *Cercet˜ari Agronomice in Moldova* **41**:134-145.

Khedari J., Charoenvai S., Hirunlabh J. (2003) New Insulating Particleboards from Durian Peel and Coconut Coir. *Journal for Building and Environment* **38**:435-441. doi: 10.1016/S0360-1323(02)00030-6.

KNBS. (2018) Economic Survey 2018. Kenya National Bureau of Statistics. Herufi House Nairobi. ISBN: 978-9966-102-06-5.

Kongkiattikajorn J., Sornvoraweat B. (2011) Comparative Study of Bioethanol Production from Cassava Peels by Monoculture and Co-Culture of Yeast. *Journal for Natural Science* **45**:268-274.

Koubaa A., Koran Z. (1995) Measure of the Internal Bond Strength of Paper/Board. *Tappi Journal* **78**:103-111.

Kowaluk G., Szymanowski K., Kozlowski P., Kukula W., Sala C., Robles E., Czarniak P. (2019) Functional Assessment of Particleboards Made of Apple and Plum Orchard Pruning. *Journal for Waste and Biomass Valorization*:2-10. doi:10.1007/s12649-018-00568-8

Kulshreshtha Y., Schlangen E., Jonkers H.M., Vardon P.J., van Paassen L.A. (2017) CoRncrete: A corn Starch Based Building Material. Construction and Building Materials **154**:411-423. DOI: https://doi.org/10.1016/j.conbuildmat.2017.07.184.

Laemlaksakul V. (2010) Physical and Mechanical Properties of Particleboard from Bamboo Waste. *Journal for Engineering and Technology* **4**:276-280.

Landrock A.H., Sina E. (2015) Adhesives Technology Handbook. (Third Edition). William Andrew. Applied Science Publishers. pp 339 - 352.

Laurichesse S., Averous L. (2014) Chemical Modification of Lignins: Towards Biobased Polymers. *Journal of Progress in Polymer Science* **39**:1266-1290.

Lawton J.W. (2016) Starch, Uses of Native Starch, *Reference Module in Food Science*, Elsevier.

Le Corre D., Dufresne A. (2013) Preparation of Starch Nanoparticles. Biopolymer Nanocomposites: Processing, Properties, and Applications, First Edition. Edited by Alain Dufresne, Sabu Thomas, and Laly A. Pothan.© 2013 John Wiley & Sons, Inc. Published 2013 by John Wiley & Sons, Inc.:153-180.

Lee H.S., Loh Y.W., H'ng P.S., Lum W.C., Tan C.K. (2010) Properties of Particleboard Produced from Admixture of Rubberwood and Mahang Species. *Journal for Applied Sciences* **3**:310-316.

Lemos P.V.F., Barbosa L.S., Ramos I.G., Coelho R.E., Druzian J.I. (2019) Characterization of Amylose and Amylopectin Fractions Separated from Potato, Banana, Corn, and Cassava Starches. *Journal for Biological Macromolecules* **132**:32-42.

Lepifre S., Baumberger S., Pollet B., Cazaux F., Coqueret X., Lapierre C. (2004) Reactivity of Sulphur-Free Alkali Lignins Within Starch Films. *Journal on Industrial Crops and Products* **20**:219-230. https://doi.org/10.1016/j.indcrop.2004.04.023.

Lewicka K., Siemion P., Kurcok P. (2015) Chemical Modifications of Starch: Microwave Effect. *Journal of Polymer Science* **2015**:1-10.

Li J., Zhang J., Zhang S., Gao Q., Li J., Zhang W. (2018) Alkali Lignin Depolymerization Under Eco-Friendly and Cost-Effective NaOH/Urea Aqueous Solution for Fast Curing Bio-Based Phenolic Resin. *Journal for Industrial Crops and Products* **120**:25-33. https://doi.org/10.1016/j.indcrop.2018.04.027.

Li Z., Wang J., Cheng L., Gu Z., Hong Y., Kowalczyk A. (2014) Improving the Performance of Starch-Based Wood Adhesive by Using Sodium Dodecyl Sulfate. *Journal on Carbohydr. Polym.* **99**:579-583.

Liew K.C., Ting P.B., Tan Y.F. (2018) Physico-Mechanical Properties of Particleboard Made from Seaweed Adhesive and Tapioca Starch Flour. *Journal for Indian Academic Wood Science* **15**:199-203.

Lim S.H., Lee W.S., Kim Y., Sohn Y., Cho D.W., Kim C., Kim E., Latham J.A., Dunaway-Mariano D., Mariano P.S. (2015) Photochemical and Enzymatic SET Promoted C–C Bond Cleavage Reactions of Lignin β-1 Model Compounds Containing Varying Number of Methoxy Substituents on their Arene Rings. Tetrahedron **71**:4236-4247. https://doi.org/10.1016/j.tet.2015.04.077.

Liu H., Xie F., Yu L., Chen L. (2016) Starch Modification Using Reactive Extrusion. *Starch* **58**:131-139.

Liu X., Wu Z., Han Y., Han L. (2017) Characteristic Modification of Alkalized Corn Stalk and Contribution to the Bonding Mechanism of Fuel Briquette. *Journal for Energy* **133**:299-305.

Liu Y., Li K. (2002) Chemical Modification of Soy Protein for Wood Adhesives. *Journal for Macromolecular Rapid Communications* **23**:739-742.

Lu J.Z., Wu Q., Negulescu I.I. (2005) Wood-Fiber/High-Density-Polyethylene Composites: Coupling Agent Performance. *Journal of Applied Polymer Science* **96**:93-102. doi: 10.1002/app.21410.

Lu K., Collins L.B., Ru H., Bermudez E., Swenberg J.A. (2010) Distribution of DNA Adducts Caused by Inhaled Formaldehyde is Consistent with Induction of Nasal Carcinoma but Not Leukemia. *Journal for Toxicol. Sci.* **116**:441-451.

Lu S., Lin S., Yao K. (2004) Study on the Synthesis and Application of Starch-graft-Poly(AM-co-DADMAC) by Using a Complex Initiation System of CS-KPS. *Journal for Starch - Stärke* **56**:138-143.

Lu Y., Lu Y.C., Hu H.-Q., Xie F.J., Wei X.Y., Fan X. (2017) Structural Characterization of Lignin and Its Degradation Products with Spectroscopic Methods. *Journal for Spectroscopy* **2017**:1-15.

Maeda H., Nakajima M., Hagiwara T., Sawaguchi T., Yano S. (2006) Bacterial Cellulose/Silica Hybrid Fabricated by Mimicking Biocomposites. *Journal for Materials Science* **41**:5646-5656.

Magalhaes F.D., Costa N.A., Pereira J., Ferra J., Cruz P., Martins J., Carvalho L.H. (2013) Scavengers for Achieving Zero Formaldehyde Emission of Wood-Based Panels. *Journal on Wood Science and Technology* **47**:1261-1272.

Majeed Z., Mansor N., Ismail S., Mathialagan R., Man Z. (2016) Gompertz Kinetics of Soil Microbial Biomass in Response to Lignin Reinforcing of Urea-Crosslinked Starch Films. *Journal on Procedia Engineering* **148**:553-560. https://doi.org/10.1016/j.proeng.2016.06.510.

Majeed Z., Mansor N., Ajab Z., Man Z., Sarwono A. (2018) Kraft Lignin Ameliorates Degradation Resistance of Starch in Urea Delivery Diocomposites. *Polymer Testing* **65**:398-406. https://doi.org/10.1016/j.polymertesting.2017.12.011.

Mamza P.A.P., Ezeh E.C., Gimba E.C., Arthur E.D. (2014) Comparative Study Of Phenol Formaldehyde And Urea Formaldehyde Particleboards From Wood Waste For Sustainable Environment. *Journal for Science and Technology Research* **3**:2277-8616. ISSN 2277-8616.

Mandal A., Chakrabarty D. (2011) Isolation of Nanocellulose from Waste Sugarcane Bagasse (SCB) and its Characterization. *Journal for Carbohydrate Polymers* **86**:1291-1299. doi:10.1016/j.carbpol.2011.06.030.

Mansor N., Majeed Z., Ismail S., Mathialagan R., Man Z. (2016) Gompertz Kinetics of Soil Microbial Biomass in Response to Lignin Reinforcing of Urea-Crosslinked

Starch Films. *Procedia Engineering* **148**:553-560. https://doi.org/10.1016/j.proeng.2016.06.510.

Mantanis G.I., Athanassiadou E.T., Barbu M.C., Wijnendaele K. (2017) Adhesive Systems Used in the European Particleboard, MDF and OSB Industries. Journal for Wood Material Science & Engineering **13**:104-116.

Marhmood N. (2005) Investigations on the Adhesion of Polyurethane Foams on Thermoplastic Material Systems.

Masina N., Choonara Y.E., Kumar P., du Toit L.C., Govender M., Indermun S., Pillay V. (2017) A review of the chemical modification techniques of starch. *Journal for Carbohydrate Polymers* **157**:1226-1236.

Mati B.N., Baynast H., Sun S., Lebert A., Petit E., Michaud P. (2015) Polysaccharidic Binders for the Conception of an Insulating Agro-Composite. *Journal on Composites Part A: Applied Science and Manufacturing* **78**:152-159. https://doi.org/10.1016/j.compositesa.2015.08.006.

Matuana M.L., Carlborn K. (2012) Composite Materials Manufactured from Wood Particles Modified Through a Reactive Extrusion Process. Polymer Composites **26**:534-541.

Meimoun J., Wiatz V., Saint-Loup R., Parcq J., Favrelle A., Bonnet F., Zinck P. (2017) Modification of starch by graft copolymerization. *Journal for Starch - Stärke* **70**:1-23.

Melo R.R.d., Stangerlin D.M., Santana R.R.C., Pedrosa T.D. (2014) Physical and Mechanical Properties of Particleboard Manufactured from Wood, Bamboo and Rice Husk. *Journal for Materials Research* **17**:682-686. doi:10.1590/s1516-14392014005000052.

Mendes R.F., Mendes L.M., Oliveira S.L., Freire T.P. (2014) Use of Sugarcane Bagasse for Particleboard Production. Journal for Engineering Materials **634**:163-171.

Mendes R.F., Mendes L.M., Carvalho A.G., Guimaraes Junior J., B., Mesquita R.G.A. (2012) Determination of the Elastic Modulus of Particleboard by Stress Wave Timer. *Journal for Floresta e Ambiente* **19**:117-122.

Mendham J., Denney R.C., Barnes J.D., Thomas M., Sivasankar B. (2000) Vogel's Textbook of Quantitative Chemical Analysis, 6th Edition, pp 338, 562.

Merline D.J., Vukusic S., Abdala A.A. (2012) Melamine Formaldehyde: Curing Studies and Reaction Mechanism. *Journal for Polymer* **45**:413-419.

Miedes E., Vanholme R., Boerjan W., Molina A. (2014) The Role of the Secondary Cell Wall in Plant Resistance to Pathogens. Frontiers in Plant Sci. **5**.

Miller J.C., Miller J.N. (1988) Basic Statistical Methods for Analytical Chemistry. Part I. Statistics of Repeated Measurements. A review Analyst **113**:1351-1356.

Milotskyi R., Bliard C., Tusseau D., Benoit C. (2018) Starch Carboxymethylation by Reactive Extrusion: Reaction Kinetics and Structure Analysis. *Journal for Carbohydrate Polymers* **194**:193-199.

Mirski R., Derkowski A., Dziurka D., Dukarska D., Czarnecki R. (2019) Effects of a Chipboard Structure on Its Physical and Mechanical Properties. *Journal for Materials* **12**:3777. doi:10.3390/ma12223777.

Mitsunaga T., Conner A.C., Hill C.G.J. (2000) Reaction of Formaldehyde with Phenols:A Computational Chemistry Study. In Proc. Int. Symp. 7th, Wood Adhesives, 2001, pp. 147–153. https://doi.org/10.1016/S0960-8524(01)00152-3.

Mittal K.L. (1995) Adhesion measurement of films and coatings, VSP, Utrecht, 5.

Mokhena T.C., Mochane M.J., Motaung T.E., Linganiso L.Z., Thekisoe O.M., Songca S.P. (2018) Sugarcane Bagasse and Cellulose Polymer Composites. Sugarcane Technology and Research. doi:10.5772/intechopen.71497.

Monteiro S., Martins J., Magalhães F.D., Carvalho L. (2019) Low Density Wood Particleboards Bonded with Starch Foam—Study of Production Process Conditions. *Journal for Materials* **12**:1975.

Monteiro S., Nunes L., Martins J., Magalhaes F.D., Carvalho L. (2020) Low-Density Cardoon (Cynara cardunculusL.)Particleboards Bound with PotatoStarch-Based Adhesive. *Journal ofor Polymers* **12**:1-16.

Moresco R., Uarrota V.G., Nunes E.d.C., Coelho B., Amante E.R., Gervin V.M., Maraschin M. (2014) Discrimination of Brazilian Cassava Genotypes (Manihot esculenta Crantz) According to Their Physicochemical Traits and Functional Properties through Bioinformatics Tools. 8th International Conference on Practical Applications of Computational Biology & Bioinformatics (PACBB 2014), 57–63. https://doi.10.1007/978-3-319-07581-5_7

Motohashi K., Tomita B., Mizumachi H., Sakaguchi H. (1984) Temperature Dependency of Bond Strength of Polyvinyl Acetate Emulsion Adhesives for Wood. *Journal for Wood and fiber science* **16**:72-85.

Mounguengui-Diallo M., Sadier A., Noly E., Da Silva Perez D., Pinel C., Perret N., Besson M. (2019) C-O Bond Hydrogenolysis of Aqueous Mixtures of Sugar Polyols and Sugars over ReOx-Rh/ZrO_2 Catalyst: Application to an Hemicelluloses Extracted Liquor. *Journal of Catalysts* **9**:740.

Moussa G., Moury R., Demirci U.B., Miele P. (2013) Borates in Hydrolysis of Ammonia borane. *International Journal of Hydrogen Energy* **38**:7888-7895. https://doi.org/10.1016/j.ijhydene.2013.04.121.

Mtibe A., Linganiso L.Z., Mathew A.P., Oksman K., John M.J., Anandjiwala R.D. (2015) A Comparative Study on Properties of Micro and Nanopapers Produced from Cellulose and Cellulose Nanofibres. *Journal for Carbohydrate Polymers* **118**:1-8.

Murphy P. (2000) Starch," in Handbook of Hydrocolloids, pp. 41–65, CRC Press, 2000.

Murphy P., Mitchell J. (2009) Starch, Handbook of Hydrocolloids, in: G.O.Phillips, P.A. Williams (Eds.), Woodhead Publishing Limited, 2009, pp. 42–65.

Muruganandam L., Ranjitha J., Harshavardhan A. (2016) A Review Report on Physical and Mechanical Properties of Particle Boards from organic Waste. *Journal for ChemTech Research* **9**:64-72.

Mwaikambo L.Y., Ansell M.P. (2002) Chemical Modification of Hemp, Sisal, Jute, and Kapok Fibers by Alkalization. *Journal of Applied Polymer Science* **84**:2222-2234. https://doi.org/10.1002/app.10460.

Myers G.E. (1985) The Effects of Temperature and Humidity on Formaldehyde Emission from UF-Bonded Boards: a Literature Critique. *Journal for For. Prod.* **35**:20-31.

Myers H.P. (2002) Introductory Solid State Physics.Taylor & Francis. ISBN 0-7484-0660-3.

Narkchamnan S., Sakdaronnarong C. (2013) Thermo-Molded Biocomposite from Cassava Starch, Natural Fibers and Lignin Associated by Laccase-Mediator System. *Carbohydrate Polymers* **96**:109-117. https://doi.org/10.1016/j.carbpol.2013.03.046.

Nasir M., Gupta A., Kumar A., Chua G. (2014) Physical and Mechanical Properties of Medium Density Fibreboards Using Soy-Lignin Adhesives. Journal on Tropical Forest Science **26**:41-49.

Nasser R.A. (2012a) Physical and Mechanical Properties of Three Layer Particleboard Manufactured from the

Tree Pruning of Seven Wood Species. *Journal for World Applied Sciences* **19**:741-753.

Nasser R.A. (2012b) Physical and Mechanical Properties of Three-Layer Particleboard Manufactured from the Tree Pruning of Seven Woodspecies. *Journal for World Application Sciences* **19**:741-753. doi: 10.5829/idosi.wasj.2012.19.05.2764.

Ndazi B., Tesha J.V., Nisanda E.T.N. (2006) Some Opportunities and Challenges of Producing Bio-Composites from Non-wood Residues. *Journal for Material Science* **41**:6984-6990. doi: 10.1007/s10853-006-0216-3.

Neelam K., Vijay S., Lalit S. (2012) Various Techniques for the Modification of Starch and the Applications of its Derivatives. *Journal for Pharmacy* **3**:25-31.

Nemli G., Aydın I., Zekovic E. (2007) Evaluation of Some of the Properties of Particleboard as Function of Manufacturing Parameters. *Journal for Materials & Design* **28**:1169-1176. doi:10.1016/j.matdes.2006.01.015.

Nemli G., Demirel S., Gumuskaya E., Aslan M., Acar C. (2009) Feasibility of Incorporating Waste Grass Clippings (*Lolium perenne L.*) in Particleboard Composites. *Journal for Waste Management* **29**:1129-1131. DOI: 10.1016/j.wasman.2008.07.011

Nerdy. (2018) Determination of Sodium, Potassium, Magnesium, and Calcium Minerals Level in Fresh and Boiled Broccoli and Cauliflower by Atomic Absorption Spectrometry. IOP Conference Series: *Materials Science and Engineering*, 288, 012113.

Neudecker P., Lundström P., Kay L.E. (2009) Relaxation Dispersion NMR Spectroscopy as a Tool for Detailed Studies of Protein Folding. *Journal for Biophysical* **96**:2045-2054. doi:10.1016/j.bpj.2008.12.3907.

Ng C.W., Yip M.W., Lai Y.C. (2018) The Study on the Effects of Sodium Silicate on Particleboard Made from Sugarcane Bagasse. *Journal for Materials Science* **911**:66-70.

Nielsen J.P. (1943) Rapid Determination of Starch Content. Journal for Ind. Eng. Chem. **15**:176-179.

Nishida J., Fayer M.D. (2017) Guest Hydrogen Bond Dynamics and Interactions in the Metal–Organic Framework MIL-53(Al) Measured with Ultrafast Infrared Spectroscopy. *Journal for Physical Chemistry* **121**:11880-11890.

Nordqvist P. (2012) Exploring the Wood Adhesive Performance of Wheat Gluten. KTH Chemical Science and Engineering, University of Stockholm.

Nurul H.B., Mazlan M., Mohd M.A., Bakri A., Noorhafiza M., Rozyanty R., Mohd N.O., Mohd H.M.A., Mohammad K.A.A., Zairi I.R. (2016) Potential of Cassava Root as a Raw Material for Bio-Composite Development. *Journal of Engineering and Applied Sciences* **11**:2016.

Obadina A.O., Oyewole O.B., Sanni L.O., Abiola S.S. (2006) Fungal enrichment of cassava peels proteins. *African Journal of Biotechnology* **5**:302.

Obiro W.C., Sinha Ray S., Emmambux M.N. (2012) V-amylose Structural Characteristics, Methods of Preparation, Significance, and Potential Applications. *Journal for Food Reviews International* **28**:412-438.

Oh S.Y., Yoo D., Shin Y., Kim H.C., Kim. H. Y., Chung Y.S., Park W.H. (2005) Crystalline Structure Analysis of Cellulose Treated with Sodium hydroxide and Carbon Dioxide by Means of X-ray Diffraction and FTIR Spectroscopy. *Journal on Carbohydrate Research* **340**:2376-2791.

Okeyo J.M., Jay N., Saidou K., Waswa B., Kihara J., Bationo A. (2016) Impact of Reduced Tillage and Crop Residue Management on Soil Properties and Crop Yields in A Long-Term Trial in Western Kenya. *International Center for Tropical Agriculture* **54**:719-729.

Okoba B., Silvestri S., Ringler C., Bryan E. (2012) Climate Change Perception and Adaptation of Agro-Pastoral Communities in Kenya. *Regional Environmental Change* **12**:791-802.

Oladele I.O., Ibrahim I.O., Adediran A.A., Akinwekomi A.D., Adetula Y.V., Olayanju T.M.A. (2020) Modified Palm Kernel Shell Fiber/Particulate Cassava Peel Hybrid Reinforced Epoxy Composites. *Journal for Results in Materials* 5:100053.

Oliveira S.L., Mendes R.F., Mendes L.M., Freire T.P. (2016) Particleboard Panels Made from Sugarcane Bagasse: Characterization for Use in the Furniture Industry. *Journal for Materials Research* **19**:914-922. doi:10.1590/1980-5373-mr-2015-0211

Olumoyewa A., Osueke C., Badiru S., Gana J., Abayomi M., Tegene G., Igbinosa I. (2019) Evaluation of Particle Board from Sugarcane Bagasse and Corn Cob. *Journal for Mechanical Engineering and Technology* 10:1193-1200.

Onyimonyi A.E., Ugwu S.O.C. (2007) Bioeconomic Indices of Broiler Chicks Fed Varying Ratios of Cassava Peel/Bovine Blood. *International Journal of Poultry Science* **6**:318-321.

Oparaku N., F.,, Ofomatah A., C., Okoroigwe E., C. (2013) Biodigestion of Cassava Peels Blended with Pig Dung for Methane Generation. *Journal of Biotechnology* 12:5956-5961.

Ouhaddouch H., Cheikh A., Idrissi M.O.B., Draoui M., Bouatia M. (2019) FT-IR Spectroscopy Applied for Identification of a Mineral Drug Substance in Drug Products: Application to Bentonite. *Journal for Spectroscopy* **2019**:1-6. doi.org/10.1155/2019/2960845.

Paiman B., Aizat A.G., Lee H.S., Zaidon A. (2019) Physico-Mechanical Properties and Formaldehyde Emission of Rubberwood Particleboard Made With UF Resin Admixed With Ammonium and Aluminium-Based Hardeners. *Journal for Science and Technology* **27**:473-488. ISSN: 0128-7680 e-ISSN: 2231-8526.

Palencia M. (2018) Functional Transformation of Fourier-Transform Mid-Infrared Spectrum for Improving Spectral Specificity by Simple Algorithm Based on Wavelet-Like Functions. *Journal for Advanced Research* **14**:53-62.

Pan Z., Cathcart A., Wang D. (2006) Properties of Particleboard Bond with Rice Bran and Polymericmethylene Diphenyl Diisocyanate Adhesives. *journal for Industrial and Products* **23**:40-45.

Papageorgiou D.G., Kinloch I.A., Young R.J. (2017) Mechanical Properties of Graphene and Graphene-Based Nanocomposites. *Journal for Progress in Materials Science* **90**:75-127.

Paranhos C.M., Santana Costa J.A. (2018) Systematic Evaluation of Amorphous Silica Production from Rice Husk Ashes. *Journal for Cleaner Production* **192**:688-697. doi.org/10.1016/j.jclepro.2018.05.028.

Parker R., Ring S.G. (2001) Aspects of the Physical Chemistry of Starch. *J. Cereal Sci.* **34**:1-17.

Parnis J.M., Oldham K.B. (2013) Beyond the Beer–Lambert Law: The Dependence of Absorbance on Time in Photochemistry. *Journal for Photochemistry and Photobiology A: Chemistry* **267**:6-10.

Patel K.F., Mehta H.U., Srivastava H.C. (1974) Kinetics and Mechanism of Oxidation of Starch with Sodium Hypochloride. *Journal on Appl. Polym. Sci.* **399**:389-399. doi.org/10.1002/app.1974.070180207.

Patel K.F., Mehta H.U., Srivastava H.C. (2013) Kinetics and Mechanism of Oxidation of Starch with Sodium Hypochloride. *J. Appl. Polym. Sci.* **399**:389-399

Paul A.P.M., Emmanuel C.E., Gimba E.C., Ebuka A.D. (2014) Comparative Study of Phenol Formaldehyde and Urea Formaldehyde Particleboards from Wood Waste for Sustainable Environment. *Journal on Scientific & Technology* **3**:53 - 61.

Peng X., Zhong L., Ren J., Sun R. (2010) Laccase and Alkali Treatments of Cellulose Fibre: Surface Lignin and its Influences on Fibre Surface Properties and Interfacial Behaviour of Sisal Fibre/Phenolic Resin Composites. *Journal for Applied Science and Manufacturing* **41**:1848-1856.

Perez J., Munoz-Dorado J., de la Rubia T., Martínez J. (2002) Biodegradation and Biological Treatments of Cellulose, Hemicellulose and Lignin: an Overview. *Journal for International Microbiology* **5**:53-63.

Pfungen L. (2015) Lignin Phenol Formaldehyde Wood Adhesives, Department of Material Sciences and Process Engineering, University of Natural Resources and Life Sciences, Vienna. pp. 75.

Polnaya F.J., Haryadi M.D.W., Cahyanto M.N. (2013) Effects of Phosphorylation and Crosslinking on the Pasting Properties and Molecular Structure of Sago Starch. *Journal for Food Research* **20**:1609-1615.

Poppe L.J., Paskevich V.F., Hathaway J.C., Blackwood D.S. (2015) A Laboratory Manual for X-Ray Powder Diffraction. U. S. Geological Survey Open-File Report 01-041.

Potthast A., Rosenau T., Kosma P. (2006) Analysis of Oxidized Functionalities in Cellulose. *Journal for Polymer Science* **205**:1-48. https://doi.0.1007/s10570-005-9040-1.

Qiang Y., Yang L., Liu J., Du C. (2013) Preparation and Properties of Cornstarch Adhesive. *Journal on advanced Food Sci. Technol.* **5**:1068-1072.

Qiao Z., Gu J., Lv S., Cao J., Tan H., Zhang Y. (2016) Preparation and Properties of Normal Temperature Cured Starch-Based Wood Adhesive. *Journal on BioResources* **11**:4839-4849. doi.10.15376/biores.11.2.4839-4849.

Qin Y., Zhang H., Dai Y., Hou H., Dong H. (2019) Effect of Alkali Treatment on Structure and Properties of High Amylose Corn Starch Film. *Journal for Materials* **12**:1705. https://doi.10.3390/ma12101705.

Rachtanapun P., Simasatitkul P., Chaiwan W., Watthanaworasakun Y. (2012) Effect of Sodium Hydroxide Concentration on Properties of Carboxymethyl Rice Starch. *Journal for Food Research* **19**:923-931.

Ragheb A.A., Abdel-Thalouth I., Tawfik S. (1995) Gelatinization of Starch in Aqueous Alkaline Solutions. *Journal for Starch - Stärke* **47**:338-345.

Raheem S.B., Arubike E.D., Awogboro O.S. (2015) Effects of Cassava Peel Ash (CPA) as Alternative Binder in Concrete. *Journal for Constructive Research in Civil Engineering* **1**:27-32.

Rahman M.M., Netravali A.N. (2018a) Advanced Green Composites Using Liquid Crystalline Cellulose Fibers and Waxy Maize Starch Based Resin. *Composites Science and Technology* **162**:110-116. https://doi.org/10.1016/j.compscitech.2018.04.023.

Rahman M.M., Netravali A.N. (2018b) Advanced Green Composites Using Liquid Crystalline Cellulose Fibers and Waxy Maize Starch Based Resin. *Journal on Composites Science and Technology* **162**:110-116. https://doi.org/10.1016/j.compscitech.2018.04.023.

Ramachandra M., Shekar H.S.S. (2018) Green Composites: A Review. *Materials Today: Proceedings* **5**:2518-2526. https://doi.org/10.1016/j.matpr.2017.11.034.

Rantala D.H., Loring R.T. (1992) Manual for the Geochemical Analysis of Marine Sediment and Suspended Particular Matter. Earth Science Review **32**:24-26.

Rautkari L., Hill C.A.S., Curling S., Jalaludin Z., Ormondroyd G. (2013) What is the Role of the Accessibility of Wood Hydroxyl Groups in Controlling Moisture Content? *Journal of Materials Science* **48**:6352-6356.

Razak W., Mohammed A.S., Othman S., Mahmud S., Hashim W.S., Mohd S.R. (2013) Properties of Engineered Oil Palm Composite Boards from 32 Year-Old Tree Stems. Journal on Agricultural and Biological Science **8**.

Rezende C., de Lima M., Maziero P., deAzevedo E., Garcia W., Polikarpov I. (2011) Chemical and Morphological Characterization of Sugarcane Bagasse Submitted to a Delignification Process for Enhanced Enzymatic Digestibility. *Journal for Biotechnology for Biofuels* **4**:54. https://doi.10.1186/1754-6834-4-54.

Roberts S., Cameron R. (2002) The Effects of Concentration and Sodium Hydroxide on the Rheological Properties of Potato Starch Gelatinisation. *Journal for Carbohydrate Polymers* **50**:133-143.

Roberts V.M., Stein V., Reiner T., Lemonidou A., Li X., Lercher J.A. (2011) Towards Quantitative Catalytic Lignin Depolymerization. *Journal for Chemistry* **17**:5939-5948.

Rokiah H., Norhafizah S., Othman S., Tomoko S., Salim H., Masatoshi S., Ryohei T. (2010) Effect of Particle Geometry on the Properties of Binderless Particleboard Manufactured from Oil Palm Trunk. *Journal on Materials and Design*:4251-4257.

Root S.E., Savagatrup S., Printz A.D., Rodriquez D., Lipomi D.J. (2017) Mechanical Properties of Organic Semiconductors for Stretchable, Highly Flexible, and Mechanically Robust Electronics. *Chemical Reviews* 117:6467-6499.

Ruel K., Nishiyama Y., Joseleau J.P. (2012) Crystalline and Amorphous Cellulose in the Secondary Walls of Arabidopsis. *Journal for Plant Science* **193-194**:48-61. https://doi.10.1016/j.plantsci.2012.05.008.

Saffari M. (2011) Effects of Hardener Type and Particles Size on Formaldehyde Emission Pollution. International Conference on Environment Science and Engineering IPCBEE vol.8 (2011) © (2011)IACSIT Press, Singapore

Salau M.A., Ikponmwosa E.E., Olonode K.A. (2012) Structural Strength Characteristics of Cement-Cassava Peel Ash Blended Concrete *Journal for Civil and Environmental* **2**:68-78.

Salleh K.M., Hashim R., Sulaiman O., Hiziroglu S., Wan Nadhari W.N.A., Abd Karim N., Ang L.Z.P. (2014) Evaluation of Properties of Starch-Based Adhesives and Particleboard Manufactured from Them. *Journal of Adhesion Science and Technology* **29**: 319-336.

Salleh K.M., Hashim R., Sulaiman S.H., Hiziroglu S., Nadhari A., Jumhuri N., Zuin L. (2015) Evaluation of Properties of Starch-Based Adhesives and Particleboard Manufactured from Them. Journal on Adhesion Science and Technology **29**:319-336.

Sam-Brew S., Smith G.D. (2017) Flax Shive and Hemp Hurd Residues as Alternative Raw Material for Particleboard Production. *Journal for BioResource* **12**:5715-5735.

Samaha S.H., Nasr H.E., Hebeish A. (2005) Synthesis and Characterization of Starch-Poly(vinyl Acetate) Graft Copolymers and their Saponified Form. *Journal for Polymer Research* **12**:343-353.

Sangwan P., Kumar S., Dhankhar R., Bidra S. (2013) Utilization of Rice Husk and their Ash: A Review. *Research Journal of Chemical and Environmental Sciences* **1**:126 - 129.

Santos S., Jones K., Abdul R., Boswell J., Paca J. (2007) Treatment of Wet Process Hardboard Plant VOC Emissions by a Pilot Scale Biological System. *Biochemical Engineering Journal*, **37**(3), 261-270.

Sattayarak T., Rachtanapun P., Ketsamak N. (2012) Correlation of Density and Properties of Particleboard from Coffee Waste with Urea–Formaldehyde and Polymeric Methylene Diphenyl Diisocyanates. *Journal for Composite Materials* **46**:1839-1850.

Sattlera S.E., Funnell-Harrisa D.L., Pedersen J.F. (2010) Brown Midrib Mutations and their Importance to the Utilization of Maize, Sorghum, and Pearl Millet Lignocellulosic Tissues. *Journal for Plant Science* **178**:229-238.

Scaccia S., Goszczynska B. (2012) Sequential Determination of Platinum, Ruthenium, and Molybdenum in Carbon-Supported Pt, PtRu, and PtMo Catalysts by Atomic Absorption Spectrometry. *J. Talanta* **63**:791-796.

Scatolino M.V., Silva D.W., Mendes R.F., Marin M.L. (2013) Use of Maize Cob for Production of Particleboard. *Journal on Cienc. Agrotec.* **37**:330-337.

Shahidan N.S., Muhammed S. (2011) Manufacture of Composite Panel from Sugarcane Bagasse. *Journal for Engineering Materials* 471-472:49-54. doi:10.4028/www.scientific.net/kem.471-472.49.

Sharif F., Arjmand M., Moud A.A., Sundararaj U., Roberts E.P.L. (2017) Segregated Hybrid Poly(methyl methacrylate)/Graphene/Magnetite Nanocomposites for Electromagnetic Interference Shielding. *Journal for ACS Applied Materials & Interfaces* **9**:14171-14179.

Shateri-Khalilabad M., Yazdanshenas M.E., Etemadifar A. (2017) Fabricating Multifunctional Silver Nanoparticles-Coated Cotton Fabric. *Arabian Journal of Chemistry* **10**:2355-2362.

Shekar H.S.S., Ramachandra M. (2018) Green Composites. *A Review* **5**:2518-2526. https://doi.org/10.1016/j.matpr.2017.11.034.

Siau C., Karim A., Norziah M., Wan Rosli W. (2004) Effects of Cationization on DSC Thermal profiles, Pasting and Emulsifying Properties of Sago Starch. *Journal of the Science of Food and Agriculture* **84**:1722-1730. doi.org/10.1002/jsfa.1871.

Siau C.L., Karim A.A., Norziah M.H., Wan Rosli W.D. (2013) Effects of Cationization on DSC Thermal Profiles, Pasting and Emulsifying Properties of Sago Starch. J. Sci. Food Agric. **84**:1722-1730.

Singha A.S., Thakur V.K. (2010) Mechanical, Morphological, and Thermal Characterization of Compression-Molded Polymer Biocomposites. *Journal for Polymer Analysis and Characterization* **15**:87-97. doi:10.1080/10236660903474506.

Sivasankarapillai G., McDonald A. (2011) Synthesis and Properties of lignin-Highly branched Poly (Ester-amine) Polymeric systems. *Journal on Biomass Bioenergy* **35**:919-931.

Spaccini R., Todisco D., Drosos M., Nebbioso A., Piccolo A. (2016) Decomposition of bio-degradable plastic polymer in a real on-farm composting process. *Journal for Chemical and Biological Technologies in Agriculture* **3**:1-12. https://doi.10.1186/s40538-016-0053-9.

Sreekala M.S. (2000) Oil Palm Fibre Reinforced Phenol FormaldehydeComposites: Influence of Fibre SurfaceModifications on the Mechanical Performance. *Journal for Applied Composite Materials* **7**:295-329.

Sridach W., Jonjankiat S., Wittaya T. (2013) Effect of Citric Acid, PVOH, and Starch Ratio on the Properties of Cross-Linked Poly(vinyl alcohol)/Starch Adhesives. *Journal of Adhesion Science and Technology* **27**:1727-1738.

Srikumar M., Vengal C.J. (2015) Processing and Study of Novel Lignin-Starch and Lignin-Gelatin Biodegradable Polymeric Films. Journal on Trends Biomater. Artif. Organs **18**.

Srivastava H.C., Parmar R.S., Dave G.B. (1970) Studies on Dextrinization. Part I. Pyrodextrinization of Corn Starch in the Absence of Any Added Catalyst. *Journal for Starch - Stärke* **22**:49-54.

Stark N.M., Cai Z., Carll C.G. (2010) Wood Handbook, Wood as an Engineering Material (General Technical Report FPL-GTR-190); Chapter 11: Wood-Based Composite–Materials-Panel Products– Glued-Laminated Timber, Structural Composite Lumber, and Wood-Nonwood Composite Materials. In: Ross, R., J. (ed.) U.S. Department of Agriculture, Forest Service, Forest Products Laboratory ed. Madison, Wisconsin: Forest Products Laboratory.

Stark N.M., Wei L., McDonald A.G. (2015) Interfacial Improvements in Biocomposites Based on Poly(3-hydroxybutyrate) and Poly(3-hydroxybutyrate-co-3-hydroxyvalerate) Bioplastics Reinforced and Grafted with α-Cellulose fibers. Green Chem. **17**:4800-4814.

Sudaryanto Y., Hartono S.B., Irawaty W., Hindarso H., Ismadji S. (2006) High Surface Area Activated Carbon Prepared from Cassava Peel by Chemical Activation. *Journal for Bioresource Technology* **97**:734-739.

Sujka M., Jamroz J. (2010) Characteristics of pores in native and hydrolyzed starch granules. *Journal for Starch - Stärke* **62**:229-235. https://doi.10.1002/star.200900226.

Sun J.X., Sun X.F., Zhao H., Sun R.C. (2004a) Isolation and Characterization of Cellulose from Sugarcane Bagasse. *Journal for Polymer Degradation and Stability* **84**:331-339. doi:10.1016/j.polymdegradstab.2004.02.008.

Sun Q., Foston M., Meng X., Sawada D., Pingali S.V., O'Neill H.M., Kumar R. (2014) Effect of Lignin Content on Changes Occurring in Poplar Cellulose Ultrastructure During Dilute Acid Pretreatment. *Journal for Biotechnology for Biofuels* **7**:2-14.

Sun S.L., Wen J.L., Xue B.L., Sun R.C. (2013) Recent Advances in Characterization of Lignin Polymer by Solution-State Nuclear Magnetic Resonance (NMR) Methodology. *Materials* **6**:359-391.

Sun X., Karr G.S., Cheng E. (2004b) Adhesive Properties of Modified Soybean Flour in Wheat Straw Particleboard. *Journal on Compos. Part A Appl. Sci. Manuf.* **35**:297-302.

Swenberg J.A., Kerns W.D., Mitchell R.I., Gralla E.J., Pavkov K.L. (1980) Induction of Squamous Cell Carcinomas of the Rat Nasal Cavity by Inhalation Exposure to Formaldehyde Vapor. *Journal for Cancer Res.* **40**:3398-3402.

Tabarsa T. (2011) Producing Particleboard Using of Mixture of Bagasse and Industrial Wood Particles. *Journal on Key Eng. Mater.* **471**:31-36.

Tadanaga K., Morita K., Mori K., Tatsumisago M. (2013) Synthesis of Monodispersed Silica Nanoparticles with High Concentration by the Stöber Process. *Journal for Sol-Gel Science and Technology* **68**:341-345.

Takagaki A., Fukai K., Nanjo F., Hara Y., Watanabe M., Sakuragawa S. (2000) Application of Green Tea Catechins as Formaldehyde Scavengers. *Journal for the Japan Wood Research* **46**:237.

Tako M., Hizukuri S. (2002) Gelatinization Mechanism of Potato Starch. *Journal for Carbohydrate Polymers* **48**:397-401. doi.org/10.1016/S0144-8617(01)00287-9.

Tan H., Zhang Y., Weng X. (2011) Preparation of the Plywood Using Starch-Based Adhesives Modified with Blocked Isocyanates. *Journal on Procedia Eng.* **15**:1171-1175.

Tan I., Flanagan B.M., Halley P.J., Whittaker A.K., Gidley M.J. (2007) A Method for Estimating the Nature and Relative Proportions of Amorphous, Single, and Double-Helical Components in Starch Granules by13C CP/MAS NMR. *Journal for Biomacromolecules* **8**:885-891. doi.org/10.1021/bm060988a.

Tana T., Zhang Z., Moghaddam L., Rackemann D.W., Rencoret J., Gutiérrez A., Río J.C., Doherty W.O.S. (2016) Structural Changes of Sugar Cane Bagasse Lignin during Cellulosic Ethanol Production Process. ACS Sustainable Chem. Eng. **4**:5483-5494.

Taramian A., Doosthoseini K., Mirshokraii S.A., Faezipour M. (2007) Particleboard Manufacturing: An Innovative Way to Recycle Paper Sludge. *Journal for Waste Management* **27**:1739-1746.

Tay C.C., Hamdan S., Osman M.S. (2016) Properties of Sago Particleboards Resinated with UF and PF Resin. *Advances in Materials Science and Engineering* **2016**:670-687.

Tester R.F., Karkalas J., Qi X. (2014) Starch—Composition, Fine Structure and Architecture. *J. Cereal Sci.* **39**:151-165.

Thomas S., Durand D., Chassenieux C., Jyotishkumar P. (2013) Handbook of Biopolymer-Based Materials: From Blends and Composites to Gels and

Complex Networks. Copyright © 2013 Wiley VCH Verlag GmbH & Co. KGaA . ISBN:9783527328840 |Online ISBN:9783527652457. doi:10.1002/9783527652457.

Tinti A., Tugnoli V., Bonora S., Francioso O. (2015) Recent Applications of Vibrational Mid-Infrared (IR) Spectroscopy for Studying Soil Components: A Review. *Journal for Central European Agriculture* **16**:1-22.

Tittelein P., Cloutier A., Bissonnette B. (2012) Design of a Low-Density Wood–Cement Particleboard for Interior Wall Finish. *Journal for Cement and Concrete Composites* **34**:218-222.

Tohmura S., Hse C.Y., Higuchi M. (2000) Formaldehyde emission and high-temperature stability of cured urea-formaldehyde resins. *Journal for Wood Science* **46**:303-309. https://doi.org/10.1007/BF00766221

Tonukari N.J. (2014) Cassava and the Future of Starch. *Electronic J. of Biotechnology* **7**:5-8.

Tout R. (2000) A Review of Adhesives for Furniture,. *Journal for Adhesion and Adhesives* **20**:269-272.

Ullah S., Bustam M.A., Nadeem M., Naz M.Y., Tan W.L., Shariff A.M. (2014) Synthesis and Thermal Degradation Studies of Melamine Formaldehyde Resins. *Scientific World Journal* **2014**:1325-1336.

Umemura K., Ueda T., Kawai S. (2012) Characterization of Wood-Based Molding Bonded with Citric Acid. *Journal of Wood Science* **58**:38-45.

Umemura K., Liao R., Xu J. (2016) Low Density Sugarcane Bagasse Particleboard Bonded with Citric Acid and Sucrose: Effect of Board Density and Additive Content. Bioresour **11**:2174-2185. doi:10.15376/biores.11.1.2174-2185.

Ummah H., Dadang A.S., Selintung M., Wahab A.W. (2015) Analysis of Chemical Composition of Rice Husk Used as Absorber Plates Sea Water into Clean Water. *Journal of Engineering and Applied Sciences* **10**:6046 - 6050.

Unger B., Bucker M., Reinsch S., Hubert T. (2012) Chemical Aspects of Wood Modification by Sol–Gel-Derived Silica. *Journal for Wood Science and Technology* **47**:83-104.

Uthumporn U., Shariffa Y.N., Fazilah A., Karim A.A. (2012) Effects of NaOH treatment of cereal starch granules on the extent of granular starch hydrolysis. *Journal for Colloid and Polymer Science* **290**:1481-1491. doi:10.1007/s00396-012-2674-2.

Vefago L.H.M., Avellaneda J. (2013) Recycling Concepts and the Index of Recyclability for Building Materials. *Journal for Resources, Conservation and Recycling* **72**:127-135. doi:10.1016/j.resconrec.2012.12.015.

Vengal C.J., Srikumar M. (2015) Processing and Study of Novel Lignin-Starch and Lignin-Gelatin Biodegradable Polymeric Films. Trends Biomater. Artif. Organs **18**.

Vengal J.C., Manu S. (2016) Processing and Study of Novel Lignin-Starch and Lignin-Gelatin Biodegradable Polymeric Films. Trends Biomater. Artif. Organs. **18**:237-241.

Visser J.H.M. (2018) Fundamentals of Alkali-Silica Gel Formation and Swelling: Condensation Under Influence of Dissolved Salts. *Journal for Cement and Concrete Research* **105**:18-30. doi:10.1016/j.cemconres.2017.11.006.

Waldron K.W., Parker M.L., Smith A.C. (2003) Plant Cell Walls and Food Quality. *Journal for Comprehensive Reviews in Food Science and Food Safety* **2**:128-146.

Wang D., Sun X.S. (2002) Low Density Particleboard from Wheat Straw and Corn Pith. *Industrial Crops Production* 15:43-50.

Wang P., Kosinski J.J., Lencka M.M., Anderko A., Springer R.D. (2013a) Thermodynamic Modeling of Boric Acid and Selected Metal Borate Systems. *Journal for Pure and Applied Chemistry* **85**:2117-2144. doi:10.1351/pac-con-12-07-09

Wang X., Cui X., Zhang L. (2013b) Preparation and Characterization of Lignin-Containing Nanofibrillar Nellulose. *Procedia Environmental Sciences* **16**:125-130.

Wankhede D.B., Shehnaj A., Raghavendra Rao M.R. (1979) Carbohydrate Composition of Finger Millet (Eleusine coracana) and Foxtail Millet (*Setaria italica*). *Qualitas Plantarum Plant Foods for Human Nutrition* **28**:293-303. https://doi.10.1007/bf01095511.

Warui S.K., Wachira J., Kawira M., Leonard G.M. (2019) Characterization of Prototype Formulated Particleboards from Agroindustrial Lignocellulose Biomass Bonded with Chemically Modified Cassava Peel Starch. *Journal for Advances in Materials Science and Engineering* **2019**:1-15. https://doi.org/10.1155/2019/1615629.

Watkins D., Nuruddin M., Hosur M., Narteh A.T., Jeelani S. (2015) Extraction and Characterization of Lignin from Different Biomass Resources. J. of Mat. Res. and Tech. **4**:26-32.

Welker C.M., Kumar B.V., Petti C., Krishan M.R., DeBolt S., Mendu V. (2015) Engineering Plant Biomass Lignin Content and Composition for Biofuels and Bioproducts. Energies **8**:7654-7676.

Wen J.L., Sun S.L., Xue B.L., Sun R.C. (2013) Recent Advances in Characterization of Lignin Polymer by Solution-State Nuclear Magnetic Resonance (NMR) Methodology. *Journal on Materials* **6**:359-391.

Widyorini R., Xu J., Umemura K., Kawai S. (2005) Manufacture and Properties of Binderless Particleboard from Bagasse I: Effects of Raw Material Type, Storage Methods, and Manufacturing Process. *Journal for Wood Science* 51:648-654.

Williams T., Hosur M., Theodore M., Netravali A., Rangari V., Jeelani S. (2011) Time Effects on Morphology and Bonding Ability in Mercerized Natural Fibers for Composite Reinforcement. *Journal for Polymer Science* **2011**:1-9. doi.org/10.1155/2011/192865.

Wu R., Wang X., Li F., Li H., Wang Y. (2009a) Green Composite Films Prepared from Cellulose, Starch and Lignin in Room-Temperature Ionic Liquid. *Journal on Bioresource Technology* **100**:2569-2574. https://doi.org/10.1016/j.biortech.2008.11.044.

Wu R., Wang X., Li F., Li H., Wang Y. (2009b) Green Composite Films Prepared from Cellulose, Starch and Lignin in Room-Temperature Ionic Liquid. *Bioresource Technology* **100**:2569-2574. https://doi.org/10.1016/j.biortech.2008.11.044.

Xiang Q., Lee Y.Y. (2000) Oxidative Cracking of Precipitated Hardwood Lignin by Hydrogen Peroxide. *Journal for Applied Biochemistry and Biotechnology* **84-86**:153-162.

Xiao C., Lu D., Xu S., Huang L. (2011) Tunable Synthesis of Starch-Poly(Vinyl Acetate) Bioconjugate. *Journal for Starch - Stärke* **63**:209-216.

Xie F., Yu L., Liu H., Chen L. (2016) Starch Modification Using Reactive Extrusion. *Journal on Starch* **58**:131-139. doi 10.1002/star.200500407.

Xu J., Hou H., Liu B., Hu J. (2017) The Integration of Different Pretreatments and Ionic Liquid Processing of Eucalyptus: Hemicellulosic Products and Regenerated Cellulose Fibers. *Industrial Crops and Products* **101**:11-20. https://doi.org/10.1016/j.indcrop.2017.02.038.

Xu Q., Wen J., Wang Z. (2016) Preparation and Properties of Cassava Starch-Based Wood Adhesives. *BioResources* **11**:6756-6767.

Yamada T., Hu Y., Ono H. (2001) Condensation Reaction of Degraded Lignocellulose during Wood Liquefaction in the Presence of PolyhydricAlcohols. *Journal for The Adhesion Society of Japan* **37**:471-478.

Yamamoto H., Makita E., Oki Y., Otani M. (2006) Flow Characteristics and Gelatinization Kinetics of Rice Starch Under Strong Alkali Conditions. *Journal for Food Hydrocolloids* **20**:9-20. doi: 10.1016/j.foodhyd.2005.02.003.

Yan N., Zhang B., Zhao Y., Farnood R.R., Shi J. (2017a) Application of Biobased Phenol Formaldehyde Novolac Resin Derived from Beetle Infested Lodgepole Pine Barks for Thermal Molding of Wood Composites. *Journal on Ind. Eng. Chem. Res.* **56**:6369-6377.

Yan N., Zhang B., Zhao Y., Farnood R.R., Shi J. (2017b) Application of Biobased Phenol Formaldehyde Novolac Resin Derived from Beetle Infested Lodgepole Pine Barks for Thermal Molding of Wood Composites. Ind. Eng. Chem. Res. **56**:6369-6377.

Yang L., Liu J., Du C., Qiang Y. (2013) Preparation and Properties of Cornstarch Adhesive. *Journal on Food Sci. Technol.* **5**:1068-1072.

Yang X., Chen Q., Zeng J., Zhang J.S., Shaw C.Y. (2001) A Mass Transfer Model for Simulating Volatile Organic Compound Emissions from 'Wet' Coating Materials Applied to Absorptive substrates. *Journal for Heat and Mass Transfer* **44**:1803-1815.

Ye P., An J., Zhang G., Wang L., Wang P., Xie Y. (2018) Preparation of Particleboard Using Dialdehyde Starch and Corn Stalk. *Journal for BioResource* **13**: 8930-8942. doi: 10.15376/biores.13.4.8930-8942.

Youngquist J.A. (2012) Wood-Based Composites and Panel Products," in Wood Handbook: Wood as an Engineering Material, Gen. Tech. Rept. FPL-GRT-113., USDA Forest Serv., Forest Prod. Lab, Madison, WI, pp. 1–31 (Chapter 10).

Yuan T.Q., Sun S.N., Xu F., Sun R.C. (2011) Structural Characterization of Lignin from Triploid of Populus tomentosa Carr. *Journal for Agricultural and Food Chemistry* **59**:6605-6615. doi:10.1021/jf2003865

Zarifa A.A., Shammala M.A., Sheikh A.A. (2018) Sustainable Manufacturing of Particleboards from Sawdust and Agricultural Waste Mixed with Recycled Plastics. *Journal for Environmental Engineering* **8**:174-180. doi:10.5923/j.ajee.20180805.02.

Zhang L., Ding Y., Song J. (2016) Crosslinked Carboxymethyl Cellulose-Sodium Borate Hybrid Binder for Advanced Silicon Anodes in Lithium-Ion Batteries. *Chinese Chemical Letters*. https://doi.org/10.1016/j.cclet.2018.03.008.

Zhang L.Z., Niu J.L. (2003) Mass Transfer of Volatile Organic Compounds from Painting Material in a Standard Field and Laboratory Emission Cell. *Journal of Heat and Mass Transfer* **46**:2415-2423.

Zhang Z., Liu J., Gao W., Sun L., Li Z. (2020) Action of Silicic Acid Derived from Sodium Silicate Precursor Toward Improving Performances of Porous Gelatin Membrane. *Journal for Applied Polymer Science* **48912**:1-10.

Zhao E., Kwak J.K., Wang Y., White J.M., Holladay J.E. (2013) Effect of Crystallinity on Dilute Acid Hydrolysis of Cellulose by Cellulose Ball-Milling Study. Energy and Fuels **20**:807-811.

Zhou P., Zhang Z. (2016) One-pot catalytic conversion of carbohydrates into furfural and 5-hydroxymethylfurfural. *Journal for Catalysis Science & Technology* **6**:3694-3712.

Zhou W., Mahato D.N., MacDonald C.A. (2010) Analysis of Powder X-ray Diffraction Resolution Using Collimating and Focusing Polycapillary Optics. *Journal for Thin Solid Films* **518**:5047-5056. https://doi. 10.1016/j.tsf.2010.02.033.

Zhou X., Li W., Zhu L., Ye H., Liu H. (2019) Polymer–Silica Hybrid Self-Healing Nano/Microcapsules with Enhanced Thermal and Mechanical Stability. *Journal for RSC Advances* **9**:1782-1791. doi: 10.1039/C8RA08396G.

Zia F., Zia K.M., Zuber M., Kamal S., Aslam N. (2015) Starch Based Polyurethanes: A Critical Review Updating Recent Literature. *Journal for Carbohydrate Polymers* **134**:784-798.

Zia K., Siddiqui T., Ali S., Farooq I., Zafar M.S., Khurshid Z. (2019) Nuclear Magnetic Resonance Spectroscopy for Medical and Dental Applications: A Comprehensive Review. *Journal of Dentistry* **13**:124-128. doi:10.1055/s-0039-1688654.

Zuo Y., Zhang X., Liu X. (2015) Study on the Effect of Organic Additives and Inorganic Fillers on Properties of Sodium Silicate Wood Adhesive Modified by Polyvinyl Alcohol. *Journal for BioResource* **10**:1528-1542.

Appendix 1. Map of Research Sites

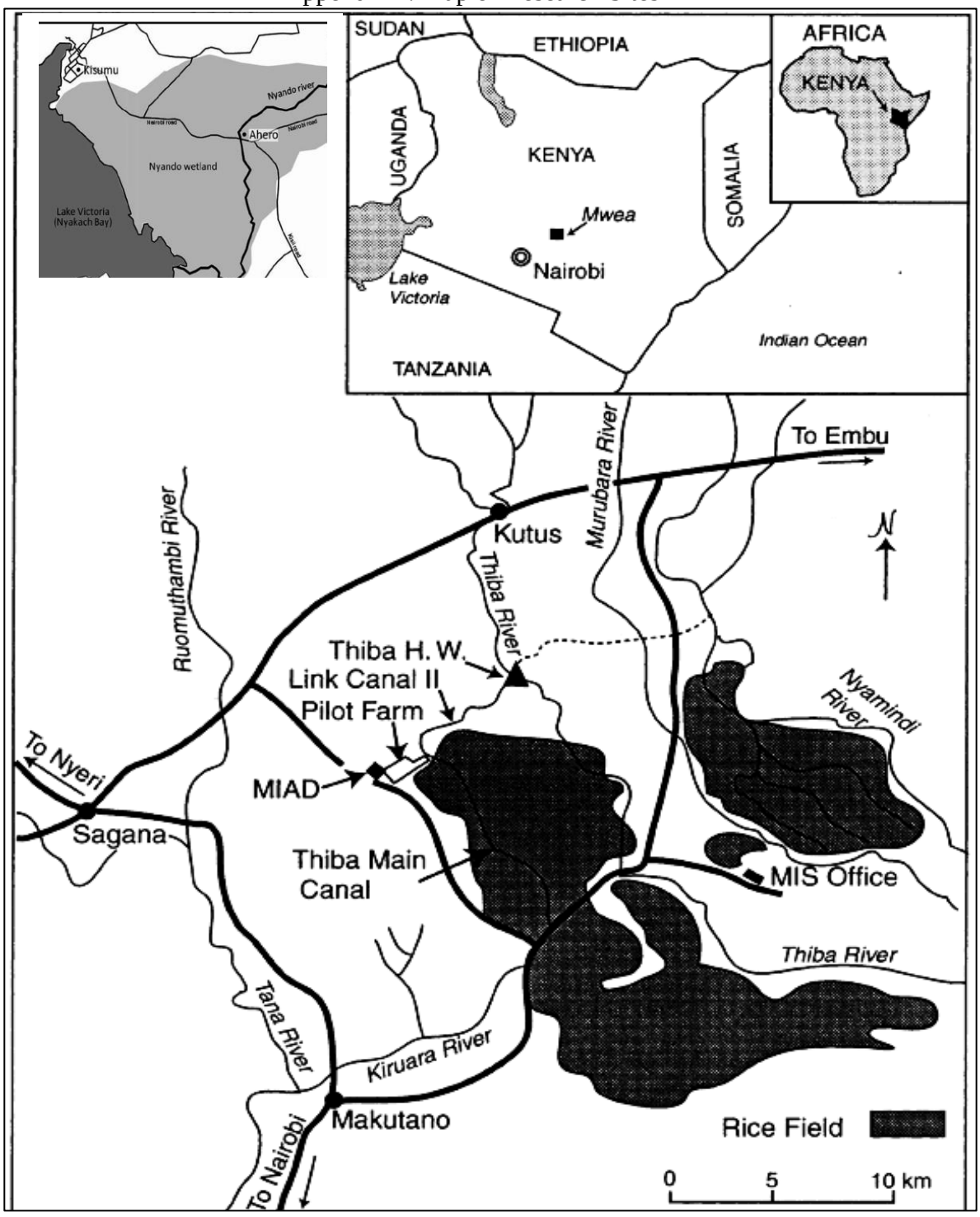

Appendix 2. Particleboard Mould

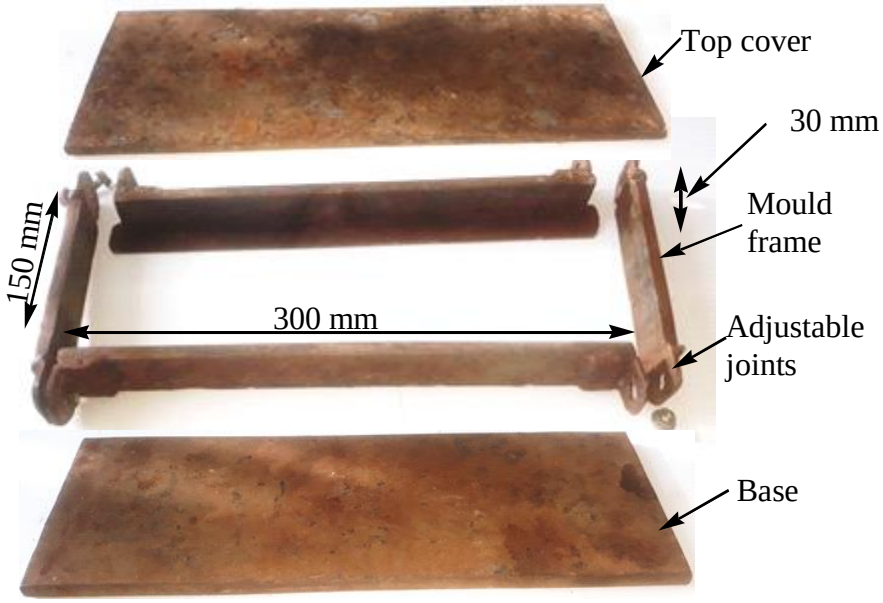

Appendix 3. XRF Analysis results for lignocellulose materials and Cassava starch

Starch Sources	Na	Zn	Ca	Mg
Cassava Tubers	0.00133^{a}±0.00058	0.03433^{a}±0.00473	9.99633^{b}±0.0953	0.00167^{a}±0.00058
Wheat Four	0.002^{a}±0.001	0.12333^{a}±0.00513	7.755^{b}±0.03568	6.55333^{bc}±0.01124
Maize Corn	0.00133^{a}±0.00058	0.132^{a}±0.00361	4.55367^{a}±0.00945	0.14387^{a}±0.18804
Sorghum Grains	0.00133^{a}±0.00058	0.21733^{a}±0.00586	5.21433^{c}±0.01756	6.24067^{cd}±0.01343
Millet Grains	0.00167^{a}±0.00058	0.23733^{a}±0.0185	5.62533^{b}±0.00586	5.953^{bc}±0.01082
Cassava Peel Starch	0.00467^{a}±0.000577	0.06333^{a}±0.00635	13.4633^{b}±0.10017	0.1270^{a}±0.00781